AN EPIGENETIC APPROACH FOR IDENTIFYING NOVEL TUMOR ASSOCIATED GENES FROM REGIONS OF LOSS OF HETEROZYGOSITY IN HUMAN NEOPLASIAS.

DISSERTATION

Presented in Partial Fulfillment of the Requirement for

the Degree of Doctor of Philosophy in

the Graduate School of The Ohio State University

By

Laura Taylor Smith

****

The Ohio State University

2005

Dissertation Committee:

Christoph Plass, PhD, Advisor

Gustavo Leone, PhD

Gail Herman, MD, PhD

James C. Lang, PhD

Approved by

_____

Advisor

Graduate Program in

Molecular Virology, Immunology,

and Medical Genetics

Abstract

The incidence of cancer is expected to be 1 in every 3 individuals. Onset of the disease in the population has been attributed to multiple genetic and environmental factors. Pathways leading to the development and progression of carcinomas, including head and neck squamous cell carcinomas (HNSCC) and non-small cell lung cancer (NSCLC), remain largely unknown. Common genetic alterations have been identified for many neoplasias, but many of the important genes of activation (oncogenes) or inactivation (tumor suppressor genes) have not yet been identified or characterized. This lack of identified cancer targets is in part due to limitations in detection techniques, as well as limited by the type of aberrations screened for. For example, researchers often search for mutations within a chromosomal region that is lost in order to identify candidate tumor suppressor genes. Epigenetic mechanisms, such as histone modifications and DNA methylation, have also become accepted modes of transcriptional inactivation in human malignancies, but are still in their beginning stages of evaluation in HNSCC, and have not been widely applied as an approach to identify tumor suppressor genes. The majority of DNA methylation studies in HNSCC have focused on genes previously identified as being inactivated in other cancer types. Efforts using genome-wide methylation scanning techniques, such

as Restriction Landmark Genomic Scanning (RLGS) have identified novel methylation targets in HNSCC. Better understanding of the role of DNA methylation in human malignancies, as well as the targets of this epigenetic inactivation, may allow for more efficient and earlier detection screenings, as well as providing an additional mechanism for identifying important cancer-related genes.

In the introductory ***chapter one***, limited information from the literature regarding DNA methylation and HNSCC is reviewed, demonstrating the void that remains in the molecular etiology of the disease. ***Chapter two*** describes the difficulty and limitations of traditional experiments used to identify tumor suppressor genes from within regions of loss of heterozygosity (LOH). Often neglected in these studies that look for genetic mutations, DNA methylation has proven to be as important for gene silencing in cancer. In this chapter, a novel application of the genome-wide methylation technique Restriction Landmark Genomic Scanning (RLGS) is used to identify genes frequently hypermethylated in a localized region of the genome frequently lost in the progression of human neoplasia for which no tumor suppressor gene has been elucidated. TCF21 is shown to be targeted for hypermethylation in the majority of HNSCC and NSCLC samples. ***Chapter three*** describes further characterization of DNA methylation of TCF21, and determines the effect of such methylation on transcription. DNA methylation along the CpG island of TCF21 is tumor specific, and removal of methylation results in transcriptional upregulation. ***Chapters four*** and ***five***

summarize the antagonistic cancer properties elicited by TCF21 expression in cancer cell lines and how they translate *in vivo.* In chapter four the tumor suppressive function of TCF21 is investigated. The role of TCF21 in mesenchymal to epithelial transitions (EMT) had been described previously as important in embryogenesis and organ differentiation. The function of TCF21 in cancer had not been investigated. TCF21 expression results in a reduced tumor growth rate *in vivo*. In cell culture, TCF21 reduces the growth rate and ability of cancer cells to aggregate into colonies, oblivious to contact inhibition by neighboring cells. Epithelial expression patterns are restored to TCF21 positive cells. Chapter five experimentally determines a link to KiSS-1, a known metastasis suppressor gene from chromosome 1q32. TCF21 expression further results in a reduced ability to invade a collagen matrix, a protein found in the extracellular matrix that is degraded in cancer to allow for migration to distant sites. Together, these experiments substantiate the conclusions that TCF21 silencing is advantageous in cancer progression and that the dual function of TCF21 as a tumor and metastasis suppressor gene is important for human malignancies.

Dedicated to all of those individuals who believed in me even when I did not, especially my husband, Eric, and my mom, Sandra.

ACKNOWLEDGMENTS

I would like to thank my advisor, Christoph Plass, for his guidance during my studies under his direction. In addition to the breadth of his knowledge in the world of epigenetics, Dr. Plass has been a source of careful and thoughtful discussion that was key to my development as a scientist. Without his unending support, both analytically and scientifically, this set of experiments would not have been possible. *"The whole art of teaching is only the art of awakening the natural curiosity of young minds for the purpose of satisfying it afterwards"* (Antole France). Dr. Plass continues to find aspects within his research to stimulate and excite researchers around him. It has been an honor to train with him.

My Plass Lab colleagues, both past and present, have also been instrumental in broadening my thought process and data analysis, while providing an environment conducive to the rapid exchange of ideas and support. It is in part because of this group of researchers that this project ensued. In particular, I would like to thank Dr. Dominic Smiraglia, a former post doc with Christoph Plass and current faculty member at Roswell Park Cancer Institute. Without Dominic, my initial training and subsequent successes would not have

been possible. In addition, I would also like to thank Dr. Zunyan Dai for his support and friendship throughout the dissertation process. Their friendships are highly regarded. Many thanks to Dr. Aparna Raval, and Dr. Linda Liu for their comments regarding improvements to my thesis.

I have also been fortunate to have been surrounded by a group of individuals that have derived from my time at OSU that have been significant to me personally that have translated into aiding me professionally. Their friendships are priceless. In particular, Ute Plass, your strength and outlook on life is amazing. This motivates me tremendously. Erin Hertlein, you have been an amazing role model for me in that you have managed to stay true to who you are throughout graduate school stresses as well as maintain your wonderful personality. I think that you are an asset wherever you go.

Collaborations made with Dr. Tom Rosol and members of his lab including Prasad Nadella, Annie Levine, and Chelsea Martin, were scientifically sound and exciting. Their clinical applications to my dissertation research are highly appreciated and their guidance was critical to the metastases studies.

My dissertation committee, consisting of Drs. Gustavo Leone, James Lang, and Gail Herman, was invaluable throughout my studies. Although devoted to their own research, they were able to provide precious time and input into guiding my own interests. In addition, individually and collectively they were able to encourage me to continue, and often praised my scientific findings.

And finally, my family continues to be inspirational to me. Matt, your

cancer echoes daily in my mind, and your remission serves as a reminder for why this is all worthwhile. Mom, you managed to always be there for me with comforting words of encouragement. I thank you for always supporting me and I am just as proud of you as you are of me. My stepfather, Greg, you were always interested in learning what was the latest development, helping to keep me motivated. My sister, Katie, although we have completely different career paths, you and I will always remain connected. I am proud of what you have accomplished in your life.

My mother- and father-in-law, Donna and Richard, were very helpful during the writing phase of the thesis. Thank you for all of your encouragement and support over these last years.

Emilie, even though you may not think you do much more than distract right now, you have been a tremendous inspiration to me. I love being able to escape from science for a short while and am amazed by your beauty, curiosity, and innocence. I love being your mom.

And most of all, Eric, your support, above all, has guided me through. You have supplied for us financially, but more importantly emotionally. I would not have been able to get this far without you. Thank you also for your grammatical corrections throughout this document, and for trying to understand the science. You are my best friend and I am happy to share this with you.

VITA

August 10, 1977……Born, Columbus, Ohio, USA

1999……Bachelor of Arts in Biology, Capital University

1999-present……..PhD candidate, Department of Molecular Virology, Immunology, and Medical Genetics, The Ohio State University

PUBLICATIONS

Research Publications

1. Yu L, Liu C, Vanduesen J, Becknell B, Dai Z, Wu Y, Raval A, Liu T, Ding W, Mao C, Liu S, **Smith LT**, Lee S, Rassenti L, Marcucci G, Byrd J, Caliguiri MA, and Plass C. "Global assessment of promoter methylation in a mouse model of cancer identifies ID4 as a putative tumor-suppressor gene in human leukemia." **Nature Genetics,** March 2005, 37 (3):265-273.
   **I established the methylated-luciferase constructs in the Plass lab that are utilized in this project.*

2. **Smith LT** and C Plass. "DNA methylation leaves its mark in Head and Neck Squamous Cell Carcinomas (HNSCC)." **Current Genomics,** 5(6), 2004.

3. Smiraglia DJ, **Smith LT**, Lang JC, Rush LJ, Dai Z, Schuller DE, Plass C. "Differential targets of CpG island hypermethylation in primary and metastatic head and neck squamous cell carcinoma (HNSCC)." **Journal of Medical Genetics,** 40(1), 2003.
   **I ran RLGS on patient samples and analyzed the methylation profiles, which identified Cullin 3 as a methylation target. I also established bisulfite sequencing reactions and confirmed Cullin 3 methylation.*

4. Dai Z, Weichenhan D, Wu YZ, Hall JL, Rush LJ, **Smith LT**, Raval A, Yu L, Krull D, Muehlisch J, Fruhwald MC, de Jong P, Cantanese J, Davuluri RV, Smiraglia DJ, and Plass C. "An *AscI* boundary library for the studies of genetic and epigenetic alterations in CpG islands." **Genome Research,** 12(10), 2002.
   **I helped to clone the AscI-EcoRV clones used to create the bacterial library.*

5. Yoon BJ, Herman H, Sikora A, **Smith LT**, Plass C, and Soloway PD. "Regulation of DNA methylation of Rasgrf1." **Nature Genetics,** 30(1), 2002.
   **I was part of designing and performing the bisulfite sequencing reactions that were used to prove methylation of Rasgrf1 was specific to the differentially methylated region (DMR).*

6. Fruhwald MC, 0'Dorisio MS, **Smith L**, Dai Z, Wright FA, Paulus W, Jurgens H, and Plass C. **"**Hypermethylation as a potential prognostic factor and a clue to a better understanding of the molecular pathogenesis of medulloblastoma--results of a genomewide methylation scan." Klin Padiatr. 213(4), 2001.
   **I designed and performed the Southern blot analysis to confirm the hypermethylation of RLGS fragment, 2F67, in medulloblastomas.*

FIELD OF STUDY

Major Field: Molecular Virology, Immunology and Medical Genetics.

Area of Emphasis: Cancer Genetics

TABLE OF CONTENTS

LIST OF TABLES

LIST OF FIGURES

LIST OF ABBREVIATIONS

HNSCC.....Head and Neck Squamous Cell Carcinomas

NSCLC .....Non-small cell lung cancer

SCLC.....Small cell lung cancer

DNA.....Deoxynucleic Acid

RLGS.....Restriction Landmark Genomic Scanning

TCF21 .....Transcription Control Factor 21

LOH .....Loss of Heterozygosity

EMT.....Epithelial to Mesenchymal Transition

MET.....Mesenchymal to Epithelial Transition

TA-4.....tumor antigen-4

CYFRA 21-1 .....cytokeratin fragment 21-1

CEA.....carcinoembryonic antigen

SPT .....Secondary Primary Tumors

DNMT .....DNA methyltransferase

SAM.....S-adenosylmethionine

rDNA.....ribosomal Deoxynucleic Acid

CpG .....Cytosine-phospho-Guanine

HDAC .....Histone Deacetylase

SUV39H1 .....suppressor of variegation 3-9 homolog 1

LOI.....Loss of Imprinting

MGMT .....O-6-methylguanine-DNA methyltransferase

RASSFIA .....Ras association domain family 1 isoform A

DAPK1.....Death-associate protein kinase 1

hMLH1 .....human homolog of mutL

MSP.....Methylation-Specific PCR

HDACi .....Histone Deacetylase inhibitors

TSA .....Trichostatin A

CDKN2A.....p16

CIS .....Carcinoma *in situ*

CGH .....Comparative Genomic Hybridization

MLR.....Minimally Lost Region

SRO.....Shortest Region of Overlap

bp .....base pairs

LN.....Natural log

BAC .....Bacterial Artificial Chromosome

NAT .....Normal Adjacent Tissue

Mb .....Megabase

EST .....Expressed sequence tag

ENPP1.....ectonucleotide pyrophosphatase/phosphodiesterase 1

MAP7.....Microtubule-associated protein 7

CITED2.....Cbp/p300-interacting transactivator, with Glu/Asp-rich carboxy-terminal domain, 2

HTF .....*Hpa*II tiny fragments

CIM.....CpG island methylation

BSA .....Bovine Serum Albumin

RT-PCR.....reverse transcriptase polymerase chain reaction

GPI .....phosphatidylinositol glycan

CoBRA .....Combined bisulfite restriction analysis

T .....thymine

A.....adenine

G.....guanine

C.....cytosine

bHLH .....basic helix loop helix

WT-1.....Wilm's Tumor-1

BMP4.....Bone morphogenic protein 4

TCF21ex.....TCF21 exon

LB .....Lurea Broth

PAGE .....Polyacrylamide gel electrophoresis

PBS .....Phosphate Buffered Saline

UTR.....Untranslated Region

GATA-1 .....Globin Transcription Factor-1

dpi.....Days post injection

RNA pol II .....Ribonucleic acid polymerase II

MMP .....Matrix Metalloprotease

PIC .....Protein Inhibitor Complex

ChIP .....Chromatin Immunoprecipitation

SDS .....Sodium Dodecyl Sulfate

wt.....wild type

nm .....nanometers

BAC-FISH.....Bacterial Artificial Chromosome Fluorescent *in situ* Hybridization

neo6q .....neomycin-tagged chromosome 6q

CRSP3 .....cofactor required for Sp1 transcriptional activation, subunit 3

CEP6 .....Centromeric probe 6

MW .....Molecular weight marker

gDNA.....Genomic deoxynucleic acid

PBL.....Peripheral blood lymphocyte

IVIS.....*In vivo* imaging system

CHAPTER 1:

DNA METHYLATION LEAVES ITS MARK IN HEAD AND NECK SQUAMOUS CELL CARCINOMAS (HNSCC)

Published in: **Current Genomics, 5(6), 2004** by **Smith LT** and C Plass.

1.1 Head and Neck Cancer – Detection Of The Disease

Ninety percent of all head and neck cancers are classified as squamous cell carcinomas (HNSCC)[1]. Annually, HNSCC accounts for approximately 500,000 new cases worldwide, making it the 6th most common cancer type[1]. In the United States, 30,000 new cases and 8,000 deaths as a result of HNSCC were estimated to occur 2002[2]. Carcinomas located predominantly in the squamous epithelium lining the larynx, pharynx, esophagus, and oral epithelium collectively form HNSCC[3]. The overall 5-year survival rate for HNSCC is a mere 50%[4]. Tobacco usage and alcohol consumption have been directly linked to approximately 85-90% of these tumors, implying that the majority of these tumors are highly preventable[5; 6]. Other factors, such as those associated with dietary and occupational exposures, including the use of mouthwash, have been implicated in HNSCC[7].

Early signs of the disease include a sore that will not heal, difficulty in swallowing, or a change in voice for longer than 2 weeks[8]. Additional symptoms are white (leukoplakia) or red patches (erythroplakia) that line the oral cavity, along with chronic sinus blockage that does not resolve upon treatment with antibiotics, frequent headaches, and persistent pain[9]. Clinical examination by a physician is often recommended with these symptoms for further diagnosis.

Available screening tools for HNSCC include tumor markers expressed by the cancer that are released into the serum such as TA-4, CYFRA 21-1 and CEA, along with visual inspection of the area[10; 11]. Visual inspections, either by eye or laboratory equipment, are limited to lesions that are large enough to detect. Even with these screening approaches, thus far no efficient detection markers for HNSCC have been identified[11]. Molecular tests, including the previously mentioned tumor markers, have limited sensitivity, especially in early diagnosis due to the low expression levels of each[11]. Earlier detection can only guarantee earlier diagnosis, and, as of yet, cannot be linked to better mortality rates[12].

Diagnosis of HNSCC is devastating in and of itself, but in addition, the standard treatment, including radical removal of the tumor-bearing area, offers little to the patient. Surgery provides its own set of complications, including physical and emotional scarring, often accompanied by difficulties in speech, hearing, and swallowing[13]. In addition, radiation treatment often follows surgery for Stage I and II tumors. More advanced Stage III and IV tumors are frequently

resistant to standard therapies, and patients succumb to second primary tumors in 10-30% of the cases as a result of microscopically undetectable tumor cells at the margins of the primary site[14]. Secondary primary tumors (SPT) are believed to arise, not as a result of therapy, but instead from continued carcinogen exposure prior to and following diagnosis[15]. Smoking cessation and the use of certain chemopreventive agents, such as retinoids, have demonstrated anti-neoplastic properties against the disease[16]. Because of a lack of fundamental understanding of the disease and its stages, the necessity for identifying genes essential for disease progression, which may also function as prognostic biomarkers, is evident.

1.2 Genetics of Head and Neck Cancer

To approach the identification of novel tumor markers, a basic molecular perception of the disease at various stages is vital. Like other tumors, HNSCC is believed to develop from a multi-step accumulation of changes in gene expression, allowing a cell (or cells) to outgrow and outlast surrounding neighbors. Because of the exposure of the entire region to the carcinogens in tobacco smoke and other contributors (field cancerization), aberrations such as chromosomal alterations, are often observed in surrounding normal epithelium as well as in the tumor itself. For example, Loss of Heterozygosity (LOH) studies identified high rates of LOH at 9p21, the location of p16, in histologically normal adjacent tissue and premalignant squamous dysplasia, as well as in advanced

invasive carcinomas[17; 18; 19]. This suggests that aberrations occurring in premalignant lesions can be used to predict those patients likely to progress to squamous carcinomas. Other genetic abnormalities have been described for HNSCC including deletions on chromosomes: 3p, 5q, 17p, 8p, 13q, 18q, 22q, 6q, and 2q, as well as DNA amplifications of 11q13, 3q, 10q, 5p, 3q, 8q, 15q, and 22q[20; 21; 22; 23; 24; 25]. Gains of 11q13 have been linked to the overexpressoin of the cell cycle gene Cyclin D1, which has clearly been associated with tumor progression and poor survival[26; 27]. The order in which the gains and/or losses occur does not appear to be as important as the overall accumulation of events[28]. In contrast, many of the candidate genes responsible have yet to be identified from the regions of chromosomal gains or losses in HNSCC.

1.3 DNA Methylation Regulates Gene Transcription

In addition to genetic events that directly alter the DNA sequence, epigenetic events that occur without changing the DNA code have also been described in HNSCC[29; 30; 31; 32; 33; 34]. DNA methylation, both hypo- and hyper-, and histone modifications are examples of epigenetic alterations described in neoplastic diseases[35; 36; 37]. Hypomethylation refers to a reduction in the overall amount of 5-methyl cytosine compared to normal tissues, while hypermethylation refers to the localized, CpG island- specific accumulation of 5-methyl cytosine. Cytosine methylation functions in long-term silencing of genetic material. DNA methylation is catalyzed by at least 3 mammalian DNA methyltransferases

(DNMTs): DNMT1, 3a, and 3b. DNMTs 3a and 3b have been shown to have *de novo* methyltransferase activity, having affinity for unmethylated DNA[38]. The maintenance methyltransferase, DNMT1, demonstrates a preference for hemi-methylated DNA molecules. All mammalian methyltransferases methylate cytosine 5' to guanine in CpG dinucleotides, following replication[39]. Enzymatic transfer of a methyl group from the methyl-donor, S-adenosylmethionine (SAM), to the carbon in position 5 of cytosine has been shown to be important in non-neoplastic, as well as neoplastic pathways[35].

It is apparent that DNA methylation is a normal process in mammals that is essential to life[40]. In mammalian development, a wave of genome-wide demethylation occurs following fertilization, followed by epigenetic reprogramming during normal embryonic development[39; 41]. This reprogramming allows for normal maternal and paternal imprints to be set[34; 42]. Further methylation occurs in female offspring during X-inactivation, allowing for proper dosing to occur by silencing genetic material in the selected X chromosome in every cell[43; 44; 45]. Repeat sequences, including rDNA and satellite sequences, as well as primitive transposable elements, including LINE1 and Alu repeats, are prevented from relocating in the genome by methylating CpG dinucleotides, which contributes to chromosomal stability[46; 47]. DNA methylation is also seen in aging tissues in mammals likely due to environmental factors, chronic infections, as well as other genetic susceptibilities[48]. Because of the accumulation of these epigenetic changes, this may contribute to the heightened incidence of cancers

in older populations[49]. A link between changes in the methylation status of DNA and chromosomal changes is evident[50; 51]. Typically, actively transcribed, euchromatic regions are less densely compact, and unmethylated, while inactive, heterochromatic regions are condensed and largely methylated. The question that remains is which came first, the chicken (DNA methylation) or the egg (histone modifications) phenomenon[52]. On the one hand, the direct binding of methyl-binding proteins to methylated cytosines supports the hypothesis that DNA methylation induces histone modifications[50; 53; 54]. These proteins have been shown to recruit histone-modifying enzymes, including Histone Deacetylases (HDACs), and other chromatin remodeling enzymes that then condense the methylated DNA, resulting in gene silencing. Opponents to this school of thought would argue that transcriptional silencing through DNA methylation is secondary to transcriptional silencing and modifications of the chromosomal architecture[55]. Recent studies have shown a direct association between chromatin remodeling proteins, such as SUV39H1, and the DNA methyltransferases[56]. It's believed that histone modifications at lysine tails on histone H3 are responsible for causing the DNA methylation mark, and this, in turn, induces further histone modifications through the interactions of the afore-mentioned methyl-binding proteins[57]. Other instances have deciphered a steric hindrance of transcription factor binding to regions of methylated DNA[58]. No matter the stance, it is agreed that these important epigenetic processes collaborate to silence genes in a reversible manner.

Neoplastic lesions are often accompanied by regions of hypomethylation[36; 39]. This occurs in regions that are normally heavily methylated, but become under-methylated in cancer, and are often sites of chromosomal breaks and rearrangements[36]. Loss of methylation in cancer, including HNSCC, is believed to result in activation of transposable elements, as well as loss of imprinting (LOI) of specific genes. Hypomethylation has also been implicated, in part, as a mechanism of oncogene activation[39; 59; 60].

In addition to a loss of methylation in repetitive elements, an increase in gene-specific methylation, as well as heightened methyltransferase activity, are also commonly associated with cancer[39]. Cytosine residues located 5' to guanine in CpG dinucleotides are not evenly distributed at the expected frequency of 1/16 in the human genome[61]. In fact, methylated cytosine spontaneously deaminates to thymine, causing a reduction in the frequency of CpG dinucleotides, except in normally unmethylated clusters called *CpG islands*. Approximately 50% of the estimated 29,000 human genes have CpG islands located within their 5' regulatory regions[39]. In human neoplasias, including HNSCC, aberrant hypermethylation of CpG dinucleotides within particular CpG islands is observed. Ten percent of the total CpG islands are estimated to be targets of aberrant DNA methylation in some cancers[57]. Current research has identified genes crucial to cell cycle regulation, DNA repair, apoptosis and angiogenesis as becoming inactivated by DNA methylation in a variety of cancers[61]. Cytosine methylation has also been linked directly to inducing genetic

mutations in vital tumor suppressor genes. Mutations within the p53 tumor suppressor have been correlated with deamination of 5-methylcytosine to thymine[62].

Like genetic events that accumulate throughout the development of HNSCC, hypermethylation is also observed at specific loci and can be found more frequently at advanced stages of disease progression, as well as in recurrent tumors[57; 63]. Greater than 90% of malignancies of the head and neck demonstrated methylation in at least one gene evaluated. In fact, tumors that contained a higher degree of methylated genes were correlated with earlier tumor recurrence and poor overall survival[64; 65].

1.4 Gene-Specific Methylation And Tumor Staging In HNSCC

Another important clinical aspect is the ability to detect aberrant methylation in HNSCC early, and by non-invasive mechanisms[9; 66]. The vast majority of research in the methylation and cancer field has been based upon a candidate gene approach by searching for methylation in genes that have been previously reported to be involved in other cancers. Studies using DNA collected from patient saliva have successfully identified promoter methylation in p16 (30-40%), MGMT (24-56%), RASSF1A (10-15%), DAPK1 (36%), and hMLH1 (31%) in head and neck cancers[22; 67; 68]. Transcriptional loss of these genes has been highly associated with the disease at varying stages. The well-known tumor suppressor gene and cell cycle regulator, p16, is often methylated and repressed

early in tumorigenesis, while loss of DAP-K function through hypermethylation is frequently associated with advanced tumor stage and metastasis[68]. Loss of the DNA mismatch repair gene, hMLH1, has been reported frequently in sporadic cancers via multiple mechanisms, but in HNSCC, promoter hypermethylation is dominant[67]. The ability to stage tumors based on the methylation of specific genes provides a novel approach for classifying HNSCC.

Interestingly, studies of HNSCC from smokers versus nonsmokers demonstrate a significant increase in p16, DAPK, E-cadherin or RASSFIA methylation[31]. Methylation of p16 alone was associated with an earlier age of smoking initiation, while E-cadherin methylation was associated with increased pack years for individuals who smoke[31]. Studies such as these, that distinguish environmental exposure differences, may be able to stratify patients for treatment, diagnosis, tumor staging, or outcome (Table 1.1).

In addition, patients that had secondary primary tumors had higher degrees of CpG island methylation[63]. On the other hand, controls did not contain methylation of these genes. Patient survival and poor prognosis have also been linked to promoter hypermethylation. For example, those patients that have increased incidences of methylated genes were less likely to survive than patients with fewer methylated targets[69]. Disease recurrence has also been significantly associated with DNA methylation analysis of several markers combined. Alone, methylation of individual genes has not been strongly predictive of disease stage, survival, or recurrence, although, taken together,

there is a significant association that can be used to classify patients with more aggressive disease.

1.5 Epigenetics And Genetics Collaborate To Silence Tumor Suppressor Genes

While it has been demonstrated that the majority of methylated targets occur independent of genetic inactivation, a subset of genes are subject to silencing through additional routes[70]. Interestingly, but not surprisingly, many of the methylated genes are located within previously identified regions of genomic loss. Studies that focused only on genetic mechanisms, such as somatic mutations, to identify candidate genes within the regions of deletion have not always been successful. For example, regions along 3p21.3 are lost in 66% of HNSCC[22]. Mutation studies of candidate genes have revealed very few inactivating mutations in this region. Studies based on DNA methylation were able to detect frequent RASSF1A methylation in primary HNSCC tumors[22]. RASSF1A has been shown in multiple cancers to be silenced through methylation, contributing to the disease phenotype. Because aberrant methylation of promoter regions of genes is as frequently utilized as an inactivating mechanism in cancer cells as genetic means (if not more so), consideration of methylation changes should also be addressed when searching for candidate tumor suppressor genes.

1.6 Global Methylation Profiling Of HNSCC

While candidate gene methylation on previously studied genes has been useful for demonstrating aberrant DNA methylation in cancer, this type of limited analysis prevents the identification of novel targets of inactivation through methylation. It is likely that genes not already acknowledged are also involved in the progression of cancer. With the advent of Restriction Landmark Genomic Scanning for screening methylated sites (RLGS-M), methylation profiles for virtually any tumor can be examined without a need for sequence information or candidate genes[33; 71; 72; 73]. In brief, RLGS-M utilizes rare-cutting, methylation-sensitive enzymes (*NotI* or *AscI*) (Figure 1.1A). Approximately 2000 *NotI* and *AscI* sites each can be assessed by a single RLGS profile (Figure 1.1B). *NotI* and *AscI* recognize a GC rich, 8bp sequence found in 86% and 83% of human CpG islands, respectively[74; 75; 76]. This global approach has the ability to distinguish unmethylated sites from methylated sites through enzymatic digestion and radioactive end labeling of the enzyme half-site of *only* unmethylated restriction sites[76]. Methylated restriction sites are inhibited from digestion and therefore cannot become radioactively end labeled, resulting in a spot loss in the profile. Because of the reproducibility of the profiles, normal and tumor tissues from individual patients are then compared to identify aberrantly methylated fragments from the tumor samples (Figure 1.1C).

In a comparison of 7 tumor types, RLGS profiles demonstrated that head and neck cancers have a lower degree of global hypermethylation compared to other tumor types examined[74]. Many of the identified methylation targets are methylated in only one to two tumor-derived HNSCC patient profiles. Several possible explanations may account for these observations. First, head and neck cancers are a collective group of tumors, located in different physical locations of the aerodigestive tract. There is evidence that the global methylation patterns are non-random, and may be tumor-type specific[74]. Other cancer-types are not grouped, representing an individual tumor location for direct comparison. Second, head and neck cancers are often a heterogeneous mixture of cells that have been exposed to the same carcinogens, but are not necessarily pure tumor DNA from a clonal population due to the field cancerization effect. In fact, tissue that is deemed uninvolved normal adjacent tissue, displaying no tumorigenic characteristics, often has similar alterations as the subsequent tumor(s)[4; 77]. Therefore, when compared to “normal” adjacent tissue, a number of methylation events may not be detected in the cancer because they are already present in the adjacent tissue. Third, because of this cellular permeation, including inflammatory cells and stromal cells, present at the time of tumor collection, it is also possible that the overall degree of methylation detected is under-represented. DNA isolated from these infiltrating cells, which are presumed to be unmethylated at CpG islands, would camouflage the methylation present in the

tumor cell populations. Fourth, if less than 30% of the cells in the given tumor sample do not contain the same hypermethylation pattern, the RLGS spot loss may be too subtle to visualize in the RLGS profile. Finally, methylation that is assessed by RLGS is dependent upon the methylation status of the "landmark" enzymes. Thus methylation that resides outside of these restriction sites would not be detected.

Regardless, methylation of HNSCC, as detected by RLGS, has demonstrated that the there is tumor-specific methylation, and likely contributes to the disease[33]. In addition, stage specific methylation patterns can be identified using metastatic DNA samples for RLGS analysis. Based on the RLGS analysis, 3 classifications of spot loss due to methylation were detectable: those lost only in primary tumors, losses only in metastasis, or losses that are shared by both primary and metastatic tumors[33]. Because of the presumed accumulation of abnormalities in cancer cells, it is not surprising that RLGS profiles from metastatic samples had a higher overall degree in the frequency of global hypermethylation than in the primary tumor[33]. Aside from the overall methylation levels detected in primary and metastatic tumors, analysis of the individual RLGS fragments resulted in different patterns. Only a small portion of the RLGS fragments methylated in the primary tumor remain methylated in the metastatic tumors[33]. This change in the methylation patterns may demonstrate the flexibility in the methylation phenomenon, allowing for gene expression to be regulated as needed in the tumor development[66] (Figure 1.2B). Differences in methylation

patterns may also reflect that many of the patients that are initially diagnosed with HNSCC have microscopically undetected primary carcinomas, and have already demonstrated cervical lymph node metastasis, or may reflect the abundance of secondary neoplastic lesions often seen in a patient. This clinical note would argue against the stepwise accumulation of alterations, and instead propose an additional mechanism utilized by cancer cells to obtain metastatic potential. Altered cells, deemed neoplastic, prior to the development of the initial invasive tumor, may acquire the ability to disseminate at a time point different than that of the primary tumor, representing a different population of genomic alterations, both genetic and epigenetic (Figure 1.2A). Whether the metastatic lesions disseminated from the primary tumor in the canonical step-wise accumulation of genetic events favorable for metastasis, or if the metastatic lesions arose independently from another tumor, differences in methylation would then be depicted in the RLGS profiles. Regardless of where these cells originated, methylation events in metastatic samples still provide insight into genes that might be essential for this aggressive behavior.

1.7 DNA Methylation And Its Application In The Clinic

A crucial clinical aspect is the relevance of DNA methylation to disease detection. Because of the early establishment of the methylation mark at certain genes, and the ability to identify this methylation in circulating cells of the blood, serum, oral rinses, urine, and stool, methylation screening as a means of cancer

detection remains an attractive idea[78]. An additional advantage is the sensitivity of tools used to assess methylation. DNA obtained from oral rinses is sufficient for use in PCR-based methylation screens, such as Methylation-Specific PCR (MSP). Arguably, potentially more important than assay sensitivity is assay specificity. Tumors, where methylation was not detected in the analyzed genes, had no false positive methylation results in DNA from their corresponding oral rinses[68]. Because of this, gene-specific methylation arrays can be designed using nanogram quantities of DNA, while eliminating false positive results.

Because of the reversibility of DNA methylation observed in cancer, the use of demethylating agents in cancer therapy is under extensive investigation. *In vitro* treatment of cell lines with these agents has been shown to restore expression of many of the genes silenced in cancer. In fact, treatment of cells in culture significantly prolonged the doubling time of neoplastic cells but not normal fibroblast cells[79]. Also of clinical importance is the finding that active concentrations of the demethylating agents used *in vitro* can be translated *in vivo*[39]. These demethylating drugs antagonize cancer cells primarily through two mechanisms: hypomethylation and cellular toxicity. Scrutiny of the application of these drugs, such as 5-aza- 2'-deoxycytidine (Decitabine) and 5'azacytidine, originates from the observation that treatment of cells results in a non-specific cytosine demethylation. In other words, the cytosine analog incorporates randomly into the genome of dividing cell populations, covalently links the catalytic domain of the DNA methyltransferases, thus inactivating the enzyme,

resulting in global (and undirected) demethylation. Demethylation of the entire genome directly causes cytotoxic effects on rapidly dividing cells in S phase of cell division, targeting neoplastic cells predominantly[39]. This genome-wide demethylation may result in the activation of many silenced genes, or chromosomal breaks and translocations of genetic material that may further enhance tumorigenic properties. But, because extensive CpG island methylation is presumed not to occur in normal cells, demethylation in tumor cells remains an attractive therapeutic approach[39].

Application of Decitabine to patients with solid and hematological tumors has resulted in varying degrees of response. In general, and for unknown reasons, hematological tumors, including leukemias and lymphomas, have demonstrated higher response rates than solid tumors, including breast, colorectal and lung cancers[39]. It is possible that because liquid tumors are known to contain higher overall frequencies of methylation than solid tumors, that the effects of the drugs are more pronounced as a result[39]. The addition of demethylating agents alone is not sufficient to reactivate all epigenetically silenced alleles. As mentioned previously, histone modifications are linked to DNA methylation. To ensure a silent chromatin structure, histone tails are deacetylated. Because of this synergy, the combination of demethylating drugs with histone deacetylase inhibitors (HDACi), such as trichostatin A (TSA) and sodium butyrate, has demonstrated gene reactivation properties for certain loci[80]. It is possible that lower dosages of both drugs, in combination with other

chemotherapeutic agents, may have less toxic effects, while having greater anti-cancer effects, *in vivo*.

In HNSCC, less information regarding efficacy using demethylating agents is available from human studies than from animal models. *In vivo* engraftment of HNSCC cell lines into nude mouse models, followed by 5-aza- 2'-deoxycytidine treatment demonstrated a reduction in tumor cell growth in approximately 40% of the cell lines investigated[81; 82]. These findings indicate that demethylating agents had equally efficient effects on engrafted HNSCC tumors as conventional chemotherapeutic agents[82].

Future Directions

The prevalent role of DNA hypermethylation in HNSCC in diagnosis, staging, and possible treatment should prompt interest in further studies to identify how methylation can be manipulated and restricted. Along with understanding targets of *de novo* methylation, the process of methylation selection is just as important. Why do certain sequences frequently become hypermethylated and others do not? Is there a sequence susceptibility that the DNMTs recognize preferentially? Or is it that methylation occurs randomly throughout the genome at frequencies higher than we are able to currently detect, and through selection, only specific sequences are carried on through tumorigenesis? In other words, does methylation occur at any site in the cancer genome, but genes that become silenced through methylation that result in

lethality for the cells are not identified? Is it likely that only those silenced genes that convey a growth advantage for the cell are selected and enriched for?

Additionally, what are the factors that direct aberrant methylation at regions in the genome, while other repetitive elements are shed of methylation in the same cancer cells? Which DNMTs are responsible for the overall methylation in these systems? Do they have overlapping functions, or is the defect instead in the timing? Could the defect instead reside in the metabolism and production of the methyl donor, S-adenosylmethionine? In order for methylation in neoplastic lesions to become understood by researchers and clinicians, we must be able to answer these questions, in addition to identifying the ensuing methylation profiles of cancer.

It is evident that methylation contributes early in the formation of HNSCC, as well as persisting into even the latest stages of metastasis and dissemination. It is possible that cancers utilize methylation because of the flexible commitment it allows the cells to undertake[66]. Gene silencing at specific times, while expression at others, is important in tumorigenesis, requiring the ability to alter the silencing patterns. Genetic alterations that modify the sequence directly are more constricting to the gene expression patterns, while epigenetic marks that do not alter the DNA sequence allow for this flexibility in cancer.

Table 1.1: **Hypermethylated genes and their association with squamous cell carcinomas located in the oral cavity, pharynx, larynx, and esophageal regions.**

Gene name	Function	Tumor subtype	Association in HNSCC	Reference
FANCF	Cisplatin sensitivity	HNSCC	Shorter tobacco usage duration; Younger smoking initiation age; Greater number of years of alcohol consumption.	83
RASSF1A	Ras associated protein	HNSCC	Inversely related to HPV infection; High methylation detected in poorly differentiated HNSCC.	30 22
CDKN2A	Cell cycle	HNSCC Esophageal	Highly methylated in plasma from patients compared with normal individuals younger age of smoking initiation; Association with dysplastic lesion development; May be an initiating event of cancer.	84 31 85
$p14^{ARF}$	Cell cycle	HNSCC	Lost in a higher percentage of recurring primary tumors	63
E-cadherin	Cell differentiation and migration	HNSCC Laryngeal	Increased number of cigarette pack years; Metastasis.	31 86
DAPK1	Apoptosis	HNSCC	Lymph node metastasis.	31; 87
TSLC1	Cell motility and invasion	Nasopharyngeal Esophageal	Depth of tumor invasion and metastasis.	88
MGMT	DNA repair	Esophageal	Methylation occurs early and may allow for damage by alkylating agents to accumulate; Accumulating p53 mutations.	89
FHIT	Spans common fragile site	Esophageal	Tumor invasion and lymphatic spread; Methylation detected in early cancer, as well as in premalignant lesions.	90; 91
p15	Cell cycle	Esophageal	Lost early in tumor development.	92
HMLH1	DNA repair	Esophageal	Increased microsatellite instability.	67
RIZ1	Chromatin-mediated gene expression	Nasopharyngeal	Methylation marker detectable in bodily fluids.	93
RAR-B	Retinoic acid signalling	Esophageal	Methylation detected in early cancer, as well as in premalignant lesions.	91
CHFR	Checkpoint control	Esophageal		94
Cullin 3	E3 ubiquitin ligase	HNSCC	RLGS methylation detected only in primary HNSCC	33

Figure 1.1: Restriction Landmark Genomic Scanning (RLGS) identifies global changes in DNA methylation. A. Genomic DNA, isolated from normal adjacent tissue, primary tumor tissue, and metastatic tumor tissue, are independently digested with methylation-sensitive enzymes, *NotI* or *AscI*. The DNA sequence recognized by *NotI* and *AscI* are GCGGCCGC and GGCGCGCC, respectively, and are located predominantly within CpG islands. In normal cells, where CpG islands are usually unmethylated, the DNA is digested, resulting in restriction enzyme overhangs. End labeling reactions, using radioactive guanine and cytosine result in a "spot" that migrates in the RLGS profile based on size. In the tumor, where certain CpG islands become aberrantly methylated, *NotI* and *AscI* enzymes are prevented from digesting at these sites, and the corresponding "spot" is absent in the profile. Comparison of patient sets allows for the global DNA methylation patterns to be distinguished in tumor and metastatic HNSCC. *(Abbreviations: D, dimension)* B. A *NotI* RLGS profile derived from normal adjacent tissue from a head and neck cancer patient. Each of the ~2000 fragments visible in the profile corresponds with a *NotI* site that was unmethylated in the original DNA sample. C. A section of the RLGS analysis of normal, primary and metastatic tumors from an individual patient, along with the corresponding Master Profile section, which identifies the unique RLGS address. The arrow distinguishes a *NotI* site that is unmethylated in the normal profile, completely methylated in the tumor profile (complete loss), and partially methylated in the metastatic profile (partial loss).

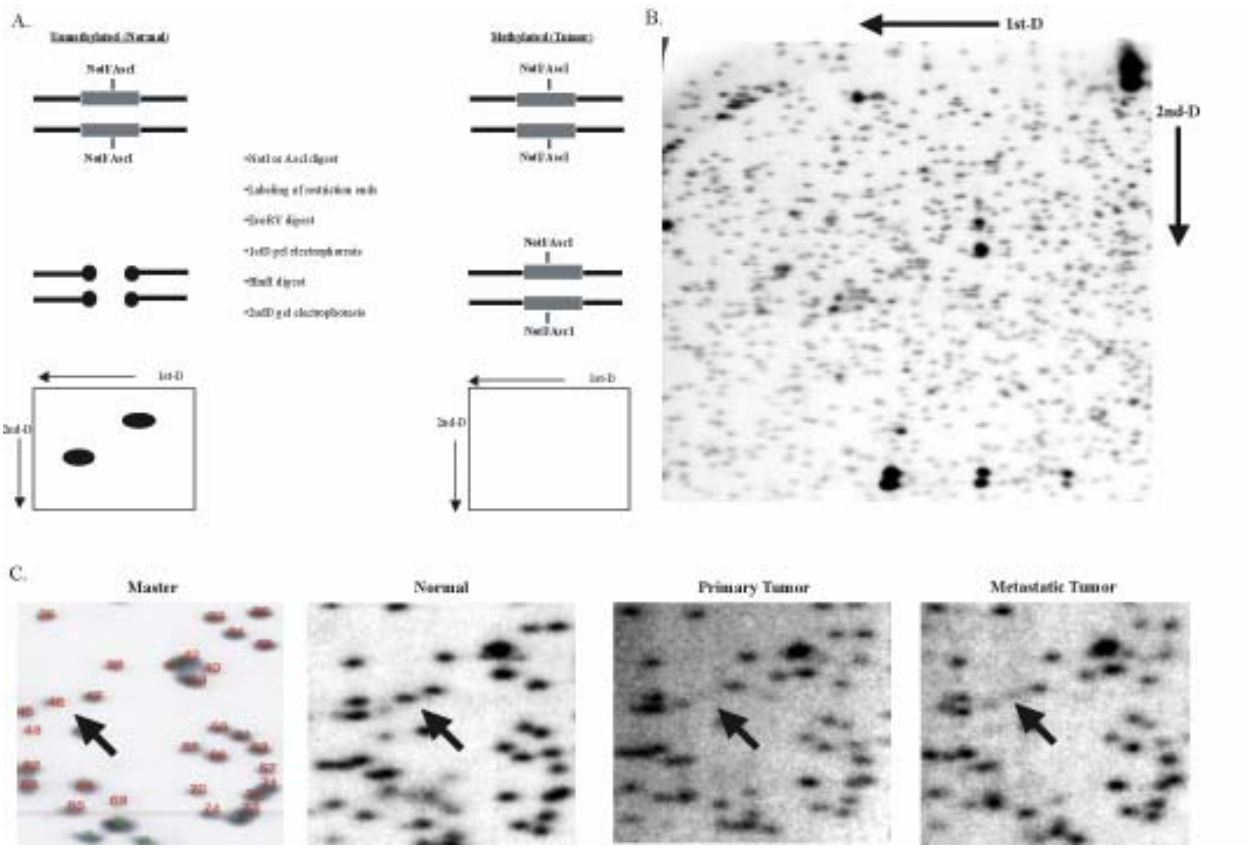
A.
Unmethylated (Normal)
Methylated (Tumor)
NotI/AscI
NotI/AscI
•NotI or AscI digest
•Labeling of restriction ends
•EcoRV digest
•1stD gel electrophoresis
•HinfI digest
•2ndD gel electrophoresis
1st-D
2nd-D
B.
1st-D
2nd-D
C.
Master
Normal
Primary Tumor
Metastatic Tumor

Figure 1.2: **Possible mechanisms to explain differential methylation patterns in RLGS profiles in HNSCC primary and metastatic tissues.** A. Squamous epithelium located in areas of the oral cavity, pharynx, larynx or trachea becomes exposed to carcinogens (indicated by the lightning bolts) that initiate epigenetic and genetic alterations. Because of the field cancerization effect, where all cells in the area are exposed to the same agents, multiple pockets of altered cells often exist in HNSCC, resulting in secondary primary tumors. Classically, it is believed that additional accumulation of abnormalities progresses the disease to primary carcinoma *in situ* (CIS) followed, ultimately, by metastatic disease to cervical lymph nodes (2). Because of the knowledge that pockets of altered cells exist throughout HNSCC, it is also possible that metastatic disease may arise from a different cell, with different epigenetic and genetic abnormalities (1). B. Head and neck squamous cell carcinomas progress through various stages of the disease by the accumulation of genetic alterations. DNA methylation, however, is believed to be a plastic alteration that changes based on gene expression patterns necessary at that time point. Therefore, in the metastatic disease, the levels of genetic alterations reach a higher level than in the preneoplastic and primary lesions, while DNA methylation patterns seen may vary.

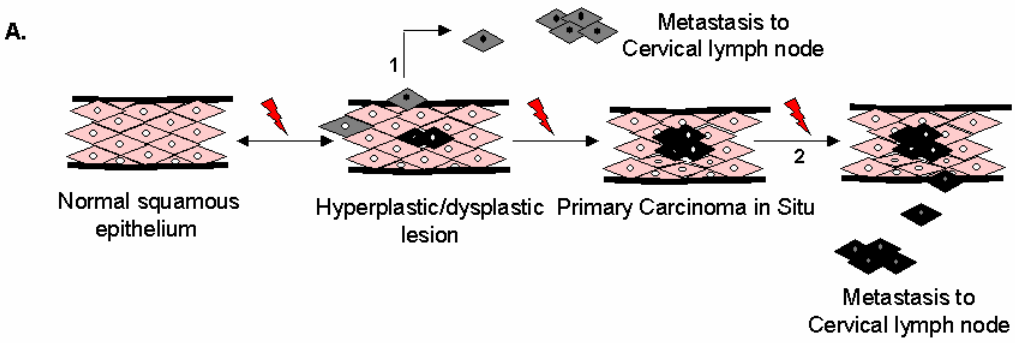
A.
Metastasis to
Cervical lymph node
1
2
Normal squamous
epithelium
Hyperplastic/dysplastic
lesion
Primary Carcinoma in Situ
Metastasis to
Cervical lymph node

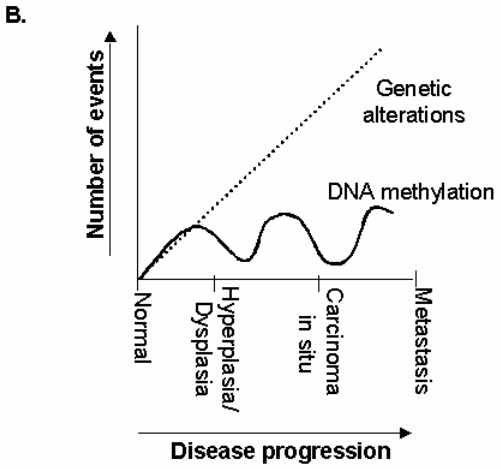
B.
Number of events
Genetic
alterations
DNA methylation
Normal
Hyperplasia/
Dysplasia
Carcinoma
in situ
Metastasis
Disease progression

CHAPTER 2:

ABERRANT DNA HYPERMETHYLATION WITHIN COMMON REGIONS OF LOH IN HNSCC AND NSCLC

2.1 Introduction

Cancer is a disease that arises from loss or untimely activation of genes in a multistep accumulation of alterations that create chaos in a normally highly regulated system[95; 96]. The search for novel tumor suppressor genes has motivated a large proportion of cancer research, providing a basic understanding for the disease process. Identification of genes somatically altered in cancer has largely been driven by Knudson's "two-hit" hypothesis of biallelic gene inactivation by mapping tumor suppressor genes within genetic regions of allelic loss followed by loss of the remaining allele via genetic mutation[97]. Comparative genomic hybridization (CGH) studies have been able to identify relatively large regions of the genome which become either over-represented or under-represented in tumors, indicating clonal expansion from a cell that possesses a selective advantage suggesting that the chromosomal irregularity is important in tumorigenesis. Higher resolution studies based on using markers with either

varying repeat lengths as determined by Southern blot analysis or PCR, restriction enzyme digestion methods, or BAC clones to map a genomic region allows for the measurement of allelic dosaging in tumor samples compared with normal tissue[98]. Differences in allelic dosaging between the two samples, where in the normal sample the paternal and maternal alleles appear to be repeats of different lengths that have lost this distinguishing characteristic in the tumor, indicates Loss of Heterozygosity (LOH) within the tumor genome[98]. LOH studies have largely defined minimally lost regions (MLR) that are used to pinpoint the position of a tumor suppressor gene[99]. It is widely accepted that aberrations occurring reproducibly at commonly lost regions serve as genetic maps, implicating the area in the genome as harboring one or more tumor-associated genes. Boundaries clearly demarking the regions, however, are difficult to define due to the use of various polymorphic markers applied in coordinating studies, making direct comparisons arduous across studies. Given that, it is interesting, however, to find recurrent losses within diverse tumor types, further supporting the importance of that region in clonal expansion.

Several regions of LOH have been identified across the tumor genomes, and as shown in chapter 1, these allelic imbalances often synchronize with specific stages in the disease progression. The goal for many of these studies is to define a shortest region of overlap (SRO) that is lost across tumor samples, minimizing the distance that must be examined to localize the tumor suppressor gene in the midst of many[99]. The loss of the remaining allele is necessary under

Knudson's definition of a true tumor suppressor gene[97]. Frequently, investigators undertake the laborious task of identifying candidate tumor suppressor genes through positional cloning and their accompanying inactivating mutations. If and when a mutation is found in the genomic sequence, functional analysis must be used to prove that the mutation renders the gene non-functional.

Over recent decades, an additional mechanism to inhibit gene function has been explored as a tool used in cancer. DNA methylation in the promoter region has been established as an alternative mechanism to heritably silence gene transcription[100]. An increasing amount of research has found that previously identified tumor suppressor genes that were found by genetic approaches are often silenced in cancer via DNA methylation. This evidence provides credence to the notion that DNA methylation is as important in cancer as mutation.

Based on the premise that retrospective analysis of known tumor suppressor genes are frequently methylated, our lab has established that novel tumor suppressor genes can be instead *prospectively* identified based on the genome-wide DNA methylation approach, Restriction Landmark Genomic Scanning (RLGS)[33; 101; 102; 103; 104; 105; 106; 107]. RLGS is based on digestion of gDNA with methylation-sensitive enzymes, *NotI* and *AscI*, which recognize GC rich sequences. These restriction sites are primarily localized within CpG islands associated with promoter regions of genes[75]. Unmethylated sites are cleaved while methylated cytosines in the restriction sites prevent enzymatic digestion. Half-sites that remain following digestion are radioactively end-labeled and

reproducibly migrate in the 2-dimension gels, appearing as RLGS fragments on the subsequent profiles, genome-wide. As a twist, these experiments aim towards identifying tumor suppressor genes from specific chromosomal locations that have not previously been identified through sequence altering mutations as "second hits".

For example, an important loss in multiple malignancies is chromosome 6q[108; 109; 110; 111]. Many researchers have identified loss of portions or the entire 6q arm in human malignancies by both CGH and LOH scanning techniques[20; 112; 113; 114; 115; 116; 117; 118; 119; 120; 121; 122; 123]. This region is frequently lost in tumors with metastatic disease, which is expounded upon in chapter 5. Analysis of cell lines derived from small cell and non-small cell lung cancer determined not only that 6q22-q23 loss occurred >50% of the time, but this region was lost more commonly in NSCLC than SCLC[121]. In fact, recent studies have provided a link with cancer predisposition with a human susceptibility locus along chromosome 6q23[124]. No candidate tumor suppressor genes have been confirmed from this region; however, studies based on DNA methylation have not, until now, been involved in the search. The purpose of this set of experiments was to identify genes that become aberrantly hypermethylated within the minimally deleted region along chromosome 6q23-q24 using RLGS as a way of identifying candidate tumor suppressor genes.

2.2 Materials and Methods

Tissue collection:

Frozen normal adjacent tissue, tumor tissues and metastatic lymph nodes from Head and Neck Squamous Cell Carcinoma as well as normal adjacent and tumor tissues from non-small cell lung cancer patients were obtained from the Ohio State University through the Cooperative Human Tissue Network. All sample collection was performed in accordance with NIH guidelines and performed under a protocol approved by The Ohio State University's Institutional Review Board. Histopathological evaluation was performed on all samples to confirm the predominance of neoplastic cells.

Identification of NotI and AscI clones:

Sequences spanning the regions of LOH were downloaded from the June 2002 BLAT resource webpage (http://genome.ucsc.edu). RLGS is based on enzymatic digestion using first methylation sensitive enzymes (*NotI* or *AscI*), followed by EcoRV digestion to limit the size of the DNA fragments in the first dimension. In order to separate the *NotI* and *AscI* sites farther, an enzyme which frequently digests, *Hinf*I, is then used prior to second dimension separation. Because of mandated size restrictions for separation in the two dimension gel electrophoresis, an *in silico* digestion of the DNA sequence from 6q23-q24 identified potential RLGS fragments and their corresponding first dimension

sequences (*NotI-NotI*, *NotI-EcoRV, AscI-AscI, or AscI-EcoRV*), as well as their second dimension sequences from the *NotI-HinfI* or *AscI-HinfI* fragments. Due to size separation constraints, *NotI-EcoRV* or *AscI-EcoRV* fragments greater than 700 bp and less than 5000 bp as well as containing a *NotI-HinfI* or *AscI-HinfI* fragment size greater than 120 bp were used for our analysis. Based on RLGS fragments that have previously been cloned in our lab, and their migration patterns within an RLGS gel are reproducible, we were able to use these known sequences, with their defined first and second dimesions, as "anchor-points" for virtual migration in RLGS. From these data points, the equation *-LN (size in base pairs/7340.3)/0.058* was used to determine the migration of fragments in RLGS in the first dimension, and *-LN (size in base pairs/1411.5)/0.0835* for the second dimension migrations. Using these equations, 1st and 2nd dimension coordinates for *NotI* and *AscI* fragments from 6q23-q24 were then calculated. Predicted migrations were then plotted using Microsoft Excel to determine which quadrant the fragments should lie in the RLGS profiles.

Isolation of Bacterial Artificial Chromosome (BAC) DNA's:

Bacterial artificial chromosome (BAC) stabs were ordered through the BACPAC Resource Center at Children's Hospital Oakland Research Institute in Oakland, California, from the RPCI-11 human BAC library. Vector pBACe3.6 contains a chloramphenicol resistance domain, which allowed for the selection of isolated clones from a streak-out plate containing 20ug/ml chloramphenicol.

Maxi preps (Qiagen) were performed on 250ml cultures according to standard protocols. BAC clones were confirmed by end-sequencing the plasmid using the Sp6 primer (5').

Restriction Trapper RLGS:

In order to isolate uncontaminated RLGS clones, free of background *EcoRV* fragments, purified *NotI-EcoRV* fragments were isolated using a *NotI* restriction trapper. Normal genomic DNA was fractionated by *NotI* and *EcoRV* digestion and passed over latex beads that were conjugated to *NotI* half sites. The cohesive ends of the fragmented genomic DNA and the latex beads allows for background *EcoRV* fragments to be washed free, leaving behind *NotI-EcoRV* fragments that were then eluted from the beads through a series of washes. This purified population was then used for RLGS as described above. Specific RLGS fragments can be isolated from the dried acrylamide gel, and used as the template in a PCR reaction.

RLGS fragment identification:

We used a previously published strategy to amplify the RLGS fragment directly from DNA eluted from RLGS gels with slight modifications. Briefly, candidate fragments from the predicted RLGS region were excised from the dried restriction trapper RLGS gels. DNA was eluted overnight in a 37^{o}C incubator/shaker in 150ul of elution buffer (0.5M ammonium acetate, pH 8; 1mM

EDTA). The supernatant containing the DNA was isolated by centrifugation at 14,000 rpm for 10 minutes to pellet the remaining debris from the original gel excision. Two micrograms of glycogen was added to the supernatant, followed by 2.5 volumes of cold 100% ethanol. The mixture was precipitated at -80^{o}C overnight. The precipitate was pelleted by centrifugation at 14,000 rpm for 25 minutes. A 70% ethanol wash was used to remove impurities, followed by a 10-minute centrifugation at 14,000 rpm. Isolated DNA pellets were partially dried in a 30^{o}C speedvac, and resuspended in 10ul of TE buffer.

Restriction Landmark Genomic Scanning:

Restriction Landmark Genomic Scanning (RLGS) was performed on normal adjacent (NAT) and primary HNSCC and NSCLC tissue samples. DNA's were digested with 20U of the methylation-sensitive, rare-cutting enzyme, *NotI* or *AscI* at 37^{o}C for 2 hours. GC restriction overhangs remaining following enzymatic digestion were filled in using Sequenase 2.0 (USB) with (^{32}P) dGTP and (^{32}P) dCTP (Amersham) for 30 minutes at 37^{o}C. Labeled DNA fragments were further digested with 20U of *EcoRV* (Promega) at 37^{o}C for 2 hours. Labeled DNA's were then separated overnight on a 0.8% agarose gel in the first dimension. Following equilibration, the first dimension gels containing separated DNA were digested in 700U of *HinfI* (Promega) at 37^{o}C for 2 hours. The agarose gels were inverted horizontally and sealed to the second dimension 5% non-denaturing polyacrylamide gel using agarose. The second dimension gels were

separated overnight at room temperature. Acrylamide gels were then dried on Whatman paper and exposed to film for 7-10 days.

RLGS BAC mixing gels

RLGS was performed as described previously with slight modifications in the initial input DNA. In brief, 3ug of genomic DNA, 50ng of BAC DNA and 5ng of clone DNA were digested with 20U of *NotI* or *AscI* (Promega) at 37^{o}C for 2 hours. Five hundred picograms of radiolabeled BAC DNAs and 250pg of radiolabeled clone DNAs were mixed with the labeled genomic DNA, and were separated in the first dimension on a 0.8% agarose gel overnight. Enhanced fragments corresponding to the *NotI* or *AscI* site from 6q23-q24 were assigned unique addresses from the Master profile.

RLGS patient analysis:

RLGS profiles from our collection of HNSCC and NSCLC were analyzed for the methylation differences between a patient's normal and tumor profiles for the loci identified within our region of LOH. Methylation was classified by either a partial or complete loss of RLGS spot intensity. The overall percentage of RLGS fragment methylation was scored by taking the (number of patients with the spot loss /the total number of patient samples analyzed) x 100.

2.3 Results

Localization of *AscI* and *NotI* RLGS fragments within chromosomal region 6q23-q24.

In order to investigate our hypothesis that aberrant promoter methylation may help pinpoint the location of a candidate tumor suppressor in regions of LOH, we chose a chromosomal region for which frequent LOH has been described not only in HNSCC and NSCLC, but also in other tumor types, but for which no tumor suppressor has been definitively identified[125]. The 9.6Mb region of LOH from 6q23-q24 has been described in >20% of HNSCC and ~50% of NSCLC, while complete loss of the long arm of chromosome 6 is even more common (Figure 2.1).

The complete 6q23-q24 sequence was obtained from the June 2002 BLAT database. *In silico* digestion using methylation-sensitive landmark restriction enzymes combinations utilized in RLGS (*NotI-EcoRV-HinfI* or *AscI-EcoRV-HinfI*) identified sequences potentially migrating in RLGS gels, which reproducibly separate fragments based on size (Figure 2.2A). The RLGS first dimension gels separate *NotI-EcoR*V or *AscI-EcoR*V fragments of 700-5000bp, while the second dimension of RLGS separates *NotI-Hinf*I or *AscI-Hinf*I fragments >120bp.

We selected bacterial artificial chromosomes (BACs) that contain *NotI* or *AscI* restriction fragments that met these size requirements for resolution via

RLGS along 6q23-q24. This region contains 49 genes or ESTs that may potentially be important for the phenotype of LOH observed. Based on our size restrictions, we identified 10 BAC clones located within the region of LOH from 6q that are used as "markers" to scan the region for patterns of methylation. First and second migration patterns were determined in centimeters for each of the fragments based on separation in the first and second dimension gels in the actual RLGS procedure, and *in silico* migration patterns were predicted (Figure 2.3A). This virtual migration aided in determining which quadrant an enhancement should be predicted and how to cluster the BAC clones for separation on RLGS. DNA isolated from the BAC clones was added into RLGS BAC mixing gels to identify the corresponding *NotI* or *AscI* fragments in the resultant RLGS profiles (Figure 2.3B). Individual clones are assigned a unique address from the universal master RLGS profile and are listed in Table 2.1. Using this approach, it was possible to identify the complete set of 10 size-matched *NotI* and *AscI* sites, representing 37% of these restriction sites residing within this chromosome 6 region (Figure 2.4A).

RLGS analysis of patient profiles

Together, *NotI* and *AscI* RLGS profiles from both normal and tumor tissues were compared to determine the frequency of methylation along this chromosomal region. The methylation status in each of the sequences from 15 HNSCC and 24 NSCLC paired normal and tumor RLGS profiles were scored for

methylation. Methylated restriction sites are represented by a partial or complete RLGS fragment loss, while no change in RLGS fragment intensity indicates that the status of the landmark enzyme site is maintained between normal and tumor tissues. Methylation frequencies varied from sample to sample, and appear to have a mosaic methylation pattern along the chromosomal fragment (Table 2.2). Methylation assessed by RLGS along this 6q region ranged from 0-86% in NSCLC samples (n=24 pairs) and 0-67% in HNSCC (n=15 pairs) (Figure 2.4B). Hypermethylation events occurred frequently at the same RLGS loci, indicating that these sequences may be "hot spots" for aberrant DNA methylation, or that epigenetic targeting of the gene residing at the corresponding RLGS locus confers a survival advantage for the tumor, serving as a foundation for clonal expansion. This methylation "hot spot" was then used as a marker to seek out genes within 5Kbp of the restriction site for their potential involvement in tumorigenesis.

Identification of a commonly methylated sequence, TCF21

BAC clone RP11-465P13, containing *AscI* fragment 6E12, was lost in 86% of NSCLC (n=19/22), 100% (n=4/4) of NSCLC cell lines, and 67% (n=10/15) of HNSCC patient profiles (Figure2.4B), making it the single most frequent methylation event identified in this sample set. BLAT search of the *AscI-EcoRV* sequence revealed that a6E12 corresponds with a CpG island within the 5' region of TCF21 (transcription control factor 21; Accession Number AF047419).

The position of the *AscI* site is within a CpG island that spans exon 1 and extends into the first intron from base pair +193 after the transcriptional start site to 493 base pairs into intron 1 (Figure 2.5). The promoter region was predicted using the FirstEF program (http://rulai.cshl.org/tools/FirstEF/), and overlaps this CpG island from –121 to +449 base pairs into exon 1 relative to the transcription start site.

2.4 Discussion

The quest for identifying tumor suppressor genes has historically focused on genetic mutations that alter the DNA sequence in a way that the gene is no longer able to perform its normal cellular function. However, only a few of the identified tumor suppressor genes have exhibited somatic mutations within the regions of LOH[126]. In recent years, the unveiling of DNA methylation as an additional and prominent tool provides the cancer cell with an alternative mechanism for transcriptional silencing of select genes. Although recognized, examination of DNA methylation has not been prospectively applied within regions of LOH to identify tumor suppressor genes, and as a result, searches for such genes have been unsuccessful. However, retrospective examination of hypermethylated genes found that they often reside within regions of LOH[70]. For example, p16, a gene that regulates cell cycle progression, resides within a region of LOH on 9q, but the "second-hit" is more often promoter methylation than mutation in many cancers[127]. Methylation studies based on RLGS have also

determined that targets of methylation occur in a non-random fashion, possibly indicating a targeting mechanism[74; 128]. In addition, RLGS is a vital tool that has been applied to simultaneously identify methylation for as many as 1300 *NotI* and *AscI* sites each, with only a 4% overlap in CpG islands containing both *NotI* and *AscI*[75]. This allows for as many as 2200 unique sites to be assessed for methylation genome-wide.

Loss of heterozygosity along chromosome 6q23-q24 has been reported in human cancers, but the localization of the tumor suppressor gene within the region has not been described through genetic or epigenetic investigation. A slight modifications of the RLGS tool changed the focus of methylation from a genome-wide scan and instead provided methylation analysis of 10 landmark sites a specific region of LOH. These data thus translate into a methylation map that provides information regarding genes within the region from a single combination of restriction enzyme digestion within a DNA sample from individual patients. This provides a more comprehensive look into the epigenetic modifications within a specific chromosomal region, whereas the hunt for somatic mutations is largely done gene by gene.

We found that CpG island methylation along the chromosome 6q23-q24 segment was not uniformly distributed. This implies that there may be sequence specificity by the methyltransferases and that DNA methylation occurs at specific loci, while adjacent DNA remains unmethylated, or that methylation at certain loci creates a growth advantage, thus promoting clonal outgrowth of cells containing

that methylation signature. By combining chromosomal regions known to be frequently altered genetically in cancer with RLGS, we have successfully identified a gene that is hypermethylated in the majority of HNSCC and NSCLC examined. In fact, our results demonstrate TCF21 promoter hypermethylation occurs at greater rates than reported LOH for the region. It is possible that other genes also localized within this region could possess tumor suppressor function, and their epigenetic inactivation is not included based on size restrictions of the assay, or that they harbor somatic mutations, also not assessed by RLGS. However, this assay allows for direct correlations to be made with TCF21, providing a novel gene target for cancer-specific methylation. Recurrent hypermethylation of TCF21 in not only the bulk of the tumor itself, but also across tumor tissues of different anatomical locations and patients, supports our hypothesis that TCF21 is frequently targeted by hypermethylation in cancer. Based on its tumor-specific methylation, we propose that TCF21 is a tumor suppressor gene in NSCLC and HNSCC.

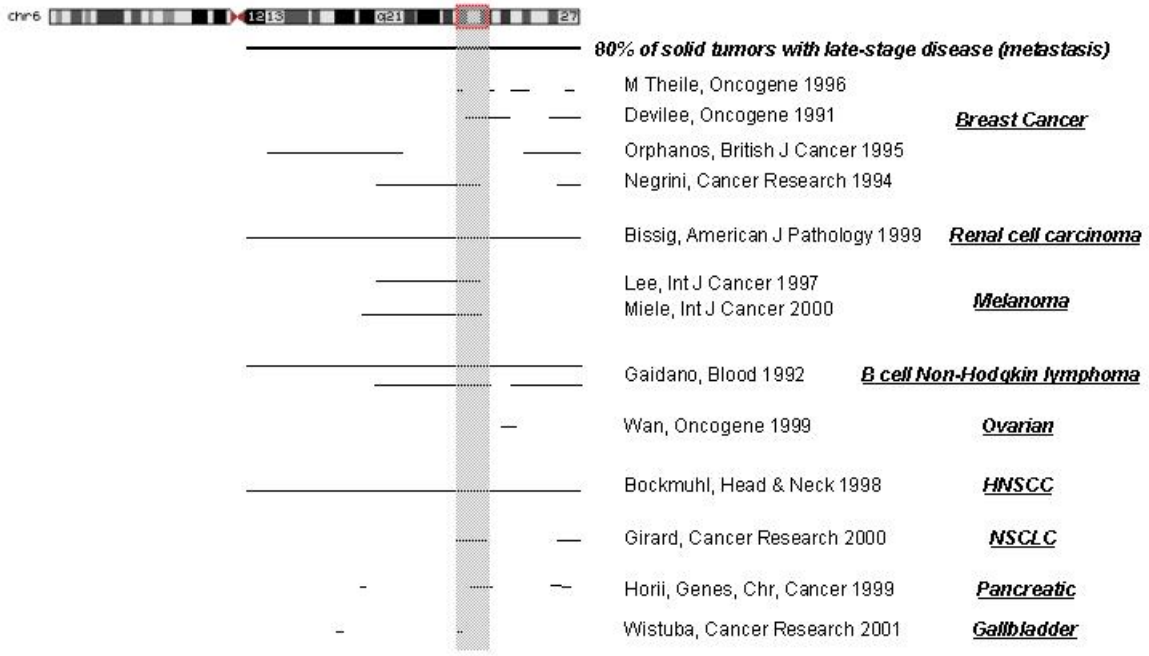

Figure 2.1: Loss of heterozygosity along chromosome 6q in cancer. Literature review of LOH along chromosome 6q determined that a crucial region commonly lost in cancers resides along 6q23-q24 as displayed in the gray vertical area, demarked by D6S262-D6S308. This 9.6 megabase pair region was used for determination of aberrant hypermethylation by RLGS.

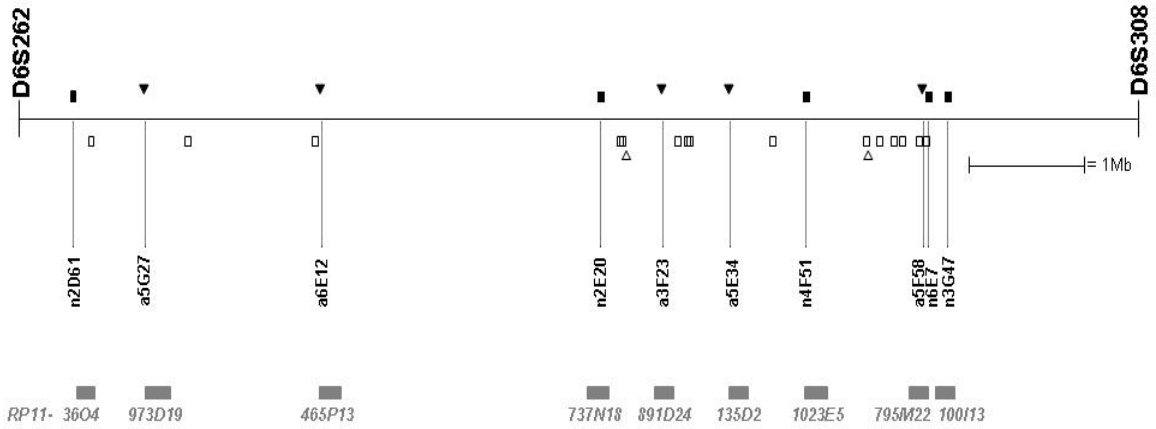

Figure 2.2: Location of *NotI* and *AscI* sites within 6q23-q24 region.

In silico digestion of the DNA obtained from the June 2002 freeze of the Human BLAT sequence from 6q23-q24 resulted in the identification of 5 *NotI* (■) and 5 *AscI* (▼) sites that will migrate on an RLGS profile based on size. Other *NotI* (n=15) and *AscI* (n=2) sites (□ and ∆, respectively) are either too large or small for separation via RLGS. The bacterial artificial chromosomes that contain the RLGS fragments are denoted with "RP11".

RLGS address	Chromosomal Location	BAC (RP11-)	Gene	Accession Number
N2D61	6q23.2	36O4	ENPP1	D12485
A5G27	6q23.2	973D19		BC018756
A6E12	6q23.2	465P13	TCF21	AF047419
N2E20	6q23.3	737N18	MAP7	BC025777
A3F23	6q23.3	891D24	ENST00000275206	
A5E34	6q23.3	135D2		
N4F51	6q23.3	1023E5		
A5F58	6q24.1	795M22	LOC51696	AB033492
N6E7	6q24.1	795M22	LOC51696	AB033492
N3G47	6q24.1	100I13	CITED2	BC004377

Table 2.1: RLGS fragments from 6q23-q24.1 (D6S262-D6S308)

A.

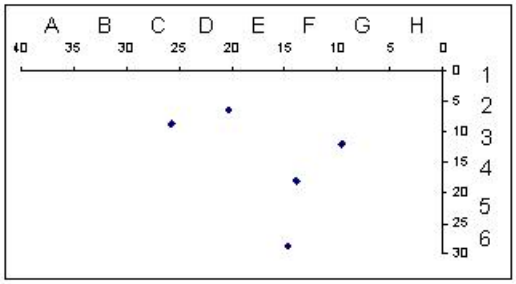

NotI (RP11-)	1D(bp)	2D (bp)	1D(cm)	2D (cm)
795M22	3116	129	14.773	28.654
36O4	1650	682	25.735	8.711
737N18	2253	827	20.364	6.4024
100I13	4211	516	9.5807	12.052
1023 E 5	3269	313	13.946	18.038

B.

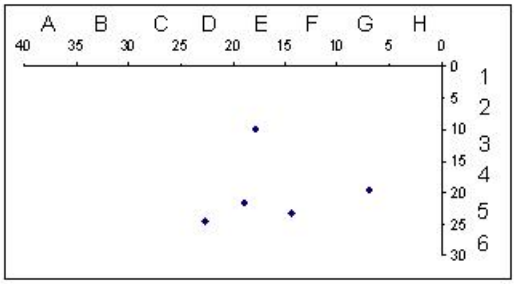

AscI (RP11-)	1D(bp)	2D (bp)	1D(cm)	2D (cm)
891D24	2621	613	17.756	9.9885
135D2	2449	232	18.926	21.625
795M22	3189	202	14.374	23.283
973D19	4905	276	6.9504	19.545
465P13	1973	182	22.652	24.532

C.

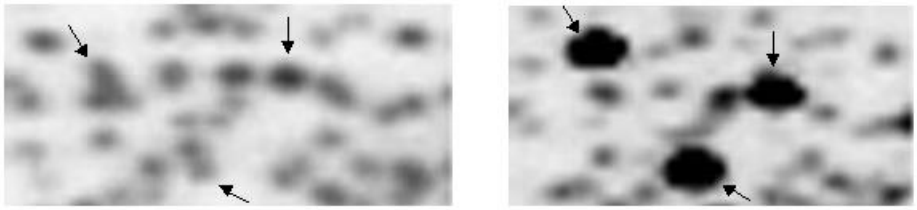

Figure 2.3: **RLGS BAC mixing gel.**

A. In silico digestion of BAC DNA using the landmark enzymes identified 5 *NotI* (A.) and 5 *AscI* (B.) clones that will migrate within an RLGS profile. Virtual RLGS patterns were determined and plotted in Microsoft Excel. C. *NotI* BAC mixing gel (right) results in increased intensity of RLGS fragments in the RLGS profile compared with the intensity of diploid fragments from normal tissue (left). Arrows indicate the fragments from the normal profile that match the DNA from the bacterial artificial chromosomes that was added in excess to identify clones from chromosome 6q.

Table 2.2: **Methylation profiling along 6q23-q24 by RLGS.**

RLGS fragment addresses (n=*NotI*, and a=*AscI*) from 6q23-q24 are depicted in columns. Analyses of tumor profiles from NSCLC and HNSCC patients are displayed in rows. Black boxes indicate a complete loss of the RLGS fragment, gray boxes indicate a partial fragment loss, and white boxes indicate no difference in fragment intensity between normal and tumor profiles. "*N/A"* denotes those RLGS fragments within the profile that were not analyzable due to the location or quality of the gel.

RLGS / Patient	n2D61	a5G27	a6E12	n2E20	a3F23	a5E34	n4F51	a5F58	n6E7	n3G47
NSCLC										
2										
3										
7										
10										
11										
13										
14										
17										
18										
2001							N/A			
2003									NA	
2768		N/A							N/A	
2802									N/A	N/A
2812									N/A	N/A
2906									N/A	
2661									N/A	
2666							N/A			
2764										
2766										
2810										
2908										
2911			N/A							
2913	N/A	N/A								
2916			N/A	N/A		N/A				
HNSCC										
11										
8										
7										
82										
49										
46										
48										
1336										
1344										
1374										
1381										
1390		N/A								
1628										
1650										
1653										

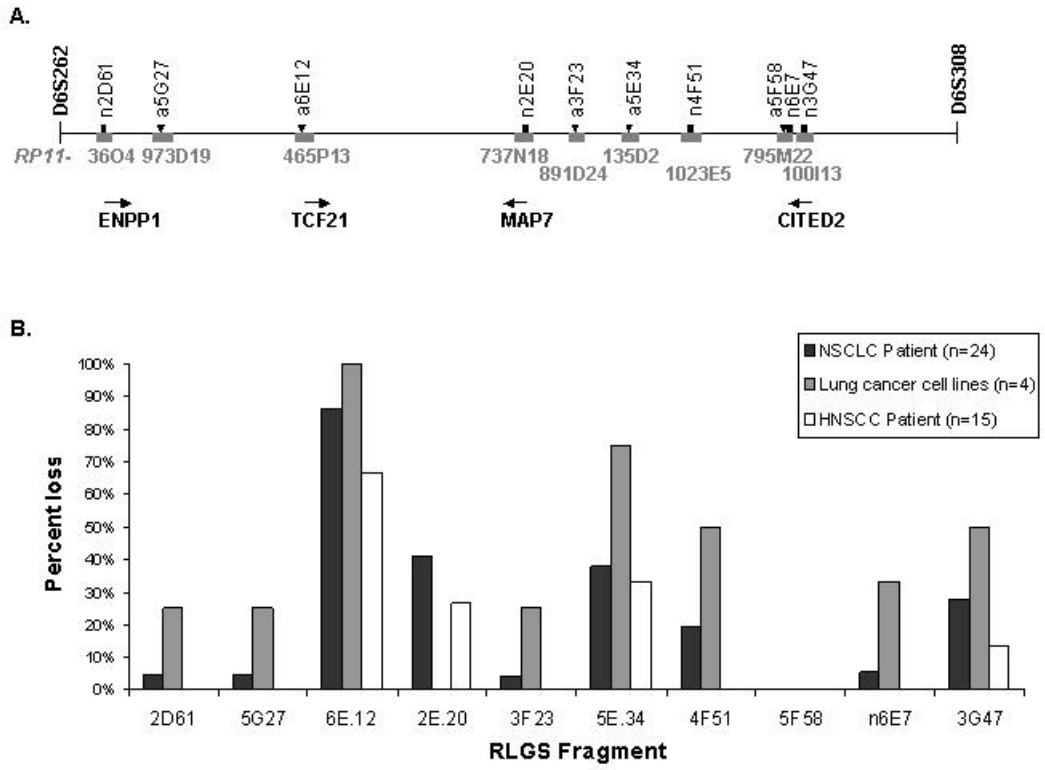

Figure 2.4: **Summary of RLGS fragments identified along 6q23-q24, and the frequency of methylation.**

A. RLGS fragments are denoted a RLGS master address, with "n" or "a" for *NotI* and *AscI*, respectively, along with a quadrant number on the top of the line. Corresponding known genes and their transcriptional orientations are denoted below the BAC clones. B. Summary of methylation percentages for each clone is denoted for NSCLC (black bars), Lung cancer cell lines (gray bars) and HNSCC (white bars).

Figure 2.5: Genomic structure of TCF21.

TCF21 contains a CpG island beginning 193 base pairs 3' of the transcriptional start site in exon 1, reaching 493 base pairs into intron 1, containing the *AscI* (A) site responsible for the RLGS landmark, a6E12. The predicted promoter region begins 121 bases upstream of the transcription start site and continues into the coding region.

CHAPTER 3:

TCF21 HYPERMETHYLATION IN CANCER CONFERS GENE SILENCING

3.1 Introduction

In chapter two, we describe the identification of TCF21 as a gene that becomes frequently hypermethylated in HNSCC and NSCLC. The location of TCF21 within a region of loss of heterozygosity and its tumor-specific methylation lends credence that it is a candidate tumor suppressor gene. Epigenetic addition of side groups to histones or cytosine in the context of cytosine 5' to guanine (CpG dinucleotides) have been shown to alter transcription without causing changes in the DNA sequence[100; 129]. The covalent addition of a methyl group from the donor, S-adenosylmethionine, to cytosine via DNA methyltransferases (DNMT1, 3a, and 3b, predominantly) results in gene silencing[100]. The addition of the methyl-group to cytosine along the DNA helix has been suggested to cause a protrusion that inhibits vital transcription factors from binding to the promoter, preventing transactivation of the corresponding gene[100; 129]. Additional mechanisms involving methyl-binding proteins that recognize the modified cytosine bind, then recruit histone deacetylase and co-repressor complexes that convert the area into compact chromatin, also creating a silent-state[100; 129].

In normal tissue, DNA methylation is limited to imprinting centers, repetitive elements, and the inactive X chromosome in female cells in part because of the spontaneous deamination of methyl-cytosine into thymine, creating point mutations[130; 131]. Tissue-specific DNA methylation of CpG islands has also been shown to occur in normal cells. Also, during aging, the process of DNA hypermethylation has also been noted at certain loci, possibly providing a correlation with increased cancer incidence with age. In cancer, hypermethylation occurs in select CpG islands that are associated with about 60% of our genes. CpG islands were first identified as *Hpa*II tiny fragments (HTF) that were found to be largely unmethylated stretches of GC-rich sequences [129]. Largely unmethylated in normal tissues, except for tissue specific methylation, CpG island methylation (CIM) is readily recognized as a mechanism frequently applied to silence genes in cancer.

Although useful as an indicator for methylation, the extent of methylation as determined by RLGS is limited to the two CpG's in the methylation-sensitive restriction sites, *NotI* or *AscI*, and does not determine the overall amount of methylation within the rest of the CpG island. The purpose of these experiments is to provide a higher resolution map of methylation-sensitive sites in order to validate that TCF21 hypermethylation extends along the CpG island into the promoter region and results in transcriptional silencing.

3.2 Materials and Methods

Bisulfite sequencing:

DNA samples from HNSCC patients and cell lines, and NSCLC patients and cell lines were modified with sodium bisulfite treatment. Two micrograms of genomic DNA from patient samples were sheared into smaller fragments by repeated rounds of freeze/thaw in a dry ice:ethanol container. In order to allow for more efficient disassociation of the DNA strands, the samples were incubated in the presence of freshly prepared 3M NaOH at 37^{o}C for 20 minutes. Denatured samples were incubated at 60^{o}C overnight with sodium bisulfite and hydroquinone in the dark. Bisulfite modified samples were purified using the Gel Extraction Kit from Qiagen, and eluted in 50ul. The reactions were desulfonated using fresh 3M NaOH at 37^{o}C. The Gel Extraction Kit was used for the final purification, eluting in 30ul, and the samples were stored at –20^{o}C. Two microliters of the DNA was used for PCR reactions following bisulfite conversion. TCF21 bisulfite sequencing primers were designed to span the 5' end of the CpG island present in the 5' region. Bis1 primers (forward 5' AGGTGGAGATGTTGGAATGTG and reverse 5' AAAAACACCCAAAACAAAATAATC) amplify a 292bp product. Bis2 primers (forward 5' AAGATTATTTTGTTTTGGGTGTTTTT and reverse 5' cacacccccactcccaac) amplify a 239bp product. Bis3 primers (forward 5' gttgggagtgggggtgtg and reverse 5' tcctctataccaactcaacacactt) amplify a 204bp product. The PCR products are checked on an 8% polyacrylamide gel and

purified using the Qiagen Gel Extraction Kit. Purified PCR products were cloned into the TOPO-TA (Invitrogen) vector using the manufacturer's standard protocol. Approximately 5-10 clones were sequenced from each sample. Complete conversion through the bisulfite reaction was confirmed by the presence of thymine where cytosine was not 5' to guanine in the original sequence. For each of the individual CpG dinucleotides, the overall methylation was scored as a percentage of (#C/(#T+#C)) x 100%.

Combined Bisulfite Restriction Analysis (CoBRA)

Sheared peripheral blood lymphocytes (PBL) DNA isolated from non-cancerous individuals was treated with 20U *SssI* methyltransferase in the presence of the methyl donor, SAM, for 4 hours at 37 ^{o}C to obtain 100% methylated standard DNA. The DNA was purified using phenol: chloroform isolation and eluted in 100ul of water. Optical densities were determined at 260nm, and concentrations were determined by the equation: OD_{260nm} ***50** * *Dilution factor=ng/ul*. *In* vitro methylated DNA and unmodified PBL from the same individual, representing 0% methylated DNA, were mixed in ratios to create 0%, 15%, 30%, 45%, 60%, 75%, and 90% methylated molecules. Two micrograms of these methylation standards and patient DNA's were bisulfite treated overnight as described. Bisulfite DNA's from both *Sss*I in vitro methylated standards and patient samples were amplified using the TCF21 bis1 primers. The bis1 PCR fragments were purified by the Qiagen Gel Extraction Kit using the following

protocol modifications: A five-minute spin following the addition of QG buffer and PE buffer were used to remove residual salt and ethanol from the membrane. The samples were ultimately eluted in 30ul. Fifteen microliters of the samples were digested in a total volume of 30ul containing 5U of *BstU*I (NEB), 1X BSA, and 1X buffer 2 at 60^{o}C for 3 hours. Fifteen microliters of each digest were then separated on an 8% polyacrylamide gel, stained with ethidium bromide, and visualized. The bis1 product contains 3 potentially methylated *BstU*I restriction sites (CGCG). Complete conversion of unmethylated cytosine to thymine abolishes the *BstU*I sites, leaving the entire PCR product intact. Tumor samples were scored as methylated upon comparison to the matching normal adjacent tissue. Specifically, methylation was determined using the following criteria as compared to the matched normal: tumors having bands corresponding to the expected 118bp, 98bp and 73bp methylated fragment, or the 216/218bp and 173bp partially methylated fragment, and/or displayed an increased banding intensity relative to the amount of product loaded on the gel.

In vitro treatment of HNSCC and NSCLC cell lines using 5-aza-2'deoxycytidine

A549, a NSCLC cell line, was plated in 10cm^2 culture dishes in triplicate. Cell cultures were treated with 1-5uM 5-aza-2'deoxycytidine for 48 hours. Media-containing drug was replaced every 24 hours to avoid drug hydrolysis and inactivation. Control plates were treated with equal amounts of dimethyl

sulfoxide, DMSO. After 48 hours of drug treatment, the cells were grown in regular culture media (10% fetal bovine serum (FBS), plus penicillin and streptomycin) for an additional 24 hours to allow transcription to occur.

RNA and DNA were isolated using Trizol reagent (Invitrogen) following the manufacturer's protocols. cDNA was synthesized using 1ug of total RNA as template by the Superscript first strand synthesis kit (Invitrogen) according to manufacturer's suggestions. Oligo dT primed and random hexamer primed cDNA's were added together for each sample following synthesis.

Semi-quantitative RT-PCR reactions using SYBR green were carried out using the IQ SYBR green Supermix (BioRad) using the icycler (BioRad). 25ul reactions containing the cDNA template and 12.5ul (2X) Master Mix, 10pmol TCF21-RT –F (5' AGCTACATCGCCCACTTGAG), 10pmol TCF21-RT-R (5' CGGTCACCACTTCTTTCAGG), and ddH_20, were amplified using the following reaction conditions: 95^{o}C (3 minutes); (40x) 95^{o}C (20s), 58^{o}C(20s), 72^{o}C(20s); a melt curve of (40x) 55-95^{o}C (increasing 0.5^{o}C increments, 10 seconds each); 72^{o}C (5 minutes); 4^{o}C hold. SYBR green fluorescence was monitored in real-time, and pipetting accuracy and cDNA amounts were measured by GAPDH amplification under the same reaction conditions using GAPDH-F (5'TGGAAGGACTCATGACCACA) and GAPDH-R (5'TTACTCCTTGGAGGCCATGT). Normalization of individual samples was calculated by threshold cycle (TCF21)-threshold cycle (GAPDH). 5azadc treated cell lines were compared to untreated cell lines by taking the normalized

threshold (untreated)- normalized threshold (treated). This difference is then used as the exponential power to determine the relative expression (2^n), where "n" equals the difference between untreated and treated samples. Expression of TCF21 in the untreated samples is given the value 1.

Construction of the TCF21 promoter luciferase constructs in pGL3:

The TCF21 sequence from 1,320 base pairs upstream of the transcription start site through 688 base pairs into exon 1 was PCR amplified using primers tagged with *Kpn*I and *Xho*I restriction sites (forward primer 5' ggtacccataggggaaagcaaacaa and reverse primer 5'ctcgagCCCGTTCTCGTATTTGTCGT).

The underlined portion of the primer sequences corresponds with the *Kpn*I and *Xho*I sequences, respectively. To ensure that these restriction sites would be properly cleaved from the ends of the product, the entact PCR products, containing a taq polymerase "A" overhang, were ligated to the TOPO-TA vector (Invitrogen) and was named TOPO- tcf21.

The RNA-tcf21 construct was designed by insertion of a *EcoR*V-*NotI*-*AscI* linker into the multiple cloning site of pGL3 using *Xho*I and *Hind*III cohesive ends. Once the linker was inserted, the plasmid clone from our RLGS bacterial library was directionally ligated into pGL3 using the *Eco*RV-*AscI* restriction sites.

Other deletion constructs along the upstream portion of TCF21 were derived from the TOPO-tcf21 plasmid. The tcf21-Δ*bgl*II construct was made by

digestion of the pGL3-tcf21 plasmid with *Bgl*II. The tcf21-ΔRV-SmaI construct was created by digestion of the pGL3-tcf21 plasmid with *EcoR*V and *Sma*I. Because *EcoR*V and *Sma*I cleave DNA sequences leaving no half-sites, the 5' and 3' ends can be directly ligated to one another, abolishing both restriction sites for future use. The tcf21-ΔsmaI construct was created by digestion with *Sma*I alone. The pGL3 plasmid contains a *Sma*I site upstream of the multiple cloning site, and an internal *Sma*I site within the tcf21 sequence allows for the removal of the sequence between. The tcf21-ΔsacI construct was created similar to the tcf21-ΔsmaI construct, instead by digestion using *SacI.* These plasmids containing the portions of the 5' region of TCF21 were extracted from a 1% agarose gel and directly ligated overnight at 16^{o}C, and assayed as described above.

Five micrograms of pGL3, TOPO-tcf21, and TOPO-predicted promoter plasmids were digested with 15 units of *Kpn*I and 20 units of *Xho*I at 37^{o}C for 2 hours. Digestions were separated on a 1% agarose gel containing ethidium bromide for visualization. Digested DNA from the TCF21 inserts and the pGL3 vector were extracted from the gel and isolated according to the Qiagen Gel Extraction kit. For each ligation, 50ng of pGL3 vector and 20-30ng of insert DNA was incubated in the presence of buffer and 0.5 units of T4 DNA ligase (Invitrogen) in a 16^{o}C water bath overnight. One fifth of the ligations were transformed into chemically competent TOP10 cells (Invitrogen) and plated on LB/ampicillin plates overnight at 37^{o}C.

To determine if a resultant colony has the correct insert, universal primers against the pGL3 vector background were designed. The forward primer sequence is 5' AGTGCAGGTGCCAGAACATT and the reverse is 5'GCCTTATGCAGTTGCTCTCC. PCR reactions were set up in the presence of 10pmol of each primer, 1X PCR buffer, 1unit of platinum taq polymerase (Invitrogen), 0.2mM dNTP's, 1.5mM $MgCl_2$, and DNA in the form of bacterial colonies. The PCR conditions were 95°C for 10 minutes, and 35 cycles of denaturing at 95°C for 30 seconds, annealing of the primers at 60°C for 30 seconds, and extension at 72°C for 30 seconds. A final extension of 72°C for 10 minutes and a 4°C hold completes the amplification. PCR products were then visualized on an 8% polyacrylamide gel and visualized by ethidium bromide staining. If a colony resulted that had self-ligated pGL3 without insert, the PCR product was 205 base pairs. Colonies with inserts were the expectant size of the insert plus 205 base pairs.

Methylated TCF21 promoter luciferase constructs:

Twenty micrograms of the pGL3-tcf21 construct were digested with 40 units of *Xho*I (NEB) in the presence of BSA in buffer 2, in a final volume of 40ul at 37°C for 2 hours. Twenty units of *KpnI* was then added in NEB buffer 1, the volume adjusted to 50ul, and returned to 37°C for an additional hour. Digested plasmids were separated on a 1% agarose gel, and the pGL3 vector and "tcf21" insert were extracted from the gel separately and purified using the Qiagen Gel

Extraction kit. Insert DNA was eluted in 50ul of buffer elution buffer and separated into two fractions, while the pGL3 vector remained free of additional modifications. In a final volume of 300ul, 20ul of insert only was incubated for 2 hours at 37^{o}C with methyl-donor, SAM, and plus/minus *SssI* (30 Units). Methylated and unmethylated insert DNA were treated identically to account for experimental artifacts; however the fraction that is unmethylated was incubated in the presence of SAM without *Sss*I methyltransferase. Immediately following this incubation, the DNA was again purified using the Qiagen Gel Extraction kit and eluted in 30ul of elution buffer.

Completeness of the *in vitro* methylation reactions was determined through methylation-sensitive and insensitive restriction enzyme digestion using *Hpa*II and *Msp*I, respectively. *Hpa*II and *Msp*I both recognize the 5' CCGG sequence. *Hpa*II, however, does not digest if the cytosine immediately 5' to guanine is methylated, whereas *MspI* will digest, regardless of methylation. Two hundred nanograms of both methylated and unmethylated insert DNA was subject to restriction digest with either 10 units of *Hpa*II or *Msp*I at 37 ^{o}C for I hour. Digested samples were separated on a 1% agarose gel and visualized. Complete methylation was determined by a loss of the 2kb band that corresponds with the expected intact "tcf21" insert length. The "tcf21" insert contains 6 *Hpa*II/*Msp*I sites and complete methylation is seen as fragments that are 99, 169, 327, 249, 427, and 839bp long.

3.3 Results

Bisulfite Sequencing of TCF21

Analysis of the RLGS profiles demonstrated that the *AscI* site located within a CpG island within exon 1 of TCF21 is hypermethylated in 67% and 84% of HNSCC and NSCLC primary tumor samples, respectively. In order to determine the extent of methylation in patient samples, bisulfite sequencing of a total of 6 pairs of normal and tumor (3 HNSCC sets and 3 NSCLC sets) as well as from a cell line derived from either HNSCC and NSCLC, was performed using bis1, 2, and 3 primer pairs that encompass the entire CpG island (Figure 3.1A). Primers were designed in sequences that are present in both methylated and unmethylated templates to allow for equal amplification upon bisulfite modification of unmethylated cytosine, present as thymine following PCR, and methylated cytosine, which remains cytosine. Bis1 PCR primers were designed at the 5' end of the CpG island from +300 to +590bp and the product contains 19 potentially methylated CpG's. Bis2 primers and bis3 primers are located at +563 to +804 and +787 to +990, respectively. Bisulfite sequencing of HNSCC patient 8, 54, and 56 normal and tumor, HNSCC cell line Scc11B, NSCLC patient 6,11, and 16 normal and tumor, and NSCLC H2086 revealed clear differences between TCF21 methylation in neoplastic and non-neoplastic samples (Figure 3.1B and C). While there is a widely mosaic distribution of methylation in the normal adjacent tissues from each of the patients, the frequency and density of methylation increases in the tumor samples, supporting our observations by

RLGS. As expected, methylation more distal to the transcriptional start site of TCF21 in bisulfite sequencing from bis2 and bis3 products were more mosaic, and differences become less obvious between normal and tumor methylation (Figure 3.1B).

Combined Bisulfite Restriction Analysis (CoBRA) on primary samples

While methylation of TCF21 was commonly noted in the patient tumor RLGS profiles analyzed as well as enriched in tumor samples that were bisulfite sequenced, methylation analysis in a larger patient population was performed to measure the extent of epigenetic regulation in TCF21. A collection of bisulfite treated DNAs from HNSCC tumor and normal pairs (n=22), normal and metastatic pairs (n=1), normal, tumor and metastatic sets (n=6) and 5 tumor and metastatic pairs from individuals (Figure 3.2B) was subject to CoBRA using *BstUI* digestion. The 292bp PCR product of TCF21 bis1 contains 3 *BstUI* sites (Figure 3.2A), whose recognition sequence is CGCG. While *BstUI* is methylation-sensitive itself, in the context of CoBRA, conversion of the unmethylated samples, or partially methylated samples results in the abolishment of the sites following bisulfite treatment to either TGTG, TGCG, or CGTG. Because of this modification following PCR, unmethylated samples remain resistant to digestion by *BstUI*, resulting in a single 292bp fragment. Conversely, complete TCF21 bis1 methylation results in 118bp, 98bp, and 73bp fragments upon *BstUI* digestion. Partial methylation of a sample appears as the combination of

methylated and unmethylated bands, as well as the addition of 216/218bp fragment and a 173bp fragment (Figure 3.2A). When available, all tumor and metastatic samples were compared with the methylation patterns seen in the corresponding normal. NSCLC samples from normal and tumor tissues (n=12) were also analyzed for methylation using this technique (Figure 3.2C). As summarized in Figure 3.2D, 82.1% of HNSCC primary tumors, 57.1% of metastatic HNSCC samples, and 84.6% of NSCLC primary tumors with matched normal adjacent tissue had observably greater amounts of DNA methylation within the TCF21 bis1 region.

CoBRA analysis confirmed a higher degree of methylation in the tumor samples than in their normal tissue controls, overall. The tumor samples had a high propensity towards TCF21 hypermethylation, displaying a mosaic pattern, where many of the bands present corresponded with complete methylation of some sequences, while others had banding patterns consistent with partial methylation (Figure 3.2B and C). Normal adjacent tissues were largely unmethylated overall, but some partial methylation represented by the 216/218bp fragment was frequently observed, indicating that this *BstUI* site is normally partially methylated. Methylation in tumor samples, where there were also metastatic lesions, also demonstrated a higher propensity towards complete methylation, indicating that there may be tumor stage-specific methylation patterns for TCF21.

Demethylation reactivates TCF21 expression

It is important to correlate methylation of TCF21 and repression of transcription. An indirect method of testing the link between methylation and TCF21 gene expression was achieved *in vitro* using a demethylating agent, Decitabine, in NSCLC cancer cell line A549, where TCF21 is methylated and silenced. Decitabine is randomly incorporated into dividing cells during replication at cytosine positions in DNA[132]. Once incorporated, the nitrogen that replaces carbon in the cytosine ring structure results in a covalent link with DNA methyltransferases as they attempt to methylate a particular sequence[132]. This linkage impedes the enzymatic activity, hence preventing additional post-replication methylation from occurring elsewhere in the genome, resulting in a release of epigenetically inhibited transcription. In this experiment, two dosages of Decitabine were selected in order to achieve optimal TCF21 re-expression through demethylation. A549 was treated for 24 and 48 hours with Decitabine (Sigma), while untreated controls were plated with equal amounts of DMSO for 48 hours. TCF21 gene reactivation was achieved in the presence of both 1uM and 3uM Decitabine for 24 and 48 hours (Figure 3.3A and B). Reactivation of TCF21 through demethylating agents indicates that TCF21 expression is regulated by DNA methylation, whether directly through demethylation of its regulatory region or through re-expression of an upstream activator of TCF21.

Promoter hypermethylation silences TCF21 activity

The promoter region of TCF21 has not previously been characterized experimentally. Promoter prediction programs have identified a ~600bp region from 121 base pairs upstream of the transcriptional start site stretching 448 base pairs into exon 1. To determine if this region, and surrounding fragments contain promoter activity, portions upstream of the transcriptional start site, as well as the CpG island portion of TCF21 were examined for promoter activity in vitro using luciferase reporter assays (Figure 3.4A). The constructs that contain the predicted promoter region demonstrate the highest levels of induced luciferase activity. The *Bgl*II construct, lacking the predicted promoter portion of TCF21, as expected, lacks transcriptional activity (Figure 3.4B).

Based on these studies, an additional experiment to determine a direct consequence of methylating the 5' regulatory region of TCF21 was done using the "tcf21" construct, as it contains not only the predicted promoter region, but also the CpG island portion of TCF21 where we have identified aberrant methylation in tumors. *In vitro* methylation of this portion of TCF21 by the *SssI* methyltransferase resulted in complete methylation as determined by methylation-sensitive, *HpaII*, and methylation-insensitive, *MspI*, digestions (Figure 3.4C). The methylated fragment was ligated to an unmethylated pGL3 plasmid backbone. Luciferase activity was normalized by co-transfection using Renilla-TK expression. Methylating this portion of TCF21 results in more than a 75% reduction in promoter activity (Figure 3.4D). This supports the effect of DNA

methylation on regulating TCF21 expression.

3.4 Discussion

With increasing experiments demonstrating that tumor suppressor genes are often hypermethylated in cancer, leading to transcriptional silencing, it is clear that epigenetic mechanisms are very common in cancer[100]. Our data demonstrate a significant inactivation of TCF21 through epigenetic silencing in primary neoplasia, as well as cancer cell lines *in vitro*, while the normal tissue tested expresses TCF21 and remains unmethylated. Methylation found within the 5' end of exon 1 can distinguish normal tissue from neoplastic tissue in more than 80% of all HNSCC and NSCLC samples investigated. TCF21 repression is reversed upon removal of DNA methylation resulting in increased expression of TCF21.

TCF21 was identified as a basic helix loop helix (bHLH) transcription factor that is expressed in the mesenchyme that encapsulates the epithelia of internal organs during embryogenesis[133]. TCF21 expression in adult tissues was highest in lung tissue, but also found in spleen, heart, liver, kidneys and testes[133]. It is the first transcription factor identified as being essential for differentiation of epithelial cells adjacent to mesenchyme, but joins the list of transcription factors to be identified as aberrantly hypermethylated in cancer[134]. bHLH proteins are transcriptional regulators that mandate cell fate differentiation[134; 135]. Despite its mesenchymal cell-specific expression in development, eliminating the expression

of TCF21 results in major phenotypic defects in the kidney, lung, spleen, facial muscles and gonad development in murine models[134; 136; 137; 138]. This is likely because cross talk between the supporting mesenchyme and the organ epithelium is essential for proper lung branching and differentiation[134; 139]. Maintaining proper expression is critical for organ development[139]. TCF21 knockout mice have been compared phenotypically with WT-1 knockouts, the Wilm's tumor suppressor gene. Further, loss of WT-1 and TCF21 transcription factors result in a loss of mesenchymal epithelialization, a process that is critical in tumorigenesis[134].

In chapters two and three, validation of epigenetic regulation of TCF21 and subsequent silencing were identified. The regulation of TCF21 is tissue-specific, but the modulators responsible for activating TCF21 have not been identified. Although DNA hypermethylation of the TCF21 CpG island correlates with a lack of gene expression, the mechanism of silencing, whether by inhibition of transcription factor binding in the upstream region of TCF21, or by structural changes in the chromatin, is not known. Using the methylated luciferase reporter assay, we were able to demonstrate that hypermethylation of the TCF21 promoter region as the initiating event is able to confer a reduction in promoter activity from the plasmid. This is likely due to the binding of methyl-binding proteins to their targets, methylated cytosine, which recruit chromatin-remodeling complexes that shut down transcription of the TCF21 promoter-luciferase product. However, there is evidence in the literature that indicates that any

methylated sequence will recruit identical protein complexes, and is not specific to methylation in CpG islands of gene promoters[140]. Methylated sequences downstream of the promoter along episomal DNA are able to prevent transcriptional elongation, but not in endogenous genes [140]. Additional studies based on methylating the endogenous locus using methylated oligos at various locations along the CpG island and promoter regions of TCF21 would provide extra validation that methylation leads to transcriptional silencing [141].

We conclude that TCF21 is targeted for epigenetic silencing rather than genetic because of its involvement in mesenchymal to epithelial transition (MET). Epithelial sheets can be dynamically converted into mesenchymal cells and back in normal developmental processes[142]. MET, and the reverse process of dedifferentiation from epithelial to mesenchymal transition (EMT), are also proposed as fluctuating during tumorigenesis[143]. The primary carcinoma *in* situ occurs in epithelial cells anchored by the extracellular matrix. These epithelial cells obtain genetic and epigenetic modifications through EMT that permit invasion along the basement membrane, establishing an opportunity for metastasis. Once in the blood or lymphatic circulation, cells reach the target organs and are able to reestablish themselves as new lesions. Propagation of these lesions at secondary sites is maintained by restructuring their gene expression patterns from migratory (mesenchymal) to stationary (epithelial) through MET[143].

Although limited in size, our data support this notion of epithelial and

mesenchymal plasticity in primary and metastatic lesions. Methylation of TCF21 is higher in HNSCC primary tumors than in metastatic lesions from patients 6,8, and 12. This may reflect that TCF21 hypermethylation allows for the dedifferentiation at the primary tumor, permitting the initial stages of the metastatic cascade. Reduction in the amount of TCF21 methylation in metastases may indicate the requirement for cells to survive in secondary sites. Reestablishing the epithelial characteristics associated with TCF21 expression, such as increased E-cadherin expression, may allow for neoplastic cells to become anchored at these distant sites. Commitment to inactivation by means of permanent genetic mutations does not allow flexibility in gene expression, nor the flexibility in differentiation states. DNA methylation, although a covalent modification, can be reversed, and expression of the silenced target restored. This elasticity in gene profiling provides plasticity in gene expression profiles at different stages in tumorigenesis.

Figure 3.1: **Bisulfite sequencing of TCF21**

A. Location of the three bisulfite sequencing primers and their association along the CpG island of TCF21. Normal and tumor PCR products from NSCLC (B.) 6, 16, 11, H2086 and HNSCC (C.) 8, 56, 54, and Scc11B, were ligated into the TOPO-TA plasmid, transformed into bacteria and grown on Lurea Broth plates containing ampicillin. Individual clones were bisulfite sequenced using the M!3 forward and reverse primer sequence adjacent to the PCR product in the plasmid. Each clone is represented by a row, and the CG being investigated is arranged in the columns. White circles represent unmethylated cytosine, and black circles are methylated.

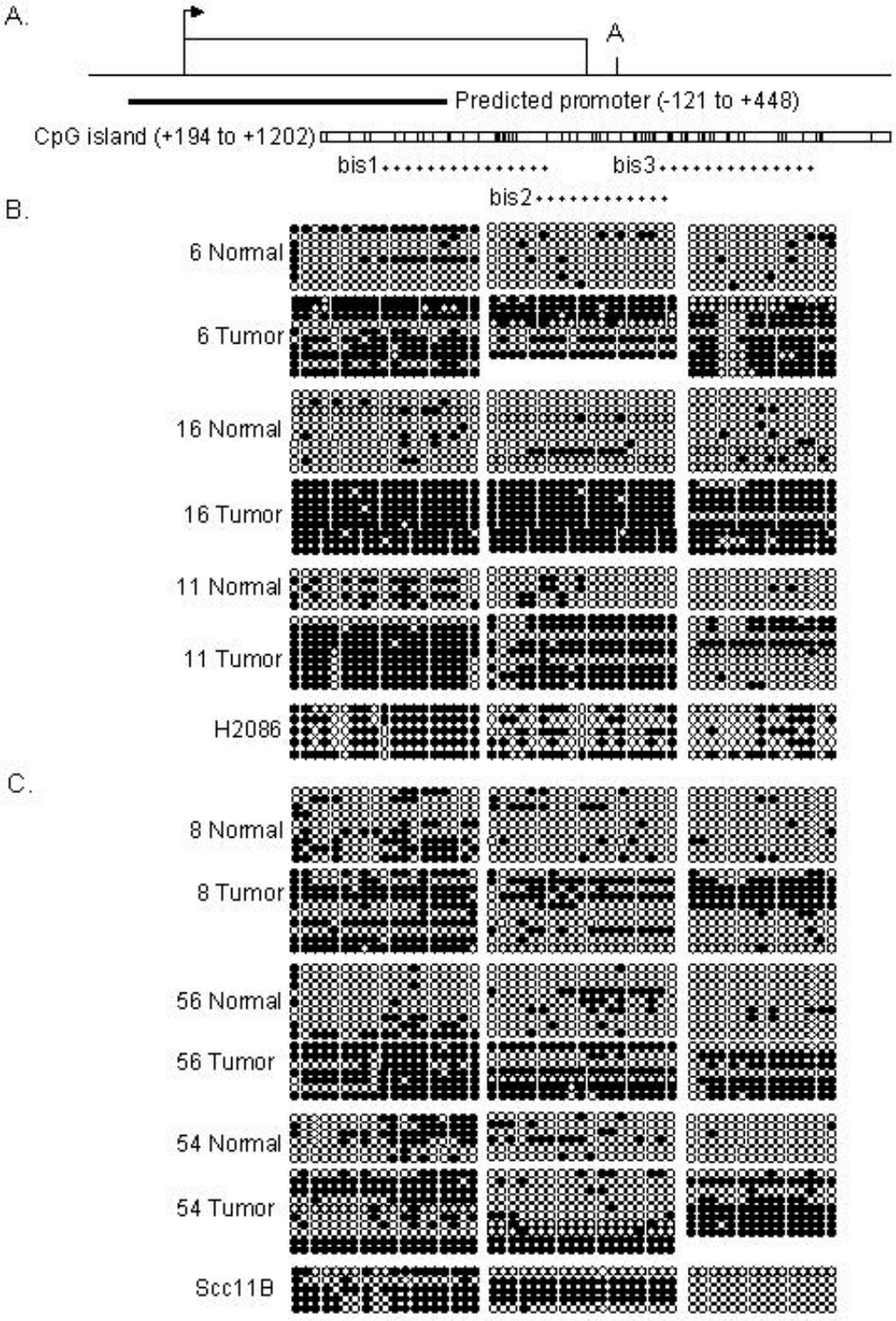
A.
A
Predicted promoter (-121 to +448)
CpG island (+194 to +1202)
bis1
bis2
bis3
B.
6 Normal
6 Tumor
16 Normal
16 Tumor
11 Normal
11 Tumor
H2086
C.
8 Normal
8 Tumor
56 Normal
56 Tumor
54 Normal
54 Tumor
Scc11B

Figure 3.2: **Combined Bisulfite Restriction Analysis (CoBRA)**

A. A schematic diagram of *BstU*I (b) sites along the TCF21 bis1 PCR product, and the expectant banding patterns following digestion. B. CoBRA results for HNSCC normal, tumor and metastatic samples. C. CoBRA results in NSCLC normal and tumor pairs. Samples in B. and C. with more methylation in the tumor than in normal are denoted with (>). Primary tumor samples with methylation equal to normal are denoted with (=), and samples with more methylation in the normal are denoted with (<). D. Summary of the methylation patterns seen across the patient samples analyzed by CoBRA.

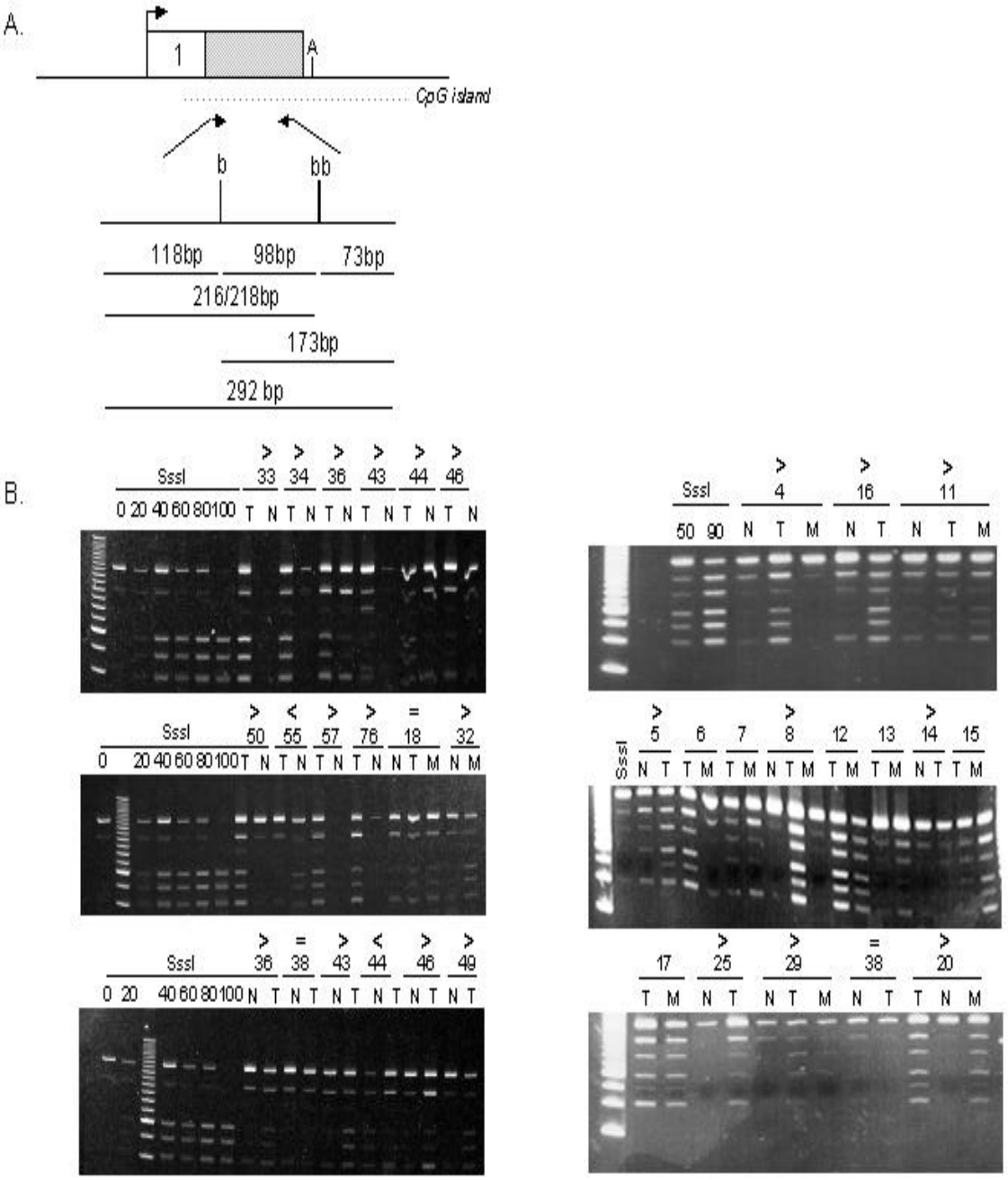

Figure 3.2 (continued)

Figure 3.2: (continued)

C.

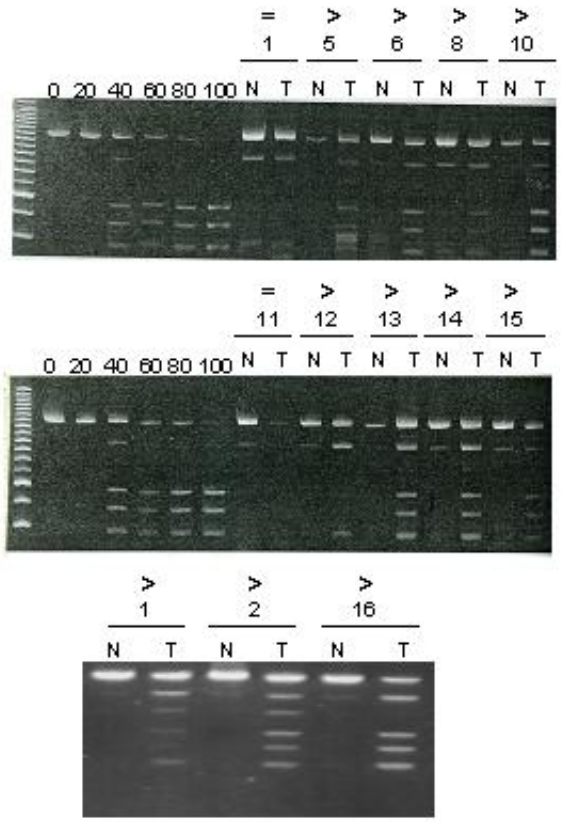

D.

Methylation Summary	>Normal (%)	<Normal (%)	=Normal (%)
HNSCC Primary Tumors (n=28)	23 (82.1)	2 (7.1)	3 (10.7)
HNSCC Metastasis (n=7)	4 (57.1)	0 (0)	3 (42.9)
NSCLC (n=13)	11 (84.6)	0 (0)	2 (15.4)

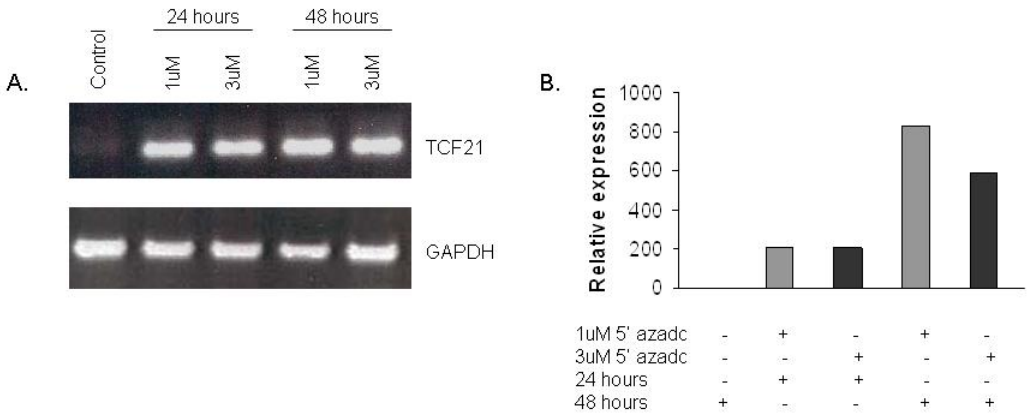

Figure 3.3: **TCF21 expression following *in vitro* demethylation.**

A. SYBR green RT-PCR determination of TCF21 expression in A549. Untreated A549 lung cancer cell line, containing hypermethylated TCF21, lacks endogenous expression (control). Following 24 and 48 hours in the presence of 1uM or 3uM 5'aza-2-deoxyctidine treatment, TCF21 expression is restored. B. Quantitation of the SYBR green RT-PCR reactions, normalized to GAPDH internal control in treated and untreated A549 cell lines.

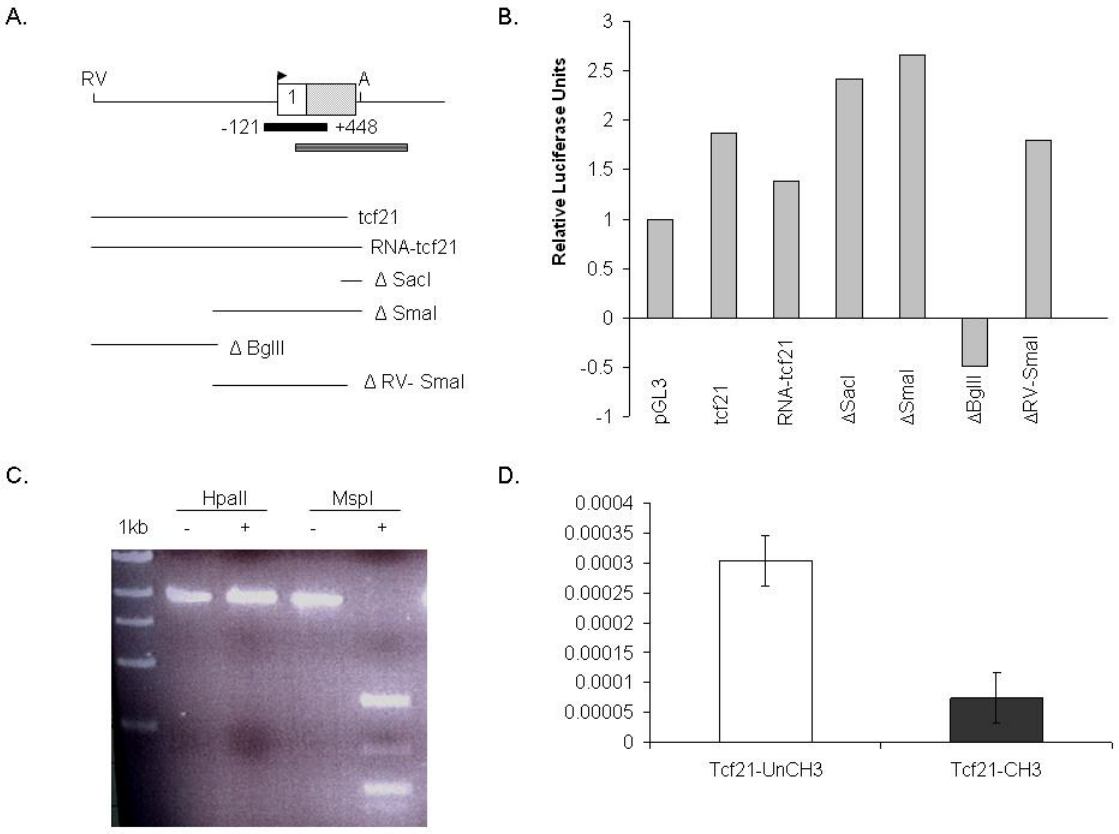

Figure 3.4: **Determining the promoter of TCF21**

A. Constructs along the 5' region and exon 1 of TCF21 cloned in front of the luciferase reporter gene in the pGL3 basic plasmid. B. Experimentally determined reporter gene activity driven by each construct. C. Enzymatic digestion by *Hpa*II or *Msp*I to determine if the *in vitro* methylation reactions were complete for the "tcf21" labeled construct from (A.). D. Luciferase activity of the "tcf21" construct upon *in vitro* methylation (black bar) or no methylation (white bar).

CHAPTER 4:

TCF21 EXPRESSION PROVIDES ANTI-TUMOR ACTIVITY

4.1 Introduction

Epithelial to mesenchymal transition (EMT) is a normal process by which a differentiated epithelial cell acquires characteristics that allow for dedifferentiation into a mobile mesenchymal cell[144]. EMT occurs during gastrulation, organ development (such as in the formation of the lungs and heart), and in the process of wound healing[137; 144]. Although clear morphological and gene expression profiles can be seen, interactions between mesenchymal and epithelial cells have been demonstrated to be important for maintaining the epithelium[145]. Alterations in signals originating from the mesenchymal component have profound effects on the adjacent epithelium and the reverse is also true[145; 146].

Normally, epithelial cells are highly organized along the basement membrane, which maintains the tissue architecture and separates the epithelial components from the stromal, as well as allowing for the exchange of extra- and intra-cellular substances[146; 147]. Epithelial cells are necessary for proper organ structure and for physiologic function, while mesenchymal cells form all migrating

cells and support for the epithelium[148]. During embryogenesis, through the process of EMT, epithelial cells lose certain defining characteristics such as E-cadherin and keratin expression, in addition to loss of the organization afforded by the polarity and inter-cellular adhesions, and instead acquire a more fibroblastic appearance[147]. Epithelial cells contain keratin filaments, and desmosomal and adherin junctions that are vital for cell-cell interactions[147]. In addition, loss of cadherin interaction between adjacent cells is essential for cells to dissociate from one another and from the extracellular matrix, which typically prevents motility.

The majority of human malignancies are derived from cells of epithelial origin and are termed carcinomas[147]. Tumor formation occurs through multiple steps that convert epithelial cells into cells that can divide indefinitely, invade surrounding tissue and migrate to target sites and eventually sustain metastatic growth[147]. To invade surrounding tissue and spread to additional sites, tumor cells adopt migration mechanisms found in normal processes[147; 149]. EMT has been described in many cancers including breast and oral squamous cell carcinomas[150]. Malignant lesions are often defined by their differentiation status, where benign tumors retain their epithelial phenotype and malignant cells acquire a more fibroblastic mesenchymal phenotype[147]. In general, less differentiated tumors are more aggressive[151; 152]. Epithelial cell plasticity obtained through EMT allows for a highly organized epithelial cell, that has polarity and multiple inter-cellular adhesion contacts, to revert to a cell that has the ability to disassociate

from neighbor cells, invade and migrate, achieving a more aggressive malignancy[144; 147; 149]. In fact, along the invasive front of a carcinoma, epithelial cells often gain mesenchymal cell characteristics and gene expression profiles[153]. Conversion into a mesenchymal cell has been demonstrated to occur through changes in gene expression within the cell, often triggered by an outside stimulus that results in induction or inactivation of important transcription factors[147].

Overexpressoin of a single transcription factor involved in the interactions between mesenchymal and epithelial cells results in a shift in the differentiation patterns[144; 147]. Because transcription factors are key to allowing the cellular plasticity of EMT and MET to occur, the understanding of these transactivating factors and their targets are important for understanding their part in human malignancies.

TCF21 was identified as a transcription factor involved in mesenchymal to epithelial transitions (MET) that occurs in embryogenesis during the development of vital organs including the heart, lungs, kidneys, spleen, and craniofacial muscles during embryogenesis[134; 136; 137]. TCF21 is a class B transcription factor. Expression of this class of transcription factors is tissue-specific, while the binding partners of class B transcription factors, known as class A, are ubiquitously expressed[133; 135]. TCF21 has been shown to heterodimerize with the class A binding partners E12 and E47.

During MET, mesenchymal cells differentiate into epithelial cells through

signaling from within the epithelium to trigger the morphological changes[134]. TCF21 expression has been shown to be mesenchyme-specific, but loss results in a loss of differentiation and branching in the surrounding epithelium[134]. In fact, lack of TCF21 based on knockout studies in mice where exon 1 is replaced by a neomycin cassette, abolishing the bHLH domain, results in live-born mice that have difficulties in respiration and die within minutes after birth[134]. This perinatal lethality is a classic feature of tumor suppressor activity[154]. The cause for the perinatal lethality has been associated with poor lung differentiation by means of down regulation of BMP4[134; 137]. Lung branching, for example, is a highly regulated process that is required to allow for increased surface area for gas exchange. The surrounding mesenchyme is essential for inducing branching, partially through TCF21 signaling.

Because of its function in inducing differentiation of mesenchymal cells into epithelial cells, and the knowledge that carcinomas often lose this epithelial state, the role of TCF21 as a tumor suppressor gene is investigated in these experiments.

4.2 Materials and Methods

Mutation screen:

Each exon of human TCF21 was amplified using two primer sets that amplify genomic DNA. The primer sets are as follows: TCF21ex1 (1a) forward, 5' CAGGAAACAGCTATGACCtgcagttgagttgatttacattacaa and reverse, 5'

tgtaaaacgacggccagtAACCCGTCACATTCCAACAT;

TCF21 ex1 (1b) forward, 5' caggaaacagctatgaccACCCTCTTCCTCGCTTTCTC and reverse, 5' TGTAAAACGACGGCCAGTcggtggtcgagatgtgtaag;

TCF21ex1 (2a) forward, 5' CAGGAAACAGCTATGACCtttacattacaagttgcaaatcagg and reverse 5' tgtaaaacgacggccagtAACCCGTCACATTCCAACAT;

TCF21ex2 (1b) forward, 5' caggaaacagctatgaccCTCGCAATGCTCCTCTCTCT and reverse 5' TGTAAAACGACGGCCAGTtccccatagtttcccactttc. Lower case letters in the mutation primer sequences denote the M13 forward and reverse primers used for the sequencing reactions of the PCR products. Fifty microliter PCR reactions were established using 10pmol of forward and reverse primers, 1X PCR Buffer (Invitrogen), Platinum Taq (Invitrogen), 0.2mM dNTPs and ~50ng genomic DNA from each patient for 35 cycles. Ten microliters from each amplification was visualized for product using ethidium bromide staining on an 8% polyacrylamide gel. Samples were then purified using the Qiagen Gel Extraction kit according to the manufacturer's suggested protocol, and eluted from the column in 30ul of elution buffer. Approximately 200ng/ul were sent for individual sequencing using the M13F and M13R tags linked to each of the 5' ends of the primers used in the initial PCR amplification reactions.

Sequencing chromatograms were analyzed using the DNA Star "Chromas" software. To confirm mutations, genomic DNA from the tumor sample as well as from its matched normal adjacent tissue were re-amplified to confirm the mutation in the tumor specifically, and not in the normal.

TCF21 ORF cloning:

Primers were designed to amplify an inframe TCF21 open reading frame when ligated to myc-tag sequence, which creates a unique peptide sequence for antibody detection. The myc tag sequence is as follows: 5' GTACCACCATGGAACAGAAGCTAATCTCTGAGGAAGTTTTGCTGGGGATCT TGGAGCAGAAATTGATAAGCGAGGAAGACCTTGGAGAACAAAAGCTGATTT CGGAAGAGGATCTGGGGATCTTGGAGCAGAAATTGATAAGCGAGGAAGAC CTTGGAGAACAAAAGCTGATTTCGGAAGAGGATCTGGGGATA. Antibodies against the myc-tag (Cell Signaling Technology) were used to measure the protein following transfection with TCF21. The TCF21 ORF and myc tag were first cloned into the Topo TA (Invitrogen) vector, utilizing the "T" overhangs on the vector and the 3' "A" overhangs incorporated onto the PCR products by the Taq polymerase. The 200bp myc-tag product was PCR amplified using primers containing a *Kpn*I restriction site at the end of the forward primer, and a *Spe*I restriction site at the end of the reverse primer. Upon restriction enzyme digestion of the Topo-myc tag plasmid, using 15 units of *Kpn*I and 10 units of *Spe*I in the multicore buffer at 37^{o}C, the myc tag portion was purified using the Qiagen Gel extraction kit. This digestion pattern allows for an in-frame and directional ligation into the topo-TCF21 plasmid upstream of TCF21 because the Topo-TA plasmid has both a *Kpn*I and *Spe*I site upstream of the multiple cloning site where TCF21 insert is located. The mycTCF21 insert was PCR amplified

from the Topo plasmids using primers that recognize the 5' portion of the myc-tag, and contain a *BamH*I site, and a TCF21 reverse primer containing a 3' *Sal*I site (5' CAGGGATCCAGCTTGGTACCACCATG and 5' GGAGTCGACTGGGACAGAGAGAGGAGCAT, respectively). PCR products were gel extracted using Qiagen's Gel Extraction Kit, and digested using *BamH*I and *Sal*I, resulting in restriction half sites on the ends of the insert. In addition, the retroviral vector, pBABE, was also digested by *BamH*I and *Sal*I, allowing for directional ligation of mycTCF21 ORF. Ligated pBABE-mycTCF21 plasmids were transformed using the chemically competent Top10 cells (Invitrogen) and plated on LB/Agar plates containing ampicillin. Colony PCR was performed on resultant clones to identify which colonies had the expected mycTCF21 insert using the forward primer specific to myc and the reverse primer specific for TCF21. Positive clones were isolated using Qiagen's Miniprep kit. Plasmid DNAs were sequenced to confirm the presence of the correctly orientated insert using SP6 and T7 primer binding sites located along the pBABE plasmid.

Transfection of pBABE mycTCF21 construct into cell lines:

Ten micrograms of pBABEmycTCF21 plasmid or pBABE vector alone were transfected into the amphotropic Pheonix packaging cell line (60% confluent) using the Superfect reagent following Qiagen's protocol at experimentally determined 1:6 ratio of DNA:Superfect, and returned to the 37^{o}C incubator. Three hours following the initial transfection, the cells were washed

once with 5ml PBS, and then 8ml of DMEM-15%FBS-Penicillin/Streptomycin was added gently to the side of the culture dish to prevent dislodging the cells. Twenty-four hours later, virus-containing medium was collected from the Pheonix cells, and cell debris was removed by centrifugation at 1000rpm for 5 minutes in the presence of 2X polybrene. Four milliliters of infectious medium, containing either pBABE mycTCF21 or pBABE vector alone, was added to the surface of 40% confluent A549 cells, and incubated at 37^{o}C. To the surface of the Pheonix cells, 8ml DMEM-15%FBS-Penicillin/Streptomycin was added. After 12 hours, the infectious medium from A549 was removed and replaced with 4ml of new infectious medium. After twenty-four hours the viral-medium was removed, the infected cells were washed with PBS, and normal RPMI-1640/10%FBS/Penicillin/Streptomycin was added to the cultures. The following day, infected cells were washed, trypsinized, and split 1:2. Selection medium was added to the cell cultures (RPMI-1640/10%FBS/Penicillin/Streptomycin + 5ug/ml Puromycin (Sigma) to select only for cells that have been infected by the viral constructs. As a control, wild type A549 cell lines were also treated with Puromycin to establish when wild type cells should be completely eliminated by the drug in the transduced cultures. Four days of selection resulted in a total loss of wild type A549 cells under puromycin drug selection.

Transfected cell lines (A549 mycTCF21 or A549 pBABE) were grown in 150mm culture dishes to allow for ample cell growth for DNA, RNA and protein isolations. RNA isolation was performed using the RNA-stabilizing agent, Trizol

according to standard protocols. Isolated RNAs were treated with DNAse to eliminate any contaminating genomic DNA that would amplify in the RT-PCR reactions. cDNA's were amplified from the Superscript RT-PCR cDNA synthesis kit (Invitrogen) by random hexamers and oligo dT primers from a total of 2ug of purified RNA. Expression levels of transfected TCF21 were analyzed using semi-quantitative SYBR green RT-PCR (forward primer 5'AGCTACATCGCCCACTTGAG; reverse, 5' CGGTCACCACTTCTTTCAGG) and normalized using primers specific for GPI (forward, 5' GACCCCCAGTTCCAGAAGCTGC; reverse, 5' GCATCACGTCCTCCGTCACC)

Expression of vimentin (forward, 5'tggcacgtcttgaccttgaa; reverse, 5'ggtcatcgtgatgctgagaa), Wnt4 (forward, 5' ctgaaggagaagtttgatggtgcc; reverse, 5' gtggaatttgcagctgcagcgttc), Snail (forward, 5' acccacactggcgagaag; reverse, 5' attccatggcagtgagaagg), and E-cadherin (forward, 5' agccatgggcccttggag; reverse, 5' ccagaggctctgtgcaccttc) were examined by SYBR green RT-PCR as described above. Normalized expression of A549 pBABE was always labeled as "1" for each gene, and the relative expression in A549 mycTCF21 is in relationship to this value.

Protein was isolated from whole cell lysate in lysis buffer (50mM Tris-HCL, pH 7.6, 250mM NaCl, 5mM EDTA, 50mM NaF, 1.5mM PMSF, 0.2% NP-40) on ice for 30 minutes. Cellular debris was removed by centrifugation at 14,000rpm (4^{o}C) for 15 minutes. Protein concentrations were determined using the Bradford Assay kit (BioRad) according to manufacturer's instructions.

Translation efficiencies of the plasmid constructs were determined by Western blot analysis using a primary antibody to detect the myc-tag of the mycTCF21 fusion protein. Briefly, 150ug of protein from whole cell lysate was separated on a 12% PAGE-SDS minigel. Semi-dry transfer of the proteins was performed at room temperature at constant amperage of 13mA for 45 minutes onto Hybond^{TM} ECL^{TM} Nitrocellulose membrane (Amersham). The resultant blots were incubated for 2 hours at room temperature using blocking buffer (1xTBS-Tween, 1% milk). Following a washing regimen that consisted of 1xTBS-Tween wash for 5 minutes, 10 minutes block, then (4x's) wash with 1xTBS-Tween (5 minutes each), the membrane was incubated with the anti-myc antibody (1:500) at 4^{o}C overnight with shaking. The membrane was washed as above, and the secondary anti-mouse antibody conjugated with HRP (1:2000) was added at room temperature for 2 hours. Following a final wash, chemiluminescence was detected using the ECL detection kit (Amersham Pharmacia). To normalize for loading differences, the blots were also incubated with anti-tubulin (1:500, Santa Cruz) antibodies and visualized.

Growth Curves and colony formation:

Cell-cycle synchronization of sub-confluent A549 pBABE and myctcf21 cells was performed by removing exogenous growth factors in culture for 12 hours in a 37^{o}C/5% CO_2 incubator. Synchronized cells were then counted in duplicate and averaged. Two hundred thousand A549 pBABE and A549

myctcf21 cells were plated in triplicate p100 for each time point of day 2, 4, and 6. Cells were incubated in the presence of RPMI-1640 containing 10% FBS, antibiotics, and 5ug/ml Puromycin for the indicated times. At each time point, the cells were washed once in PBS, trypsinized and counted, in duplicate, using the Coulter Counter.

To determine the colony-forming potential for these cells, cells were trypsinized and counted using the Coulter Counter, as before. For each line, 1000 cells were plated in triplicate 60mm dishes containing 5ml of RPMI-1640 containing FBS, antibiotics, and 5ug/ml Puromycin. Cells were incubated in a 37^{o}C/5% CO_2 incubator for 14 days. At the culmination of the experiment, cells were washed once with PBS and fixed in methanol:acetic acid (3:1) twice for 5 minutes and once for 15 minutes. Fixed colonies were stained with 0.1% crystal violet in PBS for 30 minutes at room temperature, then washed with water. Colonies consisting of ~20 cells or more were counted.

Nude mouse injection of transfected cell lines:

Two hundred microliters of PBS containing 1.5 x10$^{\wedge 6}$ A549 cells infected with mycTCF21 plasmid were injected subcutaneously into the right rear flanks of 8 athymic nude mice (Jackson Laboratories), while A549 pBABE cells were injected into the left rear flanks of the same mice as a control. Tumor volumes were determined twice weekly by caliper measurement. The radii of the tumors are calculated using the equation: *volume=((width+height+length)/3)/2.* The calculated radius was then used to determine the tumor volume using the

equation $volume=(4/3)\pi r^3$.

Five weeks post injection, mice were sacrificed using a carbon monoxide chamber. Resultant tumors from each mouse were extracted from the injection area, and measured for weight (grams) and volume (mm^3) differences. Average weight and volume were determined for each of the tumors isolated from the 8 mice injected, and the standard deviation was calculated for each group.

4.3 Results

TCF21 mutation screen

Classic determination of *bona fide* tumor suppressor genes has included the identification of mutations in the DNA sequence in addition to LOH. Although TCF21 hypermethylation is identified frequently in HNSCC and NSCLC, a mutation screen using genomic DNA and primers that amplify both exon-intron (Figure 4.1A) boundaries for TCF21 was performed on a set of samples whose methylation was determined previously by CoBRA. A total of 52 primary patient samples from 16 NSCLC, and 34 HNSCC primary tumor and 2 metastatic DNAs, were amplified, purified, and sequenced with both M13F and M13R primers to search for mutations that are present at the level of genomic DNA. Known polymorphic sequences were detected, as expected, but limited mutations were identified.

Initially, a base change was found from HNSCC patient 11-tumor tissue that was located within the third codon of amino acid 65 of TCF21, which is normally a lysine with the expected DNA sequence of AAG. The single base change identified is a transition from guanine to adenine, resulting in AAA (Figure 4.1B). However, computational translation of the sequence into protein revealed that the base substitution did not affect the amino acid code and amino acid 65 remains lysine.

An interesting mutation was noted in the non-coding 5'UTR that is part of the predicted promoter portion of TCF21 from NSCLC patient 10-tumor tissue in two independent PCR and sequencing reactions using both the forward and reverse primers. The expected sequence is cytosine located 43 base pairs 5' to the translational start site of TCF21. In the tumor DNA, there is a transversion to adenine in 50% of the product (Figure 4.2A). Because of its location in the 5'UTR, and not in the translated portion of the gene, the mutation does not cause a change in the amino acid sequence. It does, however, reside within the promoter region of the 5' UTR of TCF21, which may affect transcription. To investigate this possibility, luciferase reporter assays were applied to distinguish differences in promoter activity between the two alleles. Activity using the two isoforms revealed a reduction in promoter activity by >50% when the mutated promoter containing the adenine (Figure 4.2B) is utilized instead of the wild type allele containing cytosine. Computational analysis using http://www.cbrc.jp/research/db/TFSEARCH.html to determine changes in

transcription factor binding sites suggests that the sequence change from guanine to adenine creates a binding site for GATA-1 only on the mutant allele, possibly creating differences in the transcription potential.

Evidence in the literature suggests transcriptional repression in the cell then recruits the methyltransferases as a secondary event. The recruitment of methyltransferase then ensures transcriptional silencing through DNA methylation “marks” in subsequent daughter cells. Therefore, it is plausible that DNA methylation differences can be seen in the two alleles of TCF21, and the mutated “A” promoter, which has demonstrably reduced promoter activity is methylated to a greater extent in NSCLC patient 10T. To determine if there is a difference in DNA methylation of these alleles, bisulfite-sequencing primers designed to amplify a product containing the mutation and 9 potentially methylated CpG sites. In the product, the cytosine on the wild type allele is not located 5’ to guanine and should therefore be converted to thymine following PCR amplification, while the adenine mutation remains. Bisulfite sequencing on NSCLC-10T revealed that the mutated allele has 82% methylation over all CpG’s investigated compared to only 61% on the wild type allele (Figure 4.2C), further implying that there are differences inherent to these two promoter sequences in this patient.

TCF21 overexpressoin results in decreased cell growth

Lung cancer cell line A549 was shown by RLGS to have a hypermethylated *AscI* site in the CpG island of TCF21, as well as extensive hypermethylation in the CpG island determined by bisulfite sequencing, correlating with a lack of gene expression. Because of the lack of endogenous TCF21 expression, transfection studies were performed using this cell line through a retroviral construct of pBABE-mycTCF21 in order to understand TCF21's role in cellular control.

In vitro comparison of individual growth rates in TCF21 expressing (mycTCF21) versus non-expressing cells (pBABE) was performed in triplicate by plating equal numbers of serum-depleted, synchronized cells in p100 dishes, followed by counting the populations every other day for a total of six days. Overexpressoin of TCF21 in A549 resulted in a significant ($p<0.001$) reduction in the growth rate of the cells, without resulting in visible cell death. Cells infected with the empty vector were able to grow more than twice as rapidly as TCF21 expressing lines (Figure 4.3A).

Another hallmark of a cancer cell is the ability to grow into larger groups of cells, uninhibited by contact with neighboring cells. TCF21 expressing and non-expressing A549 cells were further analyzed for growth differences through colony formation assays. Following 14 days of growth, resultant colonies were washed, and stained with crystal violet solution. Visible colonies consisting of 20 cells or more were counted. Cells that express TCF21 were reduced in their

ability to aggregate into large populations of cells, whereas non-expressing cells were able to establish more than seven times the number of colonies as expressing lines ($p<0.004$) (Figure 4.3B). Together, these results indicate a significantly stunted ability for TCF21 over-expressing cells to maintain their tumorigenic properties of uncontrolled cell growth and aggregation.

TCF21 induces cellular differentiation

An additional hallmark of neoplastic cells is that they often lose their differentiated epithelial cell status, and express markers of an undifferentiated mesenchymal cell, which indicates their increased ability for migration and independence from surrounding cell structures. Markers such as vimentin and snail are expressed in mesenchymal cells, while E-cadherin and Wnt4 are expressed in epithelial cells. TCF21 functions to induce mesenchymal to epithelial transitions during embryogenesis, so it is possible that its exogenous expression *in vitro* induces differentiation as well. To investigate this, expression, as assessed through semi-quantitative RT-PCR from A549 cells that are stably expressing TCF21, was compared to that of A549 cells lacking TCF21 expression for the pattern of gene expression for vimentin, snail, E-cadherin, and Wnt4. As expected, A549 cells that do not express TCF21 express five times the amount of vimentin and seven fold more snail than the cell lines expressing TCF21. Expression of both E-cadherin and Wnt4 were 3 fold higher in TCF21 positive cells (Figure 4.3C).

In vivo tumor growth

Based on *in vitro* results obtained through colony formation and growth curve studies, we decided to pursue the relationship of TCF21 expression and tumor growth *in vivo*. Tumor models in murine systems allow for the evaluation of tumor formation in the presence of microenvironments. The use of athymic mice allows for the growth of allografted cells, in this situation, human cancer cells, without an immune response to irradicate the body of "non-self". Briefly, 1.5 million cells were injected subcutaneously into the rear flanks of athymic nude mice. On the left dorsal side, A549 cells not expressing TCF21 (pBABE) were injected, while the right sides of individual animals were injected with TCF21 expressing cells (mycTCF21). Following a 5-week period for tumor growth, obvious differences in the two populations were visibly and measurably observed. Tumors that developed on the pBABE side were much larger than those that formed from the TCF21 (+) population, as well as a 10-day earlier onset than the TCF21 (+) tumors (Figure 4.4A).

At the conclusion of the experiment, the mice were sacrificed and the tumors were surgically removed (Figure 4.4B). Upon tumor removal, the tumors weights (Figure 4.4C) and volumes (Figure 4.4D) were determined for each. The tumors lacking TCF21 expression were 2-3 times larger as determined by both weight and volume, than TCF21 positive tumors, obtaining statistically significant

differences (p value<0.01 and <0.0003, respectively). Of note, the tumors that lack TCF21 were also more vascular; possibly indicating that angiogenesis is affected by TCF21 expression.

4.4 Discussion

Classical studies to prove tumor suppressor gene function have gone hand-in-hand with the identification of somatic mutations in the tumor tissue that are not found in normal tissue[155]. Our data suggest that the predominant mechanism of TCF21 inactivation is epigenetic rather than genetic. However, tumor-specific changes were identified from 2 patients. The sole base change identified within the coding sequence of TCF21 does not result in a change in the protein sequence, and therefore has not been classified as a mutation. The adenine mutation in the promoter portion of TCF21 in tumor tissue from lung cancer patient number 11, however, reduced the amount of transcript made from that allele *in vitro*. The transversion from cytosine to adenine seen in the promoter region of TCF21 correlated with increased methylation in the primary tumor sample. *In silico* prediction of transcription factor binding sites reveals that the change to adenine creates a unique GATA-1 binding site not present in the wild type sequence. GATA-1 has been demonstrated to act as a repressor of expression via chromosomal confirmation changes through histone deacetylase activity[156]. We hypothesize that GATA-1 binds to the mutant allele, bringing histone deacetylase activity along to actively condense the chromosome,

preventing transcription from occurring. DNA methylation machinery is then postulated as being recruited to methylate the DNA sequence, maintaining the transcriptionally silent state long term (Figure 4.5).

Neoplastic cells have often been recognized as undifferentiated cells that no longer require recognition of neighboring cells or organization along a basement membrane. Expression of snail has been inversely correlated with differentiation, and these experiments demonstrate that overexpressoin of TCF21 results in a reduction of snail transcript. Reduced snail and vimentin expression, as well as upregulation of E-cadherin, a marker of organized epithelial cells, indicate that TCF21 has induced differentiation *in vitro*[144]. Additionally, there were notable differences in the amount of blood vessels surrounding the tumors derived from A549 cells that lack TCF21 expression compared with those that do express TCF21. This increased vasculature may indicate that TCF21 expression prevents angiogenesis to support the metabolic requirements of large tumors. This is interesting because mesenchymal cells are involved in blood vessel formation in normal placental development[157]. TCF21 also reduces expression of mesenchymal markers and results in expression patterns analogous to epithelial cells, which may further reduce the ability of tumors to create a supporting vasculature. Together, data from *in vivo* nude mice and *in vitro* cell culture experiments support the observations that targeting TCF21 for inactivation in the minimally deleted region along chromosome 6q is advantageous for neoplastic progression. Tumor cells acquire the potential to

replicate indefinitely, while karyotypically normal cells have limited growth potential in culture. Transformed cells also obtain the ability to divide without density dependence, or contact inhibition, once confluent, and they require less growth factors, such as serum, for growth in vitro. TCF21 expression in the A549 lung cancer cell line significantly reduced the growth rates of these cells as compared with equal numbers of A549 cells lacking TCF21. Further, when TCF21 is expressed, the potential to form larger populations of cell-aggregates was reduced significantly, indicating that the cells have a restored contact inhibition. In order for a transformed cell to be classified as tumorigenic, it must also produce tumors in animal models, and TCF21 tumors were diminished of this property. Together, these reduced growth rates and tumorigenic potential suggest that TCF21 is a disadvantage for cancer survival, supporting its role as a novel tumor suppressor gene from 6q23-q24.

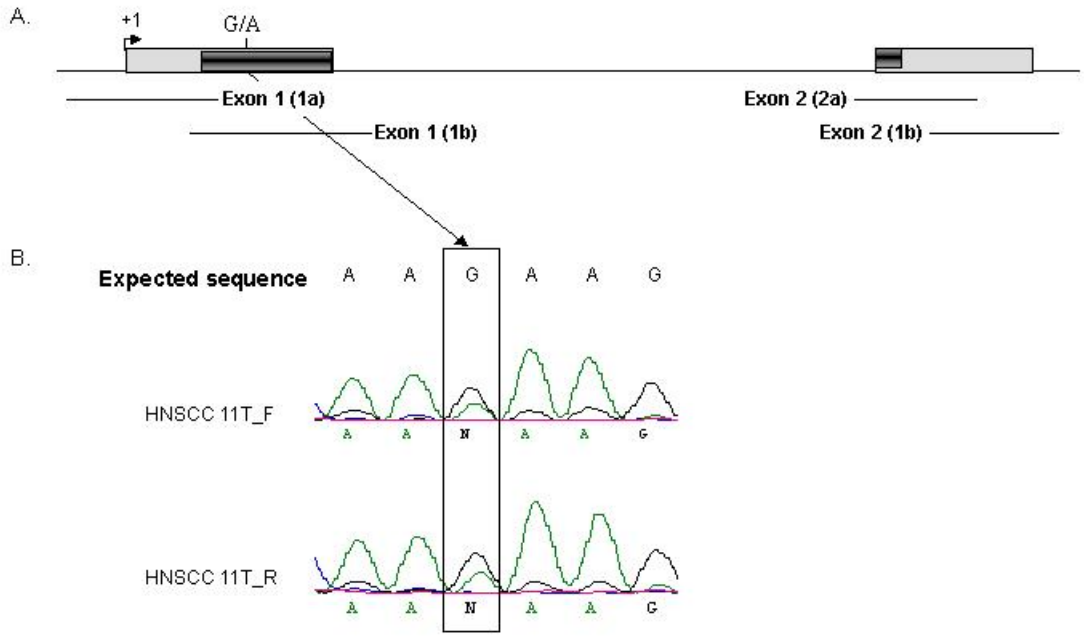

Figure 4.1: TCF21 mutation screen.

A. Primers were designed to include the exon-intron boundaries of both TCF21 exons. The primers were tagged with M13 reverse and M13 forward sequences, and were designed to overlap one another within the exon. PCR products are depicted as horizontal lines followed by "Exon…" B. A transitional base change was observed in HNSCC patient 11 tumor DNA that results in a guanine to adenine change in the third codon of amino acid 65 of the TCF21 protein product.

Figure 4.2: Cytosine to adenine transversion in the promoter of TCF21.

A. Genomic sequencing of DNA isolated from NSCLC tumor patient 10 revealed a cytosine to adenine mutation in half of the sequencing product. Sequencing of DNA from the normal adjacent tissue from the same patient revealed that the expectant homozygous cytosine is present. B. Luciferase activity of the promoter containing the mutated "A" construct results in a 50% reduction in promoter activity as compared to the wild type "C" construct. C. Bisulfite sequencing of the wild type and mutant allele demonstrate methylation differences. Each row represents a single colony that was sequenced. The columns of circles represent a single CG dinucleotide. White circles are unmethylated and black circles are methylated cytosines. The mutation is demarked with an "x", and resides between CG six and seven. Overall methylation along both the wild type and mutated allele was determined by adding up the (total number of methylated cytosines observed/the total of potentially methylated cytosines) x100.

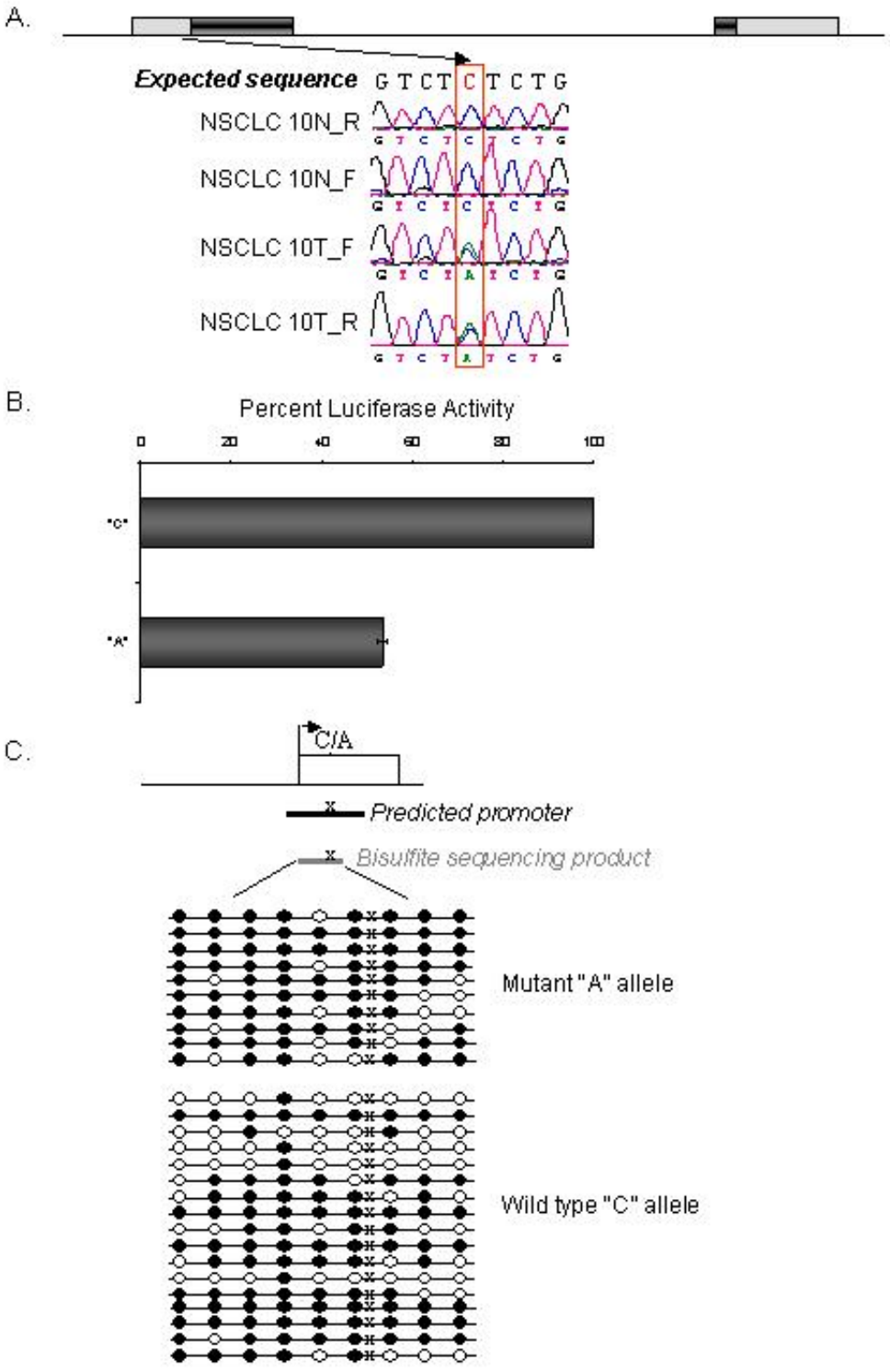
A.
Expected sequence G T C T C T C T G
NSCLC 10N_R
NSCLC 10N_F
NSCLC 10T_F
NSCLC 10T_R
B.
Percent Luciferase Activity
0
20
40
60
80
100
"C"
"A"
C.
C/A
Predicted promoter
Bisulfite sequencing product
Mutant "A" allele
Wild type "C" allele

Figure 4.3: TCF21 reduces properties associated with cancer *in vitro*.

A. A549 cells lacking or transduced to express TCF21 were synchronized using serum starvation for 12 hours. Growth curves were then determined by plating 200,000 cells in triplicate for 2, 4 and 6 days. Cellular expansion was counted on days 2, 4, and 6 using the Coulter Counter, and the averages of all 6 counts for each time point are plotted. B. Colony formation was determined by crystal violet staining following a 14-day expansion from 1000 original cells in triplicate. Visible colonies, or those containing ~20 cells, were counted and the average of all plates is plotted in the bar graph. C. TCF21 induces differentiation as determined by semi-quantitative RT-PCR on mesenchymal markers (vimentin and snail) and epithelial markers (E-cadherin and Wnt4a) in A549 TCF21 null (pBABE) and A549 TCF21 positive (myctcf21) cells.

A.

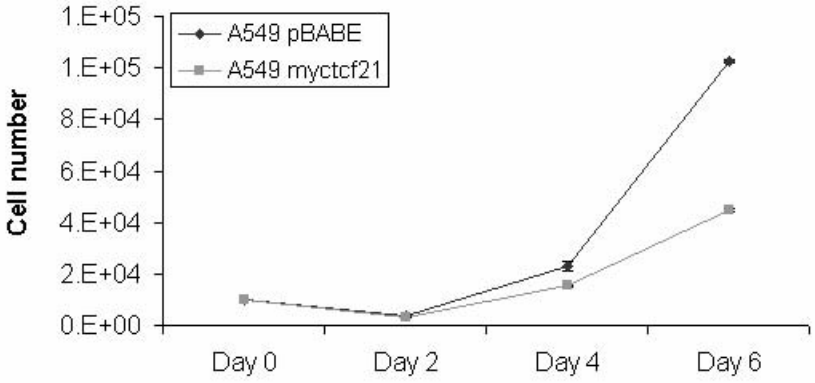
1.E+05
1.E+05
8.E+04
6.E+04
4.E+04
2.E+04
0.E+00
Cell number
A549 pBABE
A549 myctcf21
Day 0
Day 2
Day 4
Day 6

B.

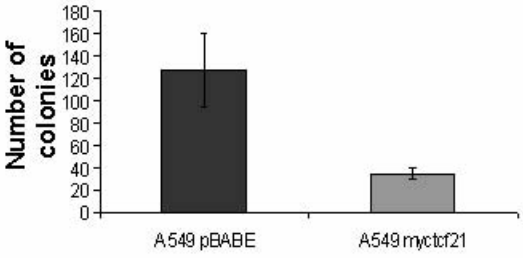
180
160
140
120
100
80
60
40
20
0
Number of colonies
A549 pBABE
A549 myctcf21

C.

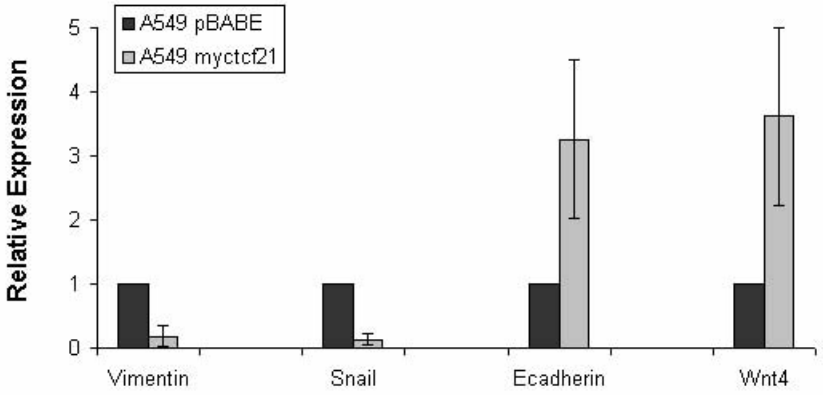
5
4
3
2
1
0
Relative Expression
A549 pBABE
A549 myctcf21
Vimentin
Snail
Ecadherin
Wnt4

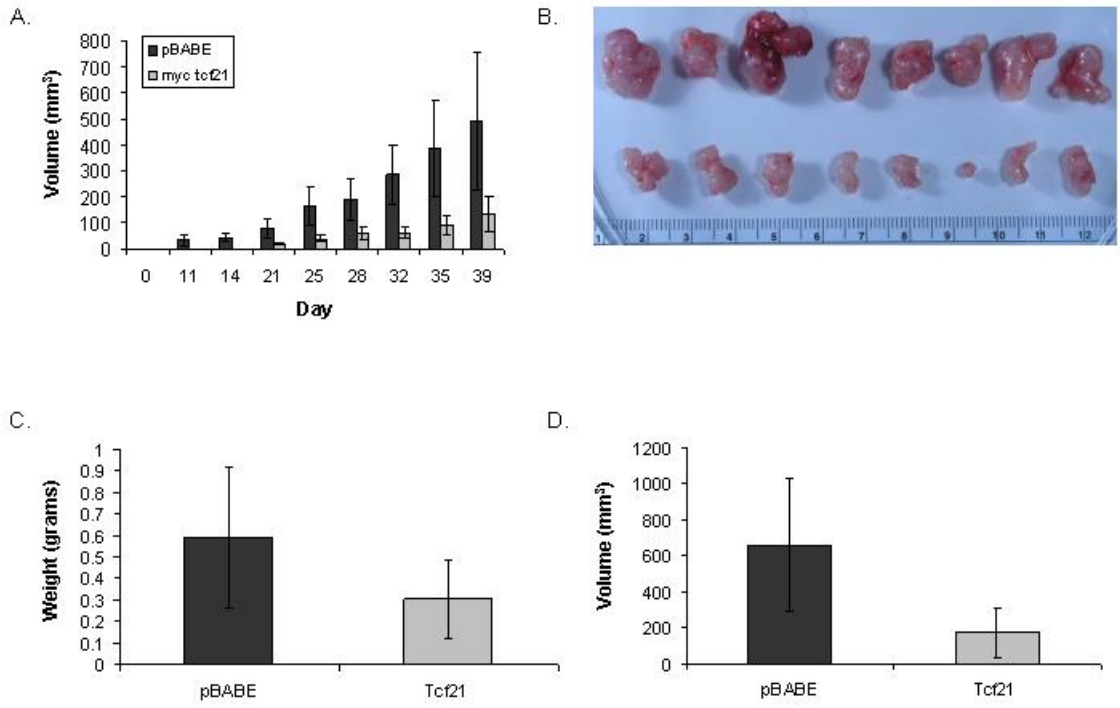

Figure 4.4: TCF21 expression results in reduced tumor potential *in vivo*.

A. *In vivo* determination of tumor volumes injected subcutaneously. Caliper measurement of tumor volumes from opposing flanks of nude mice demonstrates that TCF21 expressing tumors are delayed and markedly smaller. B. *Ex vivo* imaging of tumors isolated 40 days post injection (dpi). Tumors derived from TCF21 null cells are in the top row, while TCF21 positive tumors are on the bottom row. *Ex vivo* determination of the average tumor weights and volumes are depicted in C and D.

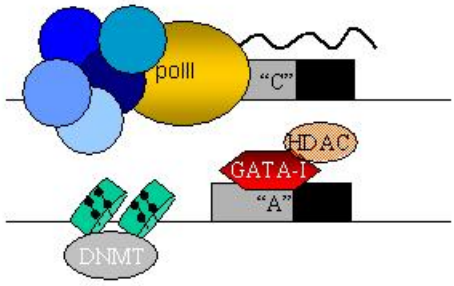

Figure 4.5: Possible model for specific regulation of the mutant TCF21 allele. Along the wild type "C" allele, transcriptional machinery, including RNA polymerase II (polII) binds the promoter portion of TCF21 and transcription of the mRNA ensues. On the mutant allele "A", GATA-1 binds to the newly created binding site, recruiting histone deacetylase proteins (HDAC) to remodel the surrounding chromatin, rendering the allele transcriptionally silent. Maintenance of the silenced allele is established by epigenetic DNA methylation of cytosine by DNA methyltransferases (DNMT).

CHAPTER 5:

TCF21 MODULATES METASTASIS

5.1 Introduction

Metastasis is the process in which tumor cells, originating from the primary tumor site, have obtained the ability to spread to distant sites via circulation in the bloodstream or the lymphatics [158]. Metastasis is the leading cause of cancer-related deaths, as these cells are often resistant to conventional anti-cancer therapies[151]. Each metastatic growth at a secondary site is from clonal growth of a single cell [158]. As previously stated, loss or translocations of chromosome 6q have been described in many human malignancies. Many of these studies correlate with advanced metastatic disease, indicating the importance of a gene or genes located along the chromosome for this process[20; 115; 116; 117; 159; 160].

In addition to the identification of tumor suppressor genes, metastasis suppressor genes have similarly been identified through these low-resolution genome scans. However, to date, only 17 metastasis suppressor genes have been identified[161]. Generally, metastasis suppressor genes have been identified by reduced expression in cell lines that are metastatic compared with cell lines

that are no longer metastatic[162]. In addition, to specify a gene as a metastasis suppressor and not a tumor suppressor gene, the expression of the gene typically inhibits only the process of metastasis, without altering the tumorigenecity[161; 162].

The importance of localizing target genes essential to the metastatic cascade is evident in HNSCC and NSCLC, where approximately 50% of the patients succumb to disseminated disease within 5 years of diagnosis[163; 164]. Fifty to sixty percent of patients already have positive lymph nodes at the time of tumor diagnosis[165]. Micro-metastatic patches, not detected at the time of surgical resection, but instead manifesting at the time of histological analysis and/or onset of secondary primary tumors in as many as 30% of the patients, account for many of the complications associated with treating and managing these malignancies[163]. This is largely because of the "field cancerization" phenomenon observed in these tumor types; presumably due to widespread tissue exposure to carcinogens from tobacco smoke[4]. Identification of markers of metastatic spread could potentially aid in diagnosis, prognosis, or serve as potential therapeutic targets. Providing a "molecular block" at one of the necessary components of the metastatic cascade is believed to block metastatic spreading[166].

Loss of heterozygosity at 6q22 and 6q23-q24 has been associated with malignant, but not benign, endocrine pancreatic tumors, tumors larger than 2cm, and more frequently lost in tumors with metastatic disease[108]. Microcell-mediated chromosome transfer of chromosome 6q, specifically a 45Mbp region

along 6q16.3-q23, was able to suppress metastasis of the highly invasive C8161 melanoma cell line, indicating an important location harboring a metastasis suppressor gene[118; 167]. Expression differences between metastatic and non-metastatic C8161 clones identified KiSS-1 as expressed exclusively in the non-metastatic cells[117]. Surprisingly, KiSS-1 was subsequently localized to chromosome 1q32, leaving the KiSS-1 transactivating factor from chromosome 6q unidentified[117; 168].

Full length KiSS-1 mRNA is comprised of 797 base pairs from 4 exons[168]. The first two exons are untranslated, while exon 3 and 4 contain 103 and 335 translated bases, respectively, resulting in a 145 amino acid protein[168]. KiSS-1 contains an amino-terminal 19 amino acid secretion signal peptide, indicating that the protein product is secreted extracellularly[169],[170]. The remaining 126 amino acid protein has no homologies to other known proteins[170]. Within the full length KiSS-1 protein there is a cleavage site that results in the 54 amino acid metastin product[169]. Metastin has been shown to be the natural ligand to the GPR54 receptor[169]. Metastin has autocrine and endocrine effects on cell motility and metastasis[170].

Correlative studies have provided credence to the suppressive function of KiSS-1 in metastasis in patient samples, as well as *in vitro*[170; 171]. The processed KiSS-1 protein, encoding 54 amino acids, termed metastin, is the portion that acts as the natural ligand for the GPR54 receptor[172]. Metastin was able to suppress metastatic melanoma cells[173]. The function of KiSS-1 is to cause an

increase in intracellular calcium that results in increased focal adhesions, preventing metastasis[172]. The ability of a cancer cell to migrate to distant sites depends, in part, on the breakdown of the basement membrane surrounding the organ containing the tumor cells[173]. Enzymes that assist in this process are matrix metalloproteases (MMP's)[173]. Metastin is bound by MMP and becomes cleaved, inactivating its metastasis suppressive ability[172].

Further studies aimed towards identifying genes involved in metastasis are essential because the most lethal feature of cancer is the ability to metastasize to distant sites[151; 152; 174]. Modifications of the restriction landmark genomic scanning (RLGS) procedure described in Chapter 2 allowed for the identification of a novel tumor suppressor gene, TCF21, located within region also associated with metastasis. TCF21, a basic helix loop helix transcription factor has been demonstrated to be involved in mesenchymal to epithelial transitions (MET) in normal embryogenesis[134; 175]. Its silencing and function in human malignancies have not been investigated previously, although the transition to mesenchymal cells has proven vital for dissemination of carcinomas. Once tumor cells have achieved a dedifferentiated status, the rate of single-cell metastasis increases, which relates with poor survival outcome[150]. Based on its physical location and its function in development, we investigate the function of TCF21 as a metastasis-suppressing gene, and its function as the much sought after KiSS-1 transactivating factor from chromosome 6q.

5.2 Materials and Methods

SYBR green RT-PCR:

Ten picomols of KiSS-1 PCR primers (forward, 5' cactttggggagccattaga and reverse, 5' ccagttgtagttcggcaggt) were used in a semi-quantitative RT-PCR reaction using SYBR green to quantitate differences in expression in C8161 in the absence or presence of TCF21. Threshold crossing values were normalized using GPI primers (forward, 5' GACCCCCAGTTCCAGAAGCTGC; reverse, 5' GCATCACGTCCTCCGTCACC). KiSS-1 expression in C8161 myctcf21 was normalized relative to C8161 pBABE levels.

Chromatin Immunoprecipitation:

Ten centimeter culture plates of C8161 pBABE and C8161 myctcf21 were grown to confluency and proteins were crosslinked to DNA using 10ml of RPMI-1640/10% FBS containing 270ul of 37% formaldehyde for 10 minutes at room temperature on a rotating platform. Five hundred microliters of 2.5M glycine was added to the crosslinking medium and rotation continued for an additional 5 minutes. The medium was removed and the plates were washed with 10ml of ice-cold PBS plus protease inhibitor complex, PIC, (P8340, Sigma) for 5 minutes. Cells were scraped into 3ml PBS+PIC and counted using the Coulter Counter. Two hundred thousand cells of each cell line were used for the remainder of the ChIP assay using the Upstate ChIP kit with slight modifications. The cells were resuspended in 200ul of SDS lysis buffer plus PIC and placed on

ice for 10 minutes. DNA was sonicated at 4°C to 0.2kb to 1kb using the Misonix XL-2020 sonicator. The samples were pelleted at 14,000rpm for 10 minutes at 4 °C. The supernatant containing the fragmented DNA was transferred to a new 2ml screw-cap microcentrifuge tube. 1.8ml of Dilution buffer (Upstate) containing PIC was added to the supernatant fractions. Twenty microliters was removed from each sample to serve as the input DNA control in each PCR reaction (1ul/reaction). The supernatant fraction was pre-cleared using 80ul of Salmon Sperm/Protein A agarose slurry (Upstate) and rotated at 4 °C for 1 hour. The supernatant and slurry was spun down at 10,000rpm for 30 seconds at 4°C. The supernatant was transferred to a new 2ml centrifuge tube. One microgram of anti-myc antibody was added to both C8161 pBABE that contains no corresponding protein and to C8161 myctcf21 supernatants and then rotated overnight at 4 °C. Sixty microliters of the salmon sperm/protein A agarose slurry was added to the mixture and the tubes were rotated for 1 hour at 4 °C. Following a 1-minute centrifugation at 1000rpm at 4 °C, the supernatant was discarded, leaving the slurry/protein A/antibody/DNA pellet. Each sample was washed with 1 ml of each of the following Upstate buffers, individually, for 5 minutes one time at 4 °C with rotation: low salt (0.1% SDS, 1% Triton X-100, 2mM EDTA, 20mM Tris-HCL, pH 8.1, and 150mM NaCl), high salt buffer (0.1% SDS, 1% Triton X-100, 2mM EDTA, 20mM Tris-HCL, pH 8.1, and 500mM NaCl) and LiCl buffer (0.25M LiCl, 1% NP40, 1% deoxycholate, 1mM EDTA, and 10mM Tris-HCL, pH 8.1). Between each wash, the slurries were recovered through a 1-

minute centrifugation step at 1000rpm. The final two wash steps were in TE buffer (10mM Tris-HCL, 1mM EDTA, pH 8) for 5 minutes each at 4 ^{o}C. After the final centrifugation, the wash was discarded, and the pellets were suspended in 250ul of elution buffer (1% SDS, 0.1M $NaHC0_3$). Twenty microliters of 5M NaCl was added to the eluate and protein/DNA cross-linking was reversed at 65 ^{o}C for 4 hours. Rnase (0.5ug/ul), 10ul 0.5M EDTA, 20ul 1M Tris (pH 6.5), and 20ug of Proteinase K was added and the samples were incubated at 45 ^{o}C for 1 hour. DNA was purified using PCI extraction, followed by ethanol precipitation in the presence of glycogen. The DNA pellet was resuspended in 200ul of H_20. Two microliters of the final DNA suspension was used in each PCR reaction.

ChIP-PCR reactions against KiSS-1 DNA were performed in the presence of several primer pairs designed in the 5' region of KiSS-1: KiSS-ChIP-1 (forward, 5' CTCTGCTCCTAGGGGCTTTT and reverse, 5' GGCAGCAGTTTTACCAGCTC), KiSS-ChIP-4 (forward, 5' TGAGATTTCTGGGGATCTGG and reverse, 5' CCAGGTGCTTCAGAGAAAGG), KiSS-ChIP-6 (forward, 5' CTCTCAAGGCCAGCTCTGTAA and reverse, 5' CCTTGAAGTCTCCGGAACAG), KiSS-ChIP-7 (forward, 5' CAAGGCACTAGCTCGATGGT and reverse, 5' GAGTCGACTTGGGGATTTGA), and KiSS-ChIP-10 (forward, 5' TTGCAGGCTCAAGAAAGAGA and reverse, 5' TGCTCAGGTACAGCACTTTGA) and an intronic KISS-1 primer pair: KiSS-ChIP-intron (forward, 5' caaccatgcctggaatttct and reverse, 5' ccatcggggcacttaacata).

The PCR reactions contained 50 pmol of each primer, were carried out

at 95 ^{o}C for 10 minutes, followed by 30 cycles of 95 ^{o}C for 30 seconds, 60 ^{o}C for 30 seconds, and 72 ^{o}C for 30 seconds, with one 10 minute extension step at 72 ^{o}C. Twenty microliters of each PCR reaction were loaded onto 8% PAGE gels, stained with ethidium bromide wash, and visualized.

TCF21 retroviral infection of C8161 cell lines:

Ten micrograms of pBABEmycTCF21 plasmid or pBABE vector alone were transfected into the amphotropic Pheonix packaging cell line (60% confluent) using the Superfect reagent following Qiagen's protocol at experimentally determined 1:6 ratio of DNA:Superfect, and returned to the 37^{o}C incubator. Three hours following the initial transfection, the cells were washed once with 5ml PBS, and then 8ml of DMEM-15%FBS-Penicillin/Streptomycin was added gently to the side of the culture dish to prevent dislodging the cells. Twenty-four hours later, virus-containing medium was collected from the Pheonix cells, and cell debris was removed by centrifugation at 1000rpm for 5 minutes in the presence of 2X polybrene. Four milliliters of infectious medium, containing either pBABEmycTCF21 or pBABE vector alone, was added to the surface of 40% confluent C8161 cells, and incubated at 37^{o}C. To surface of the Pheonix cells, 8ml DMEM-15%FBS-Penicillin/Streptomycin was added. After 12 hours, the infectious medium from C8161 was removed and replaced with 4ml of new infectious medium. Twenty-four hours following, the viral-medium was removed, the infected cells were washed with PBS, and normal RPMI-

1640/10%FBS/Penicillin/Streptomycin was added to the cultures. The following day, infected cells were washed, trypsinized, and split 1:5. Selection medium was added to the cell cultures (RPMI-1640/10%FBS/Penicillin/Streptomycin + 5ug/ml Puromycin (Sigma) to select for only cells that have been infected by the viral constructs. As a control, wild type C8161 cell lines were also treated with Puromycin to establish when wild type cells should be completely eliminated by the drug in the transduced cultures. Seven days of selection resulted in a total loss of wild type C8161 cells under puromycin drug selection.

In vitro* metastasis Assay*:

Wild type C8161 (kindly donated for these experiments from Dr. Bernard Weissman (University of North Carolina)), C8161pBABE, and C8161mycTCF21 cell lines were serum starved in RPMI-1640 medium, lacking FBS, for 18 hours. Following starvation, cells were counted using the Coulter Counter, and 200,000 cells were plated in duplicates onto the 96-well Collagen Invasion Assay (Chemicon). Twenty-four hours post cell plating, cells that had migrated to the underside of the matrix were lysed according to the manufacturer's instructions, and nuclei were fluorescently stained. Migration was determined by measuring the amount of fluorescence from each sample using at 480/520nm. Average fluorescence was plotted for each cell line, along with the corresponding standard deviation.

5.3 Results

C8161 lacks endogenous TCF21

C8161 is a highly metastatic melanoma cell line derived from an abdominal wall metastasis. Work performed in the early 1990's using the C8161 cell line demonstrated that the addition of a functional copy of 6q into the wild type cell line, which contains deletions along 6q, was able to suppress the metastatic capacity of these cells *in vivo* in athymic mice. To determine if TCF21 may abrogate metastasis, it was first important to establish if TCF21 was expressed in untreated C8161 cells. RT-PCR performed on cDNA generated from C8161 demonstrated a complete lack of TCF21 expression (Figure 5.1A). Since chromosome 6q deletions have been reported for C8161, we initially hypothesized that loss of TCF21 expression might result because of homozygous deletions along the TCF21 locus. Surprisingly, fluorescent in situ hybridization using a bacterial artificial chromosome that contains the TCF21 sequence, determined that in over 100 metaphase spreads, dual signal was detected, indicating that both chromosomal regions, at least in the context of the BAC clone, were present (Figure 5.1B). However, small intragenic deletions along TCF21 were not investigated. Bisulfite treatment followed by CoBRA digestion using *BstUI* revealed that the bis1 region of the CpG island is largely hypermethylated (Figure 5.1.C) as seen in primary patient samples and cell lines from HNSCC and NSCLC. *In vitro* demethylation allowed for TCF21 expression to be restored following 48 hours in the presence of 3uM or 5uM 5-aza-2-

deoxycytidine (Figure 5.1D). Somatic mutations at the level of genomic DNA were also not found within the TCF21 locus (not shown). Taken together, TCF21 silencing in this cell line was due to hypermethylation and not genetic alterations such as deletion or mutation.

TCF21 overexpression upregulates KiSS-1:

Microcell-mediated chromosome transfer of 6q16-q23 results in suppression of metastasis in C8161. Interestingly, the suppression was via upregulation of the metastasis suppressor gene, KiSS-1, which is located on 1q32, and not chromosome 6. From this important study, the authors concluded that a transactivating factor for KiSS-1 must reside in 6q16-q23. Because of TCF21's role as a transcription factor within this particular chromosomal region, we sought to investigate a possible relationship between TCF21 and KiSS-1.

C8161 clones that have a portion of 6q containing TCF21 and surrounding sequences through microcell-mediated chromosome transfer experiments, express not only TCF21, but have increased KiSS-1 expression as well (Figure 5.2A). However, these clones also have additional expressed genes that could increase KiSS-1 expression. Because of this possibility, we determined the effect that TCF21 confers on KiSS-1 by transducing C8161 to express TCF21. Expression of KiSS-1 was determined by RT-PCR and a 5-fold increase in KiSS-1 message was detected in the presence of TCF21 (Figure 5.2A) in C8161 neo6q clones 1, 2, and 3, as well as in C8161 cells transduced with viral TCF21.

However, this expression analysis did not determine if TCF21 is physically bound to the KiSS-1 gene or if the upregulation is a result of an intermediate player between the two genes.

Chromatin Immunoprecipitation assays using the anti-myc-tag antibody that specifically recognizes the exogenously expressed TCF21-myc fusion protein were performed to isolate DNA bound with TCF21 protein. Primers were designed within 3kbp upstream of the KiSS-1 transcription start site surrounding E box sequences (5' CANNTG), which are potentially bound by TCF21's binding partner, E2A (Figure 5.2B). Immunoprecipitation of KiSS-1 DNA using an antibody that specifically recognizes the myc-tag portion of stably integrated mycTCF21 demonstrates that TCF21 is able to bind to KiSS-1 (Figure 5.2C). The control cell line, C8161 pBABE, however, did not precipitate KiSS-1 DNA with the antibody, indicating that the protein-DNA interactions were not due to non-specific antibody artifacts. An additional primer located 461 to 606 base pairs from the 3' end of exon 1 into intron 1 of KiSS-1 that does not contain TCF21/E2A potential binding sites was negative for DNA pull-down by the antibody against the myc-tag in both cell lines (Figure 5.2C). This indicates that binding in the 5' region of KiSS-1 by TCF21 is not an artifact but a direct interaction between the protein and the KiSS-1 DNA. Hence, increased KiSS-1 expression in the presence of TCF21 is directly mediated by this protein-DNA interaction.

TCF21 involvement in metastasis:

Because of the role of TCF21 as a transcription factor involved in differentiation through mesenchymal to epithelial transitions, and the involvement of this pathway in metastatic progression, we performed *in vitro* analysis of TCF21's ability to suppress invasive properties of metastatic cells using a collagen-covered matrix system (Chemicon). All cell lines were serum starved in order to enhance the invasive migration towards the lower chamber which contains the sought after growth factors. Overexpressoin of TCF21 in the wild type C8161 cell line, which lacks endogenous TCF21 expression, resulted in a reduced capacity for the cells to invade collagen, a component of the extra-cellular matrix (Figure 5.3). These data indicate that while tumor cells expressing TCF21 remain tumorigenic in nude mice, their ability to metastasize is may be stunted.

5.4 Discussion

In this chapter, we have uncovered anti-metastatic properties of TCF21 in a melanoma cell line, C8161. TCF21, a gene encoding a basic helix loop helix transcription factor, is localized within a recognized region of LOH along chromosome 6. Previous reports have correlated losses along this region are associated with poor prognosis, tobacco smoking, and metastatic potential in several human cancers. TCF21 functions as a zinc finger, DNA binding transcription control factor involved in maintenance of the epithelial phenotype of

a cell through differentiation via MET. TCF21 is involved in crucial mesenchymal to epithelial transitions during organogenesis of the lungs, heart, kidneys, spleen, and facial structures during normal embryogenesis. Mesenchymal to epithelial transitions (MET) occur normally during endodermal lung branching, kidney and mammary gland developments[144]. Mesenchymal cells migrate and settle in areas of organ formation through MET. In fact, mesenchymal cells form all migrating cells, as well as providing structural support from the epithelium. The mesenchymal layer found in vital organs has reorganized cytoskeleton and degradation of the basal lamina [144]. Mesenchymal cells are more mobile and have lost the cell-to-cell contact that epithelial cells retain through cadherin molecules [144]. However, differentiated epithelial cells can be induced to migrate from their origin to distant locations, requiring epithelial to mesenchymal transitions (EMT).

Carcinomas, tumors derived from the epithelium, lose most of their epithelial characteristics during tumorigenesis[143]. As well as involvement in normal developmental migration, loss of differentiation from epithelial to mesenchymal cell type is often observed in metastatic carcinomas in a process known as epithelial to mesenchymal transitions (EMT)[149; 150]. EMT-induced cellular plasticity is a landmark of carcinoma progression and metastasis. In order for tumor cells to spread within primary or secondary tissues, tumor cells utilize migratory mechanisms highly similar to normal cellular processes involved in embryogenesis and wound healing. During EMT, loss of cell junctions, loss of

extracellular matrix attachment, and induced mobility have been noted[144]. In addition to enhanced metastatic characteristics, mesenchymal cells have been associated with a reduction in apoptotic-sensitivity[144]. Markers for EMT can be detected in premalignant lesions, indicating that the process begins early in tumorigenesis[144].

The timing of events, including the expression of bHLH transcription factors, is central to ensure proper embryologic development. Previous studies have reported a complete shift in differentiation by overexpressoin of a single transcription factor. Our results obtained from overexpressing TCF21 support the notion that differentiation of cancer cells ensues. Wnt4 and E-cadherin expression are restored, while vimentin and snail expression are diminished, indicating a shift in cellular phenotype from mesenchymal towards epithelial.

Our studies further demonstrate that TCF21 is a direct activator of the known metastasis suppressor along 1q32, KiSS-1. C8161 cells transduced to express TCF21 have similar levels of KiSS-1 activation as the microcell-mediated chromosome transfer C8161 clones containing DNA from the TCF21 locus and surrounding sequences (neo6q1,2,3), while the pBABE C8161 cells express minimal amounts of KiSS-1. The presence of TCF21 physically bound to KiSS-1 indicates that the upregulation is directly mediated by this protein-DNA interaction in this system. Recently, CRSP3 was identified from the chromosome 6q region in the non-metastatic C8161 clones where KiSS-1 was upregulated[176]. CRSP3 is involved in the vitamin D pathway, which regulates transcription of

another candidate metastasis suppressor gene, TXNIP[176]. CRSP3 is located 2.3Mbp centromeric to TCF21 within this core metastasis suppression region. Like KiSS-1, TXNIP localizes along chromosome 1q that is upregulated by transactivating factors from chromosome 6q[176]. Because of CRSP3 upregulation in these clones, it was concluded to be the transactivator from 6q23[176]. However, *in vivo* suppression of metastases was not complete in cell lines overexpressing CRSP3[176]. It is plausible that CRSP3 and TCF21 both function to upregulate KiSS-1, as no direct binding of CRSP3 to KiSS-1 was described, only increased transcript[176].

The ability of cells to migrate from the primary tumor requires the enzymatic degradation of the extracellular matrix through matrix metalloproteases (MMPs). MMPs are frequently targeted for increased activity in cancer, facilitating migration[150; 172]. Full length KiSS-1 protein is bound by MMP9 at the amino terminus of KiSS-1[172]. This interaction with MMP9 results in the cleavage of KiSS-1 between glycine at position 118 and leucine 119[172]. This cleavage MMP9 inactivates KiSS-1's ability to suppress metastasis[177]. As a feedback regulatory loop, KiSS-1 signaling has also been shown to downregulate MMP9 activity through decreased nuclear accumulation of p65 and p50 proteins of NFKβ[177]. These NFKβ protein subunits bind to and activate the promoter of MMP9, specifically[177]. Loss of TCF21, therefore, contributes to enhancing MMP activity through downregulation of KiSS-1, allowing for degradation of the extracellular matrix to facilitate tumor cell invasion and migration[177].

Contributing to the mesenchymal phenotypes, we propose that the loss of TCF21 function is advantageous for epithelial-derived tumors, enhancing their metastatic properties. By definition, metastasis suppressor genes only function to inhibit a step in the metastatic cascade, but allow for the tumor cells to remain tumorigenic[152]. Of the metastasis suppressor genes identified, only E-cadherin has been described as inhibiting tumorigenecity as well[178]. Akin to E-cadherin, we demonstrate anti-tumor properties of TCF21 in a lung cancer cell line in Chapter 4. While A549 cells expressing TCF21 remain able to form tumors *in vivo*, the size of the tumor growth is significantly reduced.

TCF21 is recognized as a transcription factor whose target genes and their pathways remain largely undiscovered. It is plausible that TCF21, through downstream targets, can inhibit both tumorigenesis and metastasis (i.e. through KiSS-1) in different cell types. Interestingly, metastasis suppressor genes are rarely found to contain somatic mutations[158]. Instead, metastasis suppressor genes are frequently altered epigenetically or posttranscriptionally, both mechanisms do not alter the genetic sequence[158]. Given that, the finding that TCF21 is hypermethylated frequently in the human malignancies tested, but has only one identified mutation, fits with this model.

Identification of TCF21-regulated pathways will provide insight into human malignancies. Metastasis is a highly inefficient process by which only 0.1% of cells deposited into circulation from the primary site actually lead to proliferating lesions at secondary sites[151]. Inhibition of any contributing steps in metastasis

has proven sufficient to eliminate dissemination[151]. Understanding genes involved in the cascade, including TCF21, provide potential molecular mechanisms for anti-metastatic therapies.

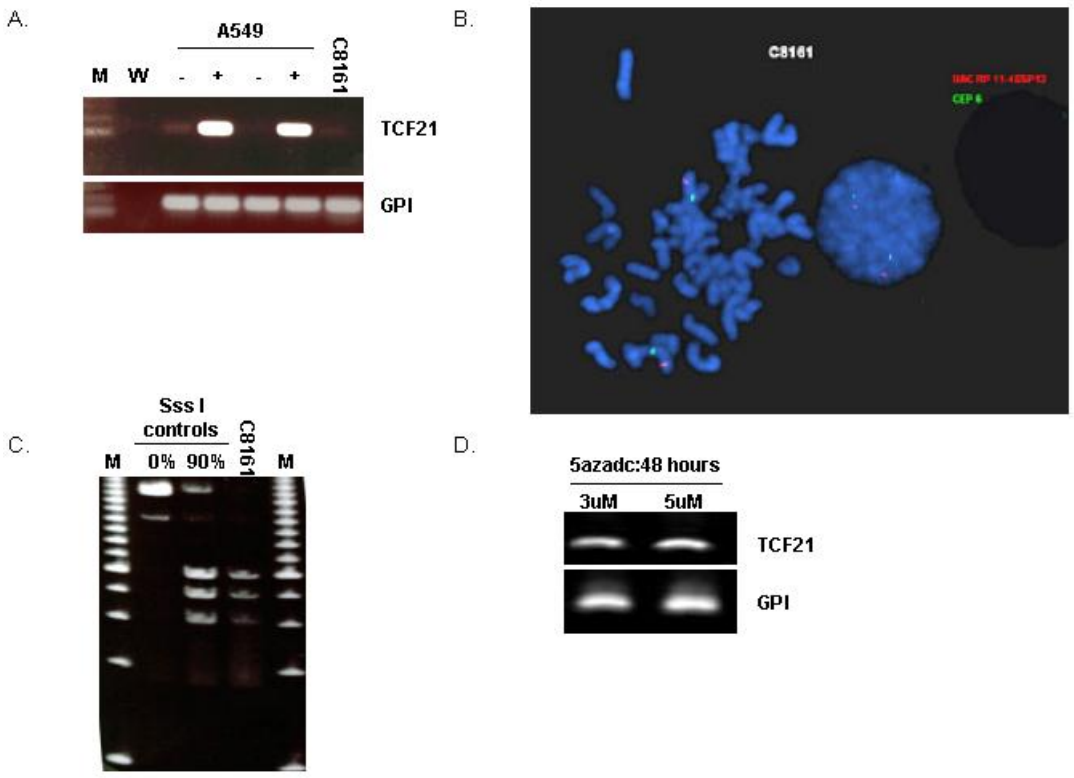

Figure 5.1: TCF21 silencing in C8161.

A. C8161 lacks TCF21 expression as determined by RT-PCR. A549 pBABE (-) cells and A549 myctcf21 (+) expression were used as controls. B. Bacterial artificial chromosomal-fluorescent *in situ* hybridization (BAC-FISH) using the BAC containing TCF21 genomic DNA, RP11-465P13 (red probe) and the centromeric probe for chromosome 6, CEP 6 (green probe). Hybridization results in dual signals indicating that both chromatids are present in the nuclei. C. CoBRA using the TCF21-bis1 primers, demonstrates that this portion of TCF21 is completely methylated in C8161. D. 5-aza- 2'-deoxycytidine treatment (3 or 5 uM) for 48 hours results in TCF21 re-expression.

Figure 5.2: KiSS-1 expression is regulated by TCF21 binding.

A. Expression of KiSS-1 in C8161 melanoma cell lines that express TCF21 (myctcf21, neo6q.1, 2, 3) and in TCF21 negative C8161 cell lines (C8161pBABE). Reference cDNA was made from a compilation of RNA from 10 different cell lines from human cancers (Stratagene). B. Physical location of KiSS-1 chromatin immunoprecipitation (ChIP) primers. E-box sequences (CANNTG) are denoted with (●). C. ChIP-PCR results precipitated with the anti-myc-tag along the upstream and intronic regions of KiSS-1 in C8161 pBABE (-TCF21) and C8161 myctcf21 (+TCF21) cell lines.

A.

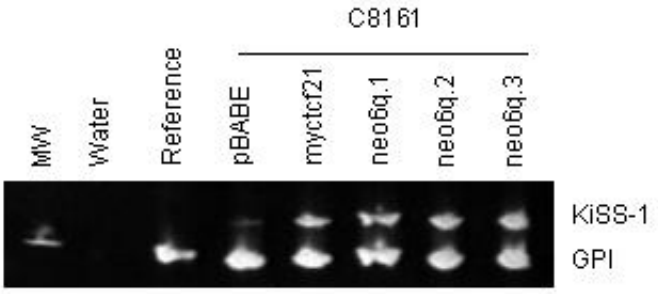
C8161
MW
Water
Reference
pBABE
myctcf21
neo6q.1
neo6q.2
neo6q.3
KiSS-1
GPI

B.

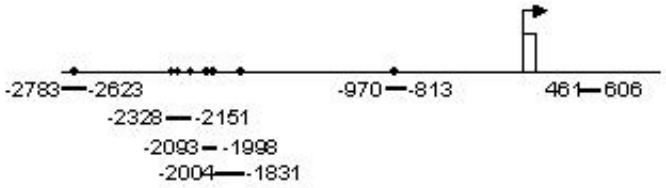
-2783—-2623
-2328—-2151
-2093—-1998
-2004—-1831
-970—-813
461—606

C.

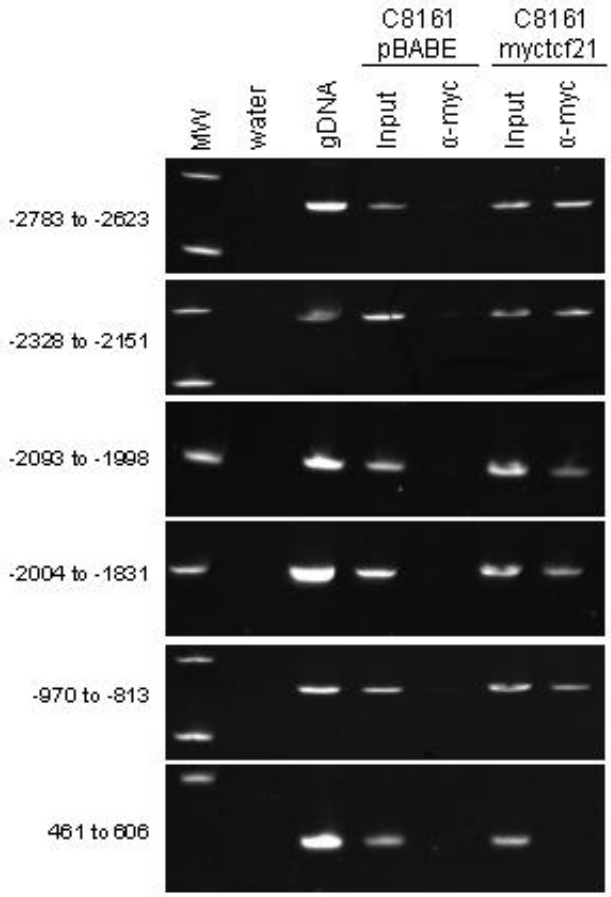
C8161 pBABE
C8161 myctcf21
MW
water
gDNA
Input
α-myc
Input
α-myc
-2783 to -2623
-2328 to -2151
-2093 to -1998
-2004 to -1831
-970 to -813
461 to 606

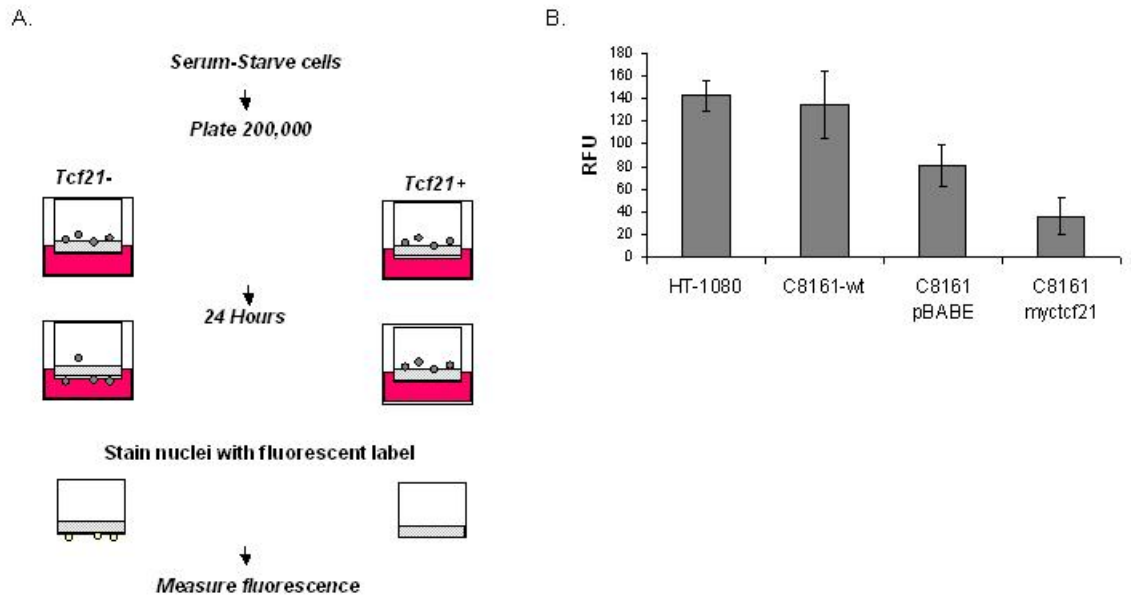

Figure 5.3: TCF21 expression reduces the metastatic potential of C8161.

A. Schematic diagram of the *in vitro* invasion assay by Chemicon. B. Fluorescent calculations of metastatic capabilities of HT-1080, a highly invasive fibrosarcoma cell line; the parental C8161-wt cell line and C8161 transfected with the empty pBABE plasmid, which lack TCF21, and C8161 mycTCF21 that expresses TCF21.

CHAPTER 6:

FUTURE DIRECTIONS

6.1 *In vivo* Metastasis Assay

The surrounding microenvironment is critical to proper tumor development[144]. Currently, experiments in athymic nude mice are underway to determine if TCF21 prevents metastasis *in vivo* are underway. C8161 cell lines (pBABE and mycTCF21) were infected with a HIV plasmid containing constitutively expressed YFP/Luciferase. The minimum number of detectable cells using the *In vivo* Imaging System (IVIS, Xenogen) was determined through a serial dilution of cells. For both C8161 pBABE/YFP/Luciferase and C8161 myctcf21/YFP/Luciferase, the least number of detectable luciferase activity was from approximately 240 cells (not shown).

One million C8161 pBABE/YFP/Luciferase or C8161 myctcf21/YFP/Luciferase cells were subcutaneously injected into the dorsal lateral flanks of 10 athymic mice per group (Jackson Lab, Maine). Biweekly caliper measurements determined the *in vivo* growth rates of the tumor cells. Once per week, mice were injected i.p. with 110ul (15ug/ul) D-Luciferin substrate,

anesthetized using an isofluorane chamber, and given 5 minutes for optimal luciferase activity prior to IVIS imaging. Metastatic lesions will be detected *in vivo* once a week for 8 weeks. Following the 8 weeks, the mice will be sacrificed and metastatic lesions will be investigated using immunohistochemistry with human-specific antibodies to distinguish the cells originating from the primary tumor that disseminated to secondary sites. Organs that will be sectioned for histology have previously been determined as targets for C8161 metastatic spread and include the lungs and spleen. In addition, upon sacrificing the animals, individual organs will be analyzed for luminescent signal, and if detected, these organs will also be sent for histological sectioning. Based on our data that TCF21 up-regulates KiSS-1 expression in C8161, a known metastasis suppressor gene, and the ability of TCF21 to inhibit invasion of the collagen matrix *in vitro*, we speculate that mice harboring tumors that express TCF21 will have less metastatic lesions than the mice that have TCF21- tumors.

6.2 Determination of TCF21 pathways and binding partners

Cells that contain or lack TCF21 expression will be screened for pathways that are deregulated, either positively or negatively, using microarrays. Although the observed data may be indirect, inferences regarding potential pathways can be discerned. Triplicate hybridizations from independent experiments will provide confidence in the identified results, thus tightening the potential list of TCF21 target genes.

The function of TCF21 has been described in embryogenesis and development without detailed description of the involved pathways, binding partners, or target genes. Because of the dual role of TCF21 as a tumor suppressor gene and a potential metastasis suppressor, it is likely that TCF21 controls several independent pathways not yet reported.

Key to understanding the function of TCF21 is identification of the binding partners that are required for the gene regulation function. Classical approaches using the yeast two-hybrid system have successfully identified interacting proteins that were confirmed by electromobility shift assay (EMSA) experiments[133; 135]. EMSA establishes binding of proteins to specific DNA sequences in the form of ~30bp radioactively labeled oligos. Once a protein(s) is bound to the labeled oligo, the migration of the oligo is retarded and migrates higher in a polyacrylamide gel. The addition of a specific antibody against a protein of interest results in a higher shift in the migration pattern of the oligo, confirming that the protein is bound to the oligo.

Because TCF21 is not expressed ubiquitously, it is possible that there are tissue specific partners; therefore libraries of protein partners from different tissues will be screened. Immunoprecipitation assays will be applied to confirm the interactions. Mutation and deletion constructs will be applied to confirm and identify how these partners cooperate with TCF21 *in vitro*.

6.3 Lung Carcinogenesis Model In TCF21 Heterozygous Mice

In vivo tumor experiments in athymic mice derived from cell lines that express TCF21 as opposed to those that don't express TCF21 significantly demonstrate stunted growth (Chapter 4). Chemically-induced tumorigenesis in mouse models have been applied to substantiate a candidate tumor suppressor gene[154]. These models closely mimic the stages of human tumor progression and allow correlations to be made with human disease. While homozygous TCF21 null mice are neonatally lethal and therefore cannot be investigated for cancer susceptibility, the heterozygous mice are phenotypically similar to wild type TCF21 mice. However, this reduction of TCF21 protein by half may confer increased tumor susceptibility *in vivo*. We want to examine this system using chemical carcinogens that will be administered to provide additional pressure for tumorigenesis. If both alleles of TCF21 are necessary for blockade, this haploinsufficient environment in the presence of carcinogens should facilitate an increase in tumors in the TCF21+/- background. If, however, the presence of any functional TCF21 is protective, or if a lack of TCF21 is, in fact, not necessary for tumors to develop, there should not be a difference between drug and vehicle administered mice. The current heterozygous mice are in a 129 background, which are less susceptible for developing lung carcinomas than an A/J mouse[179; 180]. Because of this, we plan on backcrossing the 129 mice into the A/J strain for this set of experiments.

6.4 Clinical Correlation With Patient Status

The identification of biomarkers that correlate with lymph node involvement, survival, or even therapeutic regimens is crucial in clinical practice. Because TCF21 hypermethylation is exclusively found in tumor tissue, identification of this event in patient samples may serve as a diagnostic marker. To better evaluate in which stage, early or advanced disease, TCF21 methylation occurs, a cohort of hyperplastic, dysplastic, carcinoma *in situ*, locally invasive tumor tissue and lymph node tissue should be examined. As stated in chapter 1, diagnostic and predictive markers remain elusive for HNSCC. TCF21 hypermethylation is found in the vast majority of patient samples analyzed. Further, the ability to test patient samples is benefited by increasing data that have demonstrated the utility of isolating DNA from oral swabs or sputum samples, providing a non-invasive means for detecting epigenetic alterations of TCF21.

Because of the function of TCF21 in reducing the tumor growth, and possibly inhibiting metastasis, it is likely that patients with hypermethylated TCF21 would have a poor disease outcome. Retrospective survival curves on larger patient samples based on TCF21 methylation would assist in determining a correlation with patient outcome. If patients containing unmethylated TCF21 in their tumors have significantly better outcomes than those with hypermethylation, a prospective study should then be done. The correlation with outcome often translates clinically as to what type of therapy to utilize, whether more or less

aggressive. Therapeutically, demethylating agents are included in a number of anti-cancer regimens for leukemias with positive results. In solid tumors, however, data remains limited as to their effectiveness. Trepidation using these drugs arises in part because the cause and effect has not yet been fully understood. It remains uncertain whether administering these drugs will further substantiate cancer by demethylating DNA damaging retrotransposable elements or repetitive sequences enhancing chromosomal breaks.

6.5 Closing Remarks

These experiments were driven by the premise that regions of chromosomal aberrations contain genes whose function are crucial for maintaining the tight regulation of cells *in vivo*. Discord in this regulation facilitates neoplastic progression. The redundancy in chromosomal disarray, observed as homozygous deletion, translocations, or loss of heterozygosity, lend credence that the chromosome harbors important elements for maintaining cellular balance that can be rendered inactive both genetically and epigenetically. In addition to 6q23-q24, this technique can be applied to other commonly altered chromosomal locations for the presence of epigenetically silenced genes. This approach is high-throughput in that it establishes methylation patterns simultaneously for CpG islands distributed along chromosomal regions, allowing for methylation to be assessed concurrently within a patient sample.

Although molecular by nature, techniques aimed at identifying novel targets increase the level of information about extremely complex cancer. Cancer cells have the ability to emancipate themselves from the host's defenses in ways that remain copiously intangible. The overall expectation for these studies was to provide a better understanding to the molecular foundation of cancer. Eventually, my hope is that elucidation of pathways central to cancer will translate clinically to improve in the treatment of cancer.

BIBLIOGRAPHY

1. Vokes, E. E., Weichselbaum, R. R., Lippman, S. M. & Hong, W. K. (1993). Head and neck cancer. *N Engl J Med* 328, 184-94.

2. Crowe, D. L., Hacia, J. G., Hsieh, C. L., Sinha, U. K. & Rice, H. (2002). Molecular pathology of head and neck cancer. *Histol Histopathol* 17, 909-14.

3. Lemaire, F., Millon, R., Young, J., Cromer, A., Wasylyk, C., Schultz, I., Muller, D., Marchal, P., Zhao, C., Melle, D., Bracco, L., Abecassis, J. & Wasylyk, B. (2003). Differential expression profiling of head and neck squamous cell carcinoma (HNSCC). *Br J Cancer* 89, 1940-9.

4. van Oijen, M. G., and Pieter J. Slootweg. (2000). Oral Field Cancerization: Carcinogen-induced Independent Events or Micrometastatic Deposits? *Cancer Epidemiology, Biomarkers & Prevention* 9, 249-256.

5. Blot, W. J., McLaughlin, J. K., Winn, D. M., Austin, D. F., Greenberg, R. S., Preston-Martin, S., Bernstein, L., Schoenberg, J. B., Stemhagen, A. & Fraumeni, J. F., Jr. (1988). Smoking and drinking in relation to oral and pharyngeal cancer. *Cancer Res* 48, 3282-7.

6. Nam, J. M., McLaughlin, J. K. & Blot, W. J. (1992). Cigarette smoking, alcohol, and nasopharyngeal carcinoma: a case-control study among U.S. whites. *J Natl Cancer Inst* 84, 619-22.

7. Winn, D. M., Blot, W. J., McLaughlin, J. K., Austin, D. F., Greenberg, R. S., Preston-Martin, S., Schoenberg, J. B. & Fraumeni, J. F., Jr. (1991). Mouthwash use and oral conditions in the risk of oral and pharyngeal cancer. *Cancer Res* 51, 3044-7.

8. ENH. Vol. 2003. Evanston Northwestern Healthcare (ENH), http://www.enh.org/includes/print.asp?id=277, December 30, 2003.

9. Lopez, M., Aguirre, J. M., Cuevas, N., Anzola, M., Videgain, J., Aguirregaviria, J. & Martinez de Pancorbo, M. (2003). Gene promoter hypermethylation in oral rinses of leukoplakia patients--a diagnostic and/or prognostic tool? *Eur J Cancer* 39, 2306-9.

10. Ayude, D., Gacio, G., Paez de la Cadena, M., Pallas, E., Martinez-Zorzano, V. S., de Carlos, A. & Rodriguez-Berrocal, F. J. (2003). Combined use of established and novel tumour markers in the diagnosis of head and neck squamous cell carcinoma. *Oncol Rep* 10, 1345-1350.

11. Doweck, I., M Barak, N Uri, and E Greenberg. (2000). The prognostic value of the tumour marker Cyfra 21-1 in carcinoma of the head and neck and its role in early detection of recurrent disease. *British Journal of Cancer* 83, 1696-1701.

12. NCI. (2003). Screening for Oral Cancer, Vol. 2003. National Cancer Institute, http://www.cancer.gov/cancer_information/cancer_type/head_and_neck/, December 29, 2003.

13. Birkhaug, E. J., Aarstad, H. J., Aarstad, A. K. & Olofsson, J. (2002). Relation between mood, social support and the quality of life in patients with laryngectomies. *Eur Arch Otorhinolaryngol* 259, 197-204.

14. Leemans, C. R., Tiwari, R., Nauta, J. J., van der Waal, I. & Snow, G. B. (1994). Recurrence at the primary site in head and neck cancer and the significance of neck lymph node metastases as a prognostic factor. *Cancer* 73, 187-90.

15. Do, K. A., Johnson, M. M., Doherty, D. A., Lee, J. J., Wu, X. F., Dong, Q., Hong, W. K., Khuri, F. R., Fu, K. K. & Spitz, M. R. (2003). Second primary tumors in patients with upper aerodigestive tract cancers: joint effects of smoking and alcohol (United States). *Cancer Causes Control* 14, 131-8.

16. Satake, K., Takagi, E., Ishii, A., Kato, Y., Imagawa, Y., Kimura, Y. & Tsukuda, M. (2003). Anti-tumor effect of vitamin A and D on head and neck squamous cell carcinoma. *Auris Nasus Larynx* 30, 403-12.

17. McGregor, F., Muntoni, A., Fleming, J., Brown, J., Felix, D. H., MacDonald, D. G., Parkinson, E. K. & Harrison, P. R. (2002). Molecular changes associated with oral dysplasia progression and acquisition of immortality: potential for its reversal by 5-azacytidine. *Cancer Res* 62, 4757-66.

18. Nagai, M. (1999). Genetic alteration in head and neck squamous cell carcinomas. *Brazilian Journal of Medical and Biological Research* 32, 897-904.

19. Tokugawa, T., Sugihara, H., Tani, T. & Hattori, T. (2002). Modes of silencing of p16 in development of esophageal squamous cell carcinoma. *Cancer Res* 62, 4938-44.

20. Bockmuhl, U., Wolf, G., Schmidt, S., Schwendel, A., Jahnke, V., Dietel, M. & Petersen, I. (1998). Genomic alterations associated with malignancy in head and neck cancer. *Head Neck* 20, 145-51.

21. Frank, C. J., McClatchey, K. D., Devaney, K. O. & Carey, T. E. (1997). Evidence that loss of chromosome 18q is associated with tumor progression. *Cancer Res* 57, 824-7.

22. Hogg, R. P., Honorio, S., Martinez, A., Agathanggelou, A., Dallol, A., Fullwood, P., Weichselbaum, R., Kuo, M. J., Maher, E. R. & Latif, F. (2002). Frequent 3p allele loss and epigenetic inactivation of the RASSF1A tumour suppressor gene from region 3p21.3 in head and neck squamous cell carcinoma. *Eur J Cancer* 38, 1585-92.

23. Ogawara, K., Miyakawa, A., Shiba, M., Uzawa, K., Watanabe, T., Wang, X. L., Sato, T., Kubosawa, H., Kondo, Y. & Tanzawa, H. (1998). Allelic loss of chromosome 13q14.3 in human oral cancer: correlation with lymph node metastasis. *Int J Cancer* 79, 312-7.

24. Yamamoto, K., Konishi, N., Inui, T., Kitahori, Y., Hiasa, Y., Kirita, T. & Sugimura, M. (1998). Genomic alterations in oral squamous cell carcinoma cell lines detected by two-dimensional gel analysis. *Oral Oncol* 34, 508-12.

25. Yamamoto, K., Konishi, N., Inui, T., Nakamura, M., Hiasa, Y., Kirita, T. & Sugimura, M. (1999). DNA alterations in human oral squamous cell carcinomas detected by restriction landmark genomic scanning. *J Oral Pathol Med* 28, 102-6.

26. Masuda, M., Suzui, M., Yasumatu, R., Nakashima, T., Kuratomi, Y., Azuma, K., Tomita, K., Komiyama, S. & Weinstein, I. B. (2002). Constitutive activation of signal transducers and activators of transcription 3 correlates with cyclin D1 overexpression and may provide a novel prognostic marker in head and neck squamous cell carcinoma. *Cancer Res* 62, Jun 15.

27. Quon, H., Liu, F. F. & Cummings, B. J. (2001). Potential molecular prognostic markers in head and neck squamous cell carcinomas. *Head Neck* 23, 147-59.

28. Califano, J., van der Riet, P., Westra, W., Nawroz, H., Clayman, G., Piantadosi, S., Corio, R., Lee, D., Greenberg, B., Koch, W. & Sidransky, D. (1996). Genetic progression model for head and neck cancer: implications for field cancerization. *Cancer Res* 56, 2488-92.

29. Coombes, M. M., Briggs, K. L., Bone, J. R., Clayman, G. L., El-Naggar, A. K. & Dent, S. Y. (2003). Resetting the histone code at CDKN2A in HNSCC by inhibition of DNA methylation. *Oncogene* 22, 8902-11.

30. Dong, S. M., Sun, D. I., Benoit, N. E., Kuzmin, I., Lerman, M. I. & Sidransky, D. (2003). Epigenetic inactivation of RASSF1A in head and neck cancer. *Clin Cancer Res* 9, 3635-40.

31. Hasegawa, M., Nelson, H. H., Peters, E., Ringstrom, E., Posner, M. & Kelsey, K. T. (2002). Patterns of gene promoter methylation in squamous cell cancer of the head and neck. *Oncogene* 21, 4231-6.

32. Marsit, C. J., Liu, M., Nelson, H. H., Posner, M., Suzuki, M. & Kelsey, K. T. (2003). Inactivation of the Fanconi anemia/BRCA pathway in lung and oral cancers: implications for treatment and survival. *Oncogene*.

33. Smiraglia, D. J., Smith, L. T., Lang, J. C., Rush, L. J., Dai, Z., Schuller, D. E. & Plass, C. (2003). Differential targets of CpG island hypermethylation in primary and metastatic head and neck squamous cell carcinoma (HNSCC). *J Med Genet* 40, 25-33.

34. Wutz, A., Smrzka, O. W., Schweifer, N., Schellander, K., Wagner, E. F. & Barlow, D. P. (1997). Imprinted expression of the Igf2r gene depends on an intronic CpG island. *Nature* 389, 745-9.

35. Fruhwald, M., and Christoph Plass. (2002). Global and Gene-Specific Methylation Patterns in Cancer: Aspects of Tumor Biology and Clinical Potential. *Molecular Genetics and Metabolism* 75, 1-16.

36. Gaudet, F., Hodgson, J. G., Eden, A., Jackson-Grusby, L., Dausman, J., Gray, J. W., Leonhardt, H. & Jaenisch, R. (2003). Induction of tumors in mice by genomic hypomethylation. *Science* 300, 489-92.

37. Leonhardt, H. & Cardoso, M. C. (2000). DNA methylation, nuclear structure, gene expression and cancer. *J Cell Biochem Suppl* Suppl 35, 78-83.

38. Okano, M., Bell, D. W., Haber, D. A. & Li, E. (1999). DNA methyltransferases Dnmt3a and Dnmt3b are essential for de novo methylation and mammalian development. *Cell* 99, 247-57.

39. Santini, V., Kantarjian, H. M. & Issa, J. P. (2001). Changes in DNA methylation in neoplasia: pathophysiology and therapeutic implications. *Ann Intern Med* 134, 573-86.

40. Bestor, T. H. (2000). The DNA methyltransferases of mammals. *Hum Mol Genet* 9, 2395-402.

41. Reik, W., Dean, W. & Walter, J. (2001). Epigenetic reprogramming in mammalian development. *Science* 293, 1089-93.

42. Lyon, M. F. (1999). Imprinting and X-chromosome inactivation. *Results Probl Cell Differ* 25, 73-90.

43. Csankovszki, G., Nagy, A. & Jaenisch, R. (2001). Synergism of Xist RNA, DNA methylation, and histone hypoacetylation in maintaining X chromosome inactivation. *J Cell Biol* 153, 773-84.

44. Lyon, M. F. (1999). X-chromosome inactivation. *Curr Biol* 9, R235-7.

45. O'Neill, L. P., Randall, T. E., Lavender, J., Spotswood, H. T., Lee, J. T. & Turner, B. M. (2003). X-linked genes in female embryonic stem cells carry an epigenetic mark prior to the onset of X inactivation. *Hum Mol Genet* 12, 1783-90.

46. Liang, G., Chan, M. F., Tomigahara, Y., Tsai, Y. C., Gonzales, F. A., Li, E., Laird, P. W. & Jones, P. A. (2002). Cooperativity between DNA methyltransferases in the maintenance methylation of repetitive elements. *Mol Cell Biol* 22, 480-91.

47. Yoder, J. A., Walsh, C. P. & Bestor, T. H. (1997). Cytosine methylation and the ecology of intragenomic parasites. *Trends Genet* 13, 335-40.

48. Waki, T., Tamura, G., Sato, M. & Motoyama, T. (2003). Age-related methylation of tumor suppressor and tumor-related genes: an analysis of autopsy samples. *Oncogene* 22, 4128-33.

49. Issa, J. P. (1999). Aging, DNA methylation and cancer. *Crit Rev Oncol Hematol* 32, 31-43.

50. El-Osta, A. & Wolffe, A. P. (2000). DNA methylation and histone deacetylation in the control of gene expression: basic biochemistry to human development and disease. *Gene Expr* 9, 63-75.

51. Weissmann, F. & Lyko, F. (2003). Cooperative interactions between epigenetic modifications and their function in the regulation of chromosome architecture. *Bioessays* 25, 792-7.

52. Clark, S. a. J. M. (2002). DNA methylation and gene silencing in cancer: which is the guilty party? *Oncogene* 21, 5380-5387.

53. Jones, P. L., Veenstra, G. J., Wade, P. A., Vermaak, D., Kass, S. U., Landsberger, N., Strouboulis, J. & Wolffe, A. P. (1998). Methylated DNA and MeCP2 recruit histone deacetylase to repress transcription. *Nat Genet* 19, 187-91.

54. Nan, X., Ng, H. H., Johnson, C. A., Laherty, C. D., Turner, B. M., Eisenman, R. N. & Bird, A. (1998). Transcriptional repression by the methyl-CpG-binding protein MeCP2 involves a histone deacetylase complex. *Nature* 393, 386-9.

55. Bachman, K. E., Park, B. H., Rhee, I., Rajagopalan, H., Herman, J. G., Baylin, S. B., Kinzler, K. W. & Vogelstein, B. (2003). Histone modifications and silencing prior to DNA methylation of a tumor suppressor gene. *Cancer Cell* 3, 89-95.

56. Fuks F, H. P., Deplus R, Kouzarides T. (2003). The DNA methyltransferases associate with HP1 and the SUV39H1 histone methyltransferase. *Nucleic Acids Research* 31, 2305-12.

57. Nephew, K. P. & Huang, T. H. (2003). Epigenetic gene silencing in cancer initiation and progression. *Cancer Lett* 190, 125-33.

58. Curradi, M., Izzo, A., Badaracco, G. & Landsberger, N. (2002). Molecular mechanisms of gene silencing mediated by DNA methylation. *Mol Cell Biol* 22, 3157-73.

59. Akiyama, Y., Maesawa, C., Ogasawara, S., Terashima, M. & Masuda, T. (2003). Cell-type-specific repression of the maspin gene is disrupted frequently by demethylation at the promoter region in gastric intestinal metaplasia and cancer cells. *Am J Pathol* 163, 1911-9.

60. Oshimo, Y., Nakayama, H., Ito, R., Kitadai, Y., Yoshida, K., Chayama, K. & Yasui, W. (2003). Promoter methylation of cyclin D2 gene in gastric carcinoma. *Int J Oncol* 23, 1663-70.

61. Herman, J. G. & Baylin, S. B. (2003). Gene silencing in cancer in association with promoter hypermethylation. *N Engl J Med* 349, 2042-54.

62. Pfeifer, G. (2000). p53 mutational spectra and the role of methylated CpG sequences. *Mutat Res* 450, 155-66.

63. Weber, A., Bellmann, U., Bootz, F., Wittekind, C. & Tannapfel, A. (2002). INK4a-ARF alterations and p53 mutations in primary and consecutive squamous cell carcinoma of the head and neck. *Virchows Arch* 441, 133-42.

64. Brock, M. V., Gou, M., Akiyama, Y., Muller, A., Wu, T. T., Montgomery, E., Deasel, M., Germonpre, P., Rubinson, L., Heitmiller, R. F., Yang, S. C., Forastiere, A. A., Baylin, S. B. & Herman, J. G. (2003). Prognostic importance of promoter hypermethylation of multiple genes in esophageal adenocarcinoma. *Clin Cancer Res* 9, 2912-9.

65. Ogi, K., Toyota, M., Ohe-Toyota, M., Tanaka, N., Noguchi, M., Sonoda, T., Kohama, G. & Tokino, T. (2002). Aberrant methylation of multiple genes and clinicopathological features in oral squamous cell carcinoma. *Clin Cancer Res* 8, 3164-71.

66. Baylin, S. B., Esteller, M., Rountree, M. R., Bachman, K. E., Schuebel, K. & Herman, J. G. (2001). Aberrant patterns of DNA methylation, chromatin formation and gene expression in cancer. *Hum Mol Genet* 10, 687-92.

67. Liu, K., Zuo, C., Luo, Q. K., Suen, J. Y., Hanna, E. & Fan, C. Y. (2003). Promoter hypermethylation and inactivation of hMLH1, a DNA mismatch repair gene, in head and neck squamous cell carcinoma. *Diagn Mol Pathol* 12, 50-6.

68. Rosas, S. L., Koch, W., da Costa Carvalho, M. G., Wu, L., Califano, J., Westra, W., Jen, J. & Sidransky, D. (2001). Promoter hypermethylation patterns of p16, O6-methylguanine-DNA-methyltransferase, and death-associated protein kinase in tumors and saliva of head and neck cancer patients. *Cancer Res* 61, 939-42.

69. Issa, J. P. (2003). Methylation and prognosis: of molecular clocks and hypermethylator phenotypes. *Clin Cancer Res* 9, 2879-81.

70. Zardo, G., Tiirikainen, M. I., Hong, C., Misra, A., Feuerstein, B. G., Volik, S., Collins, C. C., Lamborn, K. R., Bollen, A., Pinkel, D., Albertson, D. G. & Costello, J. F. (2002). Integrated genomic and epigenomic analyses pinpoint biallelic gene inactivation in tumors. *Nat Genet* 32, 453-8.

71. Akama, T. O., Okazaki, Y., Ito, M., Okuizumi, H., Konno, H., Muramatsu, M., Plass, C., Held, W. A. & Hayashizaki, Y. (1997). Restriction landmark genomic scanning (RLGS-M)-based genome-wide scanning of mouse liver tumors for alterations in DNA methylation status. *Cancer Res* 57, 3294-9.

72. Plass, C., Yu, F., Yu, L., Strout, M. P., El-Rifai, W., Elonen, E., Knuutila, S., Marcucci, G., Young, D. C., Held, W. A., Bloomfield, C. D. & Caligiuri, M. A. (1999). Restriction landmark genome scanning for aberrant methylation in primary refractory and relapsed acute myeloid leukemia; involvement of the WIT-1 gene. *Oncogene* 18, 3159-65.

73. Hayashizaki, Y., Hirotsune, S., Okazaki, Y., Hatada, I., Shibata, H., Kawai, J., Hirose, K., Watanabe, S., Fushiki, S., Wada, S. & et al. (1993). Restriction landmark genomic scanning method and its various applications. *Electrophoresis* 14, 251-8.

74. Costello, J. F., Fruhwald, M. C., Smiraglia, D. J., Rush, L. J., Robertson, G. P., Gao, X., Wright, F. A., Feramisco, J. D., Peltomaki, P., Lang, J. C., Schuller, D. E., Yu, L., Bloomfield, C. D., Caligiuri, M. A., Yates, A., Nishikawa, R., Su Huang, H., Petrelli, N. J., Zhang, X., O'Dorisio, M. S., Held, W. A., Cavenee, W. K. & Plass, C. (2000). Aberrant CpG-island methylation has non-random and tumour-type-specific patterns. *Nat Genet* 24, 132-8.

75. Dai, Z., Weichenhan, D., Wu, Y. Z., Hall, J. L., Rush, L. J., Smith, L. T., Raval, A., Yu, L., Kroll, D., Muehlisch, J., Fruhwald, M. C., De Jong, P., Catanese, J., Davuluri, R. V., Smiraglia, D. J. & Plass, C. (2002). An AscI Boundary Library for the Studies of Genetic and Epigenetic Alterations in CpG Islands. *Genome Res* 12, 1591-8.

76. Rush, L. J. & Plass, C. (2002). Restriction landmark genomic scanning for DNA methylation in cancer: past, present, and future applications. *Anal Biochem* 307, 191-201.

77. Tabor, M. P., Brakenhoff, R. H., van Houten, V. M., Kummer, J. A., Snel, M. H., Snijders, P. J., Snow, G. B., Leemans, C. R. & Braakhuis, B. J. (2001). Persistence of genetically altered fields in head and neck cancer patients: biological and clinical implications. *Clin Cancer Res* 7, 1523-32.

78. Muller, H. M. & Widschwendter, M. (2003). Methylated DNA as a possible screening marker for neoplastic disease in several body fluids. *Expert Rev Mol Diagn* 3, 443-58.

79. Bender, C. M., Zingg, J. M. & Jones, P. A. (1998). DNA methylation as a target for drug design. *Pharm Res* 15, 175-87.

80. Zhu, W. G. & Otterson, G. A. (2003). The interaction of histone deacetylase inhibitors and DNA methyltransferase inhibitors in the treatment of human cancer cells. *Curr Med Chem Anti-Canc Agents* 3, 187-99.

81. Braakhuis, B. J., van Dongen, G. A., Bagnay, M., van Walsum, M. & Snow, G. B. (1989). Preclinical chemotherapy on human head and neck cancer xenografts grown in athymic nude mice. *Head Neck* 11, 511-5.

82. van Dongen, G., Braakhuis, B. J., Bagnay, M., Leyva, A. & Snow, G. B. (1988). Activity of differentiation-inducing agents and conventional drugs in head and neck cancer xenografts. *Acta Otolaryngol* 105, 488-93.

83. Marsit CJ, L. M., Nelson HH, Posner M, Suzuki M, Kelsey KT. (2003). Inactivation of the Fanconi anemia/BRCA pathway in lung and oral cancers: implications for treatment and survival. *Oncogene*, 1-5.

84. Wong, T. S., Man, M. W., Lam, A. K., Wei, W. I., Kwong, Y. L. & Yuen, A. P. (2003). The study of p16 and p15 gene methylation in head and neck squamous cell carcinoma and their quantitative evaluation in plasma by real-time PCR. *Eur J Cancer* 39, 1881-7.

85. Hibi, K., Koike, M., Nakayama, H., Fujitake, S., Kasai, Y., Ito, K., Akiyama, S. & Nakao, A. (2003). A cancer-prone case with a background of methylation of p16 tumor suppressor gene. *Clin Cancer Res* 9, 1053-6.

86. Azarschab, P., Stembalska, A., Loncar, M. B., Pfister, M., Sasiadek, M. M. & Blin, N. (2003). Epigenetic control of E-cadherin (CDH1) by CpG methylation in metastasising laryngeal cancer. *Oncol Rep* 10, 501-3.

87. Sanchez-Cespedes, M., Esteller, M., Wu, L., Nawroz-Danish, H., Yoo, G. H., Koch, W. M., Jen, J., Herman, J. G. & Sidransky, D. (2000). Gene promoter hypermethylation in tumors and serum of head and neck cancer patients. *Cancer Res* 60, 892-5.

88. Tetsuo, I., Shimada, Y., Hashimoto, Y., Kaganoi, J., Takatsugu, K., Watanabe, G., Murakami, Y. & Imamura, M. (2003). Involvement of TSLC1 in progression of esophageal squamous cell carcinoma. *Cancer Research* 63, 6320-6326.

89. Zhang, L., Lu, W., Miao, X., Xing, D., Tan, W. & Lin, D. (2003). Inactivation of DNA repair gene O6-methylguanine-DNA methyltransferase by promoter hypermethylation and its relation to p53 mutations in esophageal squamous cell carcinoma. *Carcinogenesis* 24, 1039-44.

90. Noguchi, T., Takeno, S., Kimura, Y., Uchida, Y., Daa, T., Yokoyama, S., Gabbert, H. E. & Mueller, W. (2003). FHIT expression and hypermethylation in esophageal squamous cell carcinoma. *Int J Mol Med* 11, 441-7.

91. Kuroki, T., Trapasso, F., Yendamuri, S., Matsuyama, A., Alder, H., Mori, M. & Croce, C. M. (2003). Allele loss and promoter hypermethylation of VHL, RAR-beta, RASSF1A, and FHIT tumor suppressor genes on chromosome 3p in esophageal squamous cell carcinoma. *Cancer Res* 63, 3724-8.

92. Nie, Y., Liao, J., Zhao, X., Song, Y., Yang, G. Y., Wang, L. D. & Yang, C. S. (2002). Detection of multiple gene hypermethylation in the development of esophageal squamous cell carcinoma. *Carcinogenesis* 23, 1713-20.

93. Chang, H. W., Chan, A., Kwong, D. L., Wei, W. I., Sham, J. S. & Yuen, A. P. (2003). Detection of hypermethylated RIZ1 gene in primary tumor, mouth, and throat rinsing fluid, nasopharyngeal swab, and peripheral blood of nasopharyngeal carcinoma patient. *Clin Cancer Res* 9, 1033-8.

94. Shibata, Y., Haruki, N., Kuwabara, Y., Ishiguro, H., Shinoda, N., Sato, A., Kimura, M., Koyama, H., Toyama, T., Nishiwaki, T., Kudo, J., Terashita, Y., Konishi, S., Sugiura, H. & Fujii, Y. (2002). Chfr expression is downregulated by CpG island hypermethylation in esophageal cancer. *Carcinogenesis* 23, 1695-9.

95. Kim, M. M. & Califano, J. A. (2004). Molecular pathology of head-and-neck cancer. *Int J Cancer* 112, 545-53.

96. Pan, H., Califano, J., Ponte, J. F., Russo, A. L., Cheng, K. H., Thiagalingam, A., Nemani, P., Sidransky, D. & Thiagalingam, S. (2005). Loss of heterozygosity patterns provide fingerprints for genetic heterogeneity in multistep cancer progression of tobacco smoke-induced non-small cell lung cancer. *Cancer Res* 65, 1664-9.

97. Knudson, A. G. (2001). Two genetic hits (more or less) to cancer. *Nat Rev Cancer* 1, 157-62.

98. Lasko, D., Cavenee, W. & Nordenskjold, M. (1991). Loss of constitutional heterozygosity in human cancer. *Annu Rev Genet* 25, 281-314.

99. Kim, S. K., Ro, J. Y., Kemp, B. L., Lee, J. S., Kwon, T. J., Hong, W. K. & Mao, L. (1998). Identification of two distinct tumor-suppressor loci on the long arm of chromosome 10 in small cell lung cancer. *Oncogene* 17, 1749-53.

100. Garinis, G. A., Patrinos, G. P., Spanakis, N. E. & Menounos, P. G. (2002). DNA hypermethylation: when tumour suppressor genes go silent. *Hum Genet* 111, 115-27.

101. Smiraglia, D. J. & Plass, C. (2002). The study of aberrant methylation in cancer via restriction landmark genomic scanning. *Oncogene* 21, 5414-26.

102. Costello, J. F., Smiraglia, D. J. & Plass, C. (2002). Restriction landmark genome scanning. *Methods* 27, 144-9.

103. Dai, Z., Lakshmanan, R. R., Zhu, W. G., Smiraglia, D. J., Rush, L. J., Fruhwald, M. C., Brena, R. M., Li, B., Wright, F. A., Ross, P., Otterson, G. A. & Plass, C. (2001). Global methylation profiling of lung cancer identifies novel methylated genes. *Neoplasia* 3, 314-23.

104. Fruhwald, M. C., O'Dorisio, M. S., Smith, L., Dai, Z., Wright, F. A., Paulus, W., Jurgens, H. & Plass, C. (2001). [Hypermethylation as a potential prognostic factor and a clue to a better understanding of the molecular pathogenesis of medulloblastoma--results of a genomewide methylation scan]. *Klin Padiatr* 213, 197-203.

105. Rush, L. J., Dai, Z., Smiraglia, D. J., Gao, X., Wright, F. A., Fruhwald, M., Costello, J. F., Held, W. A., Yu, L., Krahe, R., Kolitz, J. E., Bloomfield, C. D., Caligiuri, M. A. & Plass, C. (2001). Novel methylation targets in de novo acute myeloid leukemia with prevalence of chromosome 11 loci. *Blood* 97, 3226-33.

106. Costello, J. F., Fruhwald, M. C., Smiraglia, D. J., Rush, L. J., Robertson, G. P., Gao, X., Wright, F. A., Feramisco, J. D., Peltomaki, P., Lang, J. C., Schuller, D. E., Yu, L., Bloomfield, C. D., Caligiuri, M. A., Yates, A., Nishikawa, R., Su Huang, H., Petrelli, N. J., Zhang, X., O'Dorisio, M. S., Held, W. A., Cavenee, W. K. & Plass, C. (2000). Aberrant CpG-island methylation has non-random and tumour-type-specific patterns. *Nat Genet* 24, 132-8.

107. Plass, C., Yu, F., Yu, L., Strout, M. P., El-Rifai, W., Elonen, E., Knuutila, S., Marcucci, G., Young, D. C., Held, W. A., Bloomfield, C. D. & Caligiuri, M. A. (1999). Restriction landmark genome scanning for aberrant methylation in primary refractory and relapsed acute myeloid leukemia; involvement of the WIT-1 gene. *Oncogene* 18, 3159-65.

108. Barghorn, A., Speel, E. J., Farspour, B., Saremaslani, P., Schmid, S., Perren, A., Roth, J., Heitz, P. U. & Komminoth, P. (2001). Putative tumor suppressor loci at 6q22 and 6q23-q24 are involved in the malignant progression of sporadic endocrine pancreatic tumors. *Am J Pathol* 158, 1903-11.

109. Stenman, G., Sandros, J., Dahlenfors, R., Juberg-Ode, M. & Mark, J. (1986). 6q- and loss of the Y chromosome--two common deviations in malignant human salivary gland tumors. *Cancer Genet Cytogenet* 22, 283-93.

110. Stenman, G., Sandros, J., Mark, J. & Edstrom, S. (1989). Partial 6q deletion in a human salivary gland adenocarcinoma. *Cancer Genet Cytogenet* 39, 153-6.

111. Sandros, J., Mark, J., Happonen, R. P. & Stenman, G. (1988). Specificity of 6q- markers and other recurrent deviations in human malignant salivary gland tumors. *Anticancer Res* 8, 637-43.

112. Theile, M., Seitz, S., Arnold, W., Jandrig, B., Frege, R., Schlag, P. M., Haensch, W., Guski, H., Winzer, K. J., Barrett, J. C. & Scherneck, S. (1996). A defined chromosome 6q fragment (at D6S310) harbors a putative tumor suppressor gene for breast cancer. *Oncogene* 13, 677-85.

113. Orphanos, V., McGown, G., Hey, Y., Boyle, J. M. & Santibanez-Koref, M. (1995). Proximal 6q, a region showing allele loss in primary breast cancer. *Br J Cancer* 71, 290-3.

114. Devilee, P., van Vliet, M., van Sloun, P., Kuipers Dijkshoorn, N., Hermans, J., Pearson, P. L. & Cornelisse, C. J. (1991). Allelotype of human breast carcinoma: a second major site for loss of heterozygosity is on chromosome 6q. *Oncogene* 6, 1705-11.

115. Negrini, M., Sabbioni, S., Possati, L., Rattan, S., Corallini, A., Barbanti-Brodano, G. & Croce, C. M. (1994). Suppression of tumorigenicity of breast cancer cells by microcell-mediated chromosome transfer: studies on chromosomes 6 and 11. *Cancer Res* 54, 1331-6.

116. Bissig, H., Richter, J., Desper, R., Meier, V., Schraml, P., Schaffer, A. A., Sauter, G., Mihatsch, M. J. & Moch, H. (1999). Evaluation of the clonal relationship between primary and metastatic renal cell carcinoma by comparative genomic hybridization. *Am J Pathol* 155, 267-74.

117. Lee, J. H. & Welch, D. R. (1997). Identification of highly expressed genes in metastasis-suppressed chromosome 6/human malignant melanoma hybrid cells using subtractive hybridization and differential display. *Int J Cancer* 71, 1035-44.

118. Miele, M. E., Jewett, M. D., Goldberg, S. F., Hyatt, D. L., Morelli, C., Gualandi, F., Rimessi, P., Hicks, D. J., Weissman, B. E., Barbanti-Brodano, G. & Welch, D. R. (2000). A human melanoma metastasis-suppressor locus maps to 6q16.3-q23. *Int J Cancer* 86, 524-8.

119. Gaidano, G., Hauptschein, R. S., Parsa, N. Z., Offit, K., Rao, P. H., Lenoir, G., Knowles, D. M., Chaganti, R. S. & Dalla-Favera, R. (1992). Deletions involving two distinct regions of 6q in B-cell non-Hodgkin lymphoma. *Blood* 80, 1781-7.

120. Wan, M., Sun, T., Vyas, R., Zheng, J., Granada, E. & Dubeau, L. (1999). Suppression of tumorigenicity in human ovarian cancer cell lines is controlled by a 2 cM fragment in chromosomal region 6q24-q25. *Oncogene* 18, 1545-51.

121. Girard, L., Zochbauer-Muller, S., Virmani, A. K., Gazdar, A. F. & Minna, J. D. (2000). Genome-wide allelotyping of lung cancer identifies new regions of allelic loss, differences between small cell lung cancer and non-small cell lung cancer, and loci clustering. *Cancer Res* 60, 4894-906.

122. Abe, T., Makino, N., Furukawa, T., Ouyang, H., Kimura, M., Yatsuoka, T., Yokoyama, T., Inoue, H., Fukushige, S., Hoshi, M., Hayashi, Y., Sunamura, M., Kobari, M., Matsuno, S. & Horii, A. (1999). Identification of three commonly deleted regions on chromosome arm 6q in human pancreatic cancer. *Genes Chromosomes Cancer* 25, 60-4.

123. Wistuba, II, Tang, M., Maitra, A., Alvarez, H., Troncoso, P., Pimentel, F. & Gazdar, A. F. (2001). Genome-wide allelotyping analysis reveals multiple sites of allelic loss in gallbladder carcinoma. *Cancer Res* 61, 3795-800.

124. Bailey-Wilson, J. E., Amos, C. I., Pinney, S. M., Petersen, G. M., de Andrade, M., Wiest, J. S., Fain, P., Schwartz, A. G., You, M., Franklin, W., Klein, C., Gazdar, A., Rothschild, H., Mandal, D., Coons, T., Slusser, J., Lee, J., Gaba, C., Kupert, E., Perez, A., Zhou, X., Zeng, D., Liu, Q., Zhang, Q., Seminara, D., Minna, J. & Anderson, M. W. (2004). A major lung cancer susceptibility locus maps to chromosome 6q23-25. *Am J Hum Genet* 75, 460-74.

125. Knuutila, S., Aalto, Y., Autio, K., Bjorkqvist, A. M., El-Rifai, W., Hemmer, S., Huhta, T., Kettunen, E., Kiuru-Kuhlefelt, S., Larramendy, M. L., Lushnikova, T., Monni, O., Pere, H., Tapper, J., Tarkkanen, M., Varis, A., Wasenius, V. M., Wolf, M. & Zhu, Y. (1999). DNA copy number losses in human neoplasms. *Am J Pathol* 155, 683-94.

126. Presneau, N., Manderson, E. N. & Tonin, P. N. (2003). The quest for a tumor suppressor gene phenotype. *Curr Mol Med* 3, 605-29.

127. Lee, J. K., Kim, M. J., Hong, S. P. & Hong, S. D. (2004). Inactivation patterns of p16/INK4A in oral squamous cell carcinomas. *Exp Mol Med* 36, 165-71.

128. Feltus, F. A., Lee, E. K., Costello, J. F., Plass, C. & Vertino, P. M. (2003). Predicting aberrant CpG island methylation. *Proc Natl Acad Sci U S A* 100, 12253-8.

129. Fazzari, M. J. & Greally, J. M. (2004). Epigenomics: beyond CpG islands. *Nat Rev Genet* 5, 446-55.

130. Wolf, S. F. & Migeon, B. R. (1982). Studies of X chromosome DNA methylation in normal human cells. *Nature* 295, 667-71.

131. Morgan, H. D., Dean, W., Coker, H. A., Reik, W. & Petersen-Mahrt, S. K. (2004). Activation-induced cytidine deaminase deaminates 5-methylcytosine in DNA and is expressed in pluripotent tissues: implications for epigenetic reprogramming. *J Biol Chem* 279, 52353-60.

132. Sheikhnejad, G., Brank, A., Christman, J. K., Goddard, A., Alvarez, E., Ford, H., Jr., Marquez, V. E., Marasco, C. J., Sufrin, J. R., O'Gara, M. & Cheng, X. (1999). Mechanism of inhibition of DNA (cytosine C5)-methyltransferases by oligodeoxyribonucleotides containing 5,6-dihydro-5-azacytosine. *J Mol Biol* 285, 2021-34.

133. Lu, J., Richardson, J. A. & Olson, E. N. (1998). Capsulin: a novel bHLH transcription factor expressed in epicardial progenitors and mesenchyme of visceral organs. *Mech Dev* 73, 23-32.

134. Quaggin, S. E., Schwartz, L., Cui, S., Igarashi, P., Deimling, J., Post, M. & Rossant, J. (1999). The basic-helix-loop-helix protein pod1 is critically important for kidney and lung organogenesis. *Development* 126, 5771-83.

135. Funato, N., Ohyama, K., Kuroda, T. & Nakamura, M. (2003). Basic helix-loop-helix transcription factor epicardin/capsulin/Pod-1 suppresses differentiation by negative regulation of transcription. *J Biol Chem* 278, 7486-93.

136. Lu, J. R., Bassel-Duby, R., Hawkins, A., Chang, P., Valdez, R., Wu, H., Gan, L., Shelton, J. M., Richardson, J. A. & Olson, E. N. (2002). Control of facial muscle development by MyoR and capsulin. *Science* 298, 2378-81.

137. Lu, J., Chang, P., Richardson, J. A., Gan, L., Weiler, H. & Olson, E. N. (2000). The basic helix-loop-helix transcription factor capsulin controls spleen organogenesis. *Proc Natl Acad Sci U S A* 97, 9525-30.

138. Cui, S., Ross, A., Stallings, N., Parker, K. L., Capel, B. & Quaggin, S. E. (2004). Disrupted gonadogenesis and male-to-female sex reversal in Pod1 knockout mice. *Development* 131, 4095-105.

139. Shannon, J. M. & Hyatt, B. A. (2004). Epithelial-mesenchymal interactions in the developing lung. *Annu Rev Physiol* 66, 625-45.

140. Lorincz, M. C., Dickerson, D. R., Schmitt, M. & Groudine, M. (2004). Intragenic DNA methylation alters chromatin structure and elongation efficiency in mammalian cells. *Nat Struct Mol Biol* 11, 1068-75.

141. Ishii, T., Fujishiro, M., Masuda, M., Teramoto, S. & Matsuse, T. (2004). A methylated oligonucleotide induced methylation of GSTP1 promoter and suppressed its expression in A549 lung adenocarcinoma cells. *Cancer Lett* 212, 211-23.

142. Boyer, B., Valles, A. M. & Edme, N. (2000). Induction and regulation of epithelial-mesenchymal transitions. *Biochem Pharmacol* 60, 1091-9.

143. Thiery, J. P. (2002). Epithelial-mesenchymal transitions in tumour progression. *Nat Rev Cancer* 2, 442-54.

144. Prindull, G. & Zipori, D. (2004). Environmental guidance of normal and tumor cell plasticity: epithelial mesenchymal transitions as a paradigm. *Blood* 103, 2892-9.

145. Bukovsky, A., Caudle, M. R., Keenan, J. A., Upadhyaya, N. B., Van Meter, S. E., Wimalasena, J. & Elder, R. F. (2001). Association of mesenchymal cells and immunoglobulins with differentiating epithelial cells. *BMC Dev Biol* 1, 11.

146. Gibson, M. C. & Perrimon, N. (2003). Apicobasal polarization: epithelial form and function. *Curr Opin Cell Biol* 15, 747-52.

147. Kiemer, A. K., Takeuchi, K. & Quinlan, M. P. (2001). Identification of genes involved in epithelial-mesenchymal transition and tumor progression. *Oncogene* 20, 6679-88.

148. Sipp, D. (2004). There and back again, Vol. 2005. EurekAlert.

149. Thiery, J. P. (2003). Epithelial-mesenchymal transitions in development and pathologies. *Curr Opin Cell Biol* 15, 740-6.

150. Friedl, P. & Wolf, K. (2003). Tumour-cell invasion and migration: diversity and escape mechanisms. *Nat Rev Cancer* 3, 362-74.

151. Welch, D. R. & Rinker-Schaeffer, C. W. (1999). What defines a useful marker of metastasis in human cancer? *J Natl Cancer Inst* 91, 1351-3.

152. Yoshida, B. A., Sokoloff, M. M., Welch, D. R. & Rinker-Schaeffer, C. W. (2000). Metastasis-suppressor genes: a review and perspective on an emerging field. *J Natl Cancer Inst* 92, 1717-30.

153. Miyazawa, J., Mitoro, A., Kawashiri, S., Chada, K. K. & Imai, K. (2004). Expression of mesenchyme-specific gene HMGA2 in squamous cell carcinomas of the oral cavity. *Cancer Res* 64, 2024-9.

154. Meuwissen, R. & Berns, A. (2005). Mouse models for human lung cancer. *Genes Dev* 19, 643-64.

155. Chen, W., Cooper, T. K., Zahnow, C. A., Overholtzer, M., Zhao, Z., Ladanyi, M., Karp, J. E., Gokgoz, N., Wunder, J. S., Andrulis, I. L., Levine, A. J., Mankowski, J. L. & Baylin, S. B. (2004). Epigenetic and genetic loss of Hic1 function accentuates the role of p53 in tumorigenesis. *Cancer Cell* 6, 387-98.

156. Grass, J. A., Boyer, M. E., Pal, S., Wu, J., Weiss, M. J. & Bresnick, E. H. (2003). GATA-1-dependent transcriptional repression of GATA-2 via disruption of positive autoregulation and domain-wide chromatin remodeling. *Proc Natl Acad Sci U S A* 100, 8811-6.

157. Nishishita, T., Ouchi, K., Zhang, X., Inoue, M., Inazawa, T., Yoshiura, K., Kuwabara, K., Nakaoka, T., Watanabe, N., Igura, K., Takahashi, T. A. & Yamashita, N. (2004). A potential pro-angiogenic cell therapy with human placenta-derived mesenchymal cells. *Biochem Biophys Res Commun* 325, 24-31.

158. Kauffman, E. C., Robinson, V. L., Stadler, W. M., Sokoloff, M. H. & Rinker-Schaeffer, C. W. (2003). Metastasis suppression: the evolving role of metastasis suppressor genes for regulating cancer cell growth at the secondary site. *J Urol* 169, 1122-33.

159. Goeze, A., Schluns, K., Wolf, G., Thasler, Z., Petersen, S. & Petersen, I. (2002). Chromosomal imbalances of primary and metastatic lung adenocarcinomas. *J Pathol* 196, 8-16.

160. Sheng, Z. M., Marchetti, A., Buttitta, F., Champeme, M. H., Campani, D., Bistocchi, M., Lidereau, R. & Callahan, R. (1996). Multiple regions of chromosome 6q affected by loss of heterozygosity in primary human breast carcinomas. *Br J Cancer* 73, 144-7.

161. Shevde, L. A. & Welch, D. R. (2003). Metastasis suppressor pathways--an evolving paradigm. *Cancer Lett* 198, 1-20.

162. Steeg, P. S. (2003). Metastasis suppressors alter the signal transduction of cancer cells. *Nat Rev Cancer* 3, 55-63.

163. Warner, G. C., Reis, P. P., Jurisica, I., Sultan, M., Arora, S., Macmillan, C., Makitie, A. A., Grenman, R., Reid, N., Sukhai, M., Freeman, J., Gullane, P., Irish, J. & Kamel-Reid, S. (2004). Molecular classification of oral cancer by cDNA microarrays identifies overexpressed genes correlated with nodal metastasis. *Int J Cancer* 110, 857-68.

164. Maula, S. M., Luukkaa, M., Grenman, R., Jackson, D., Jalkanen, S. & Ristamaki, R. (2003). Intratumoral lymphatics are essential for the metastatic spread and prognosis in squamous cell carcinomas of the head and neck region. *Cancer Res* 63, 1920-6.

165. Bockmuhl, U., Schluns, K., Schmidt, S., Matthias, S. & Petersen, I. (2002). Chromosomal alterations during metastasis formation of head and neck squamous cell carcinoma. *Genes Chromosomes Cancer* 33, 29-35.

166. Keller, E. T., Fu, Z., Yeung, K. & Brennan, M. (2004). Raf kinase inhibitor protein: a prostate cancer metastasis suppressor gene. *Cancer Lett* 207, 131-7.

167. Shirasaki, F., Takata, M., Hatta, N. & Takehara, K. (2001). Loss of expression of the metastasis suppressor gene KiSS1 during melanoma progression and its association with LOH of chromosome 6q16.3-q23. *Cancer Res* 61, 7422-5.

168. West, A., Vojta, P. J., Welch, D. R. & Weissman, B. E. (1998). Chromosome localization and genomic structure of the KiSS-1 metastasis suppressor gene (KISS1). *Genomics* 54, 145-8.

169. Kotani, M., Detheux, M., Vandenbogaerde, A., Communi, D., Vanderwinden, J. M., Le Poul, E., Brezillon, S., Tyldesley, R., Suarez-Huerta, N., Vandeput, F., Blanpain, C., Schiffmann, S. N., Vassart, G. & Parmentier, M. (2001). The metastasis suppressor gene KiSS-1 encodes kisspeptins, the natural ligands of the orphan G protein-coupled receptor GPR54. *J Biol Chem* 276, 34631-6.

170. Harms, J. F., Welch, D. R. & Miele, M. E. (2003). KISS1 metastasis suppression and emergent pathways. *Clin Exp Metastasis* 20, 11-8.

171. Dhar, D. K., Naora, H., Kubota, H., Maruyama, R., Yoshimura, H., Tonomoto, Y., Tachibana, M., Ono, T., Otani, H. & Nagasue, N. (2004). Downregulation of KiSS-1 expression is responsible for tumor invasion and worse prognosis in gastric carcinoma. *Int J Cancer* 111, 868-72.

172. Takino, T., Koshikawa, N., Miyamori, H., Tanaka, M., Sasaki, T., Okada, Y., Seiki, M. & Sato, H. (2003). Cleavage of metastasis suppressor gene product KiSS-1 protein/metastin by matrix metalloproteinases. *Oncogene* 22, 4617-26.

173. Ohtaki, T., Shintani, Y., Honda, S., Matsumoto, H., Hori, A., Kanehashi, K., Terao, Y., Kumano, S., Takatsu, Y., Masuda, Y., Ishibashi, Y., Watanabe, T., Asada, M., Yamada, T., Suenaga, M., Kitada, C., Usuki, S., Kurokawa, T., Onda, H., Nishimura, O. & Fujino, M. (2001). Metastasis suppressor gene KiSS-1 encodes peptide ligand of a G-protein-coupled receptor. *Nature* 411, 613-7.

174. You, J., Miele, M. E., Dong, C. & Welch, D. R. (1995). Suppression of human melanoma metastasis by introduction of chromosome 6 may be partially due to inhibition of motility, but not to inhibition of invasion. *Biochem Biophys Res Commun* 208, 476-84.

175. Quaggin, S. E., Vanden Heuvel, G. B. & Igarashi, P. (1998). Pod-1, a mesoderm-specific basic-helix-loop-helix protein expressed in mesenchymal and glomerular epithelial cells in the developing kidney. *Mech Dev* 71, 37-48.

176. Goldberg, S. F., Miele, M. E., Hatta, N., Takata, M., Paquette-Straub, C., Freedman, L. P. & Welch, D. R. (2003). Melanoma metastasis suppression by chromosome 6: evidence for a pathway regulated by CRSP3 and TXNIP. *Cancer Res* 63, 432-40.

177. Yan, C., Wang, H. & Boyd, D. D. (2001). KiSS-1 represses 92-kDa type IV collagenase expression by down-regulating NF-kappa B binding to the promoter as a consequence of Ikappa Balpha -induced block of p65/p50 nuclear translocation. *J Biol Chem* 276, 1164-72.

178. Chambers, A. F., Groom, A. C. & MacDonald, I. C. (2002). Dissemination and growth of cancer cells in metastatic sites. *Nat Rev Cancer* 2, 563-72.

179. You, M. & Bergman, G. (1998). Preclinical and clinical models of lung cancer chemoprevention. *Hematol Oncol Clin North Am* 12, 1037-53.

180. Wang, Y., Zhang, Z., Kastens, E., Lubet, R. A. & You, M. (2003). Mice with alterations in both p53 and Ink4a/Arf display a striking increase in lung tumor multiplicity and progression: differential chemopreventive effect of budesonide in wild-type and mutant A/J mice. *Cancer Res* 63, 4389-95.